Иммунохимические методы детекции

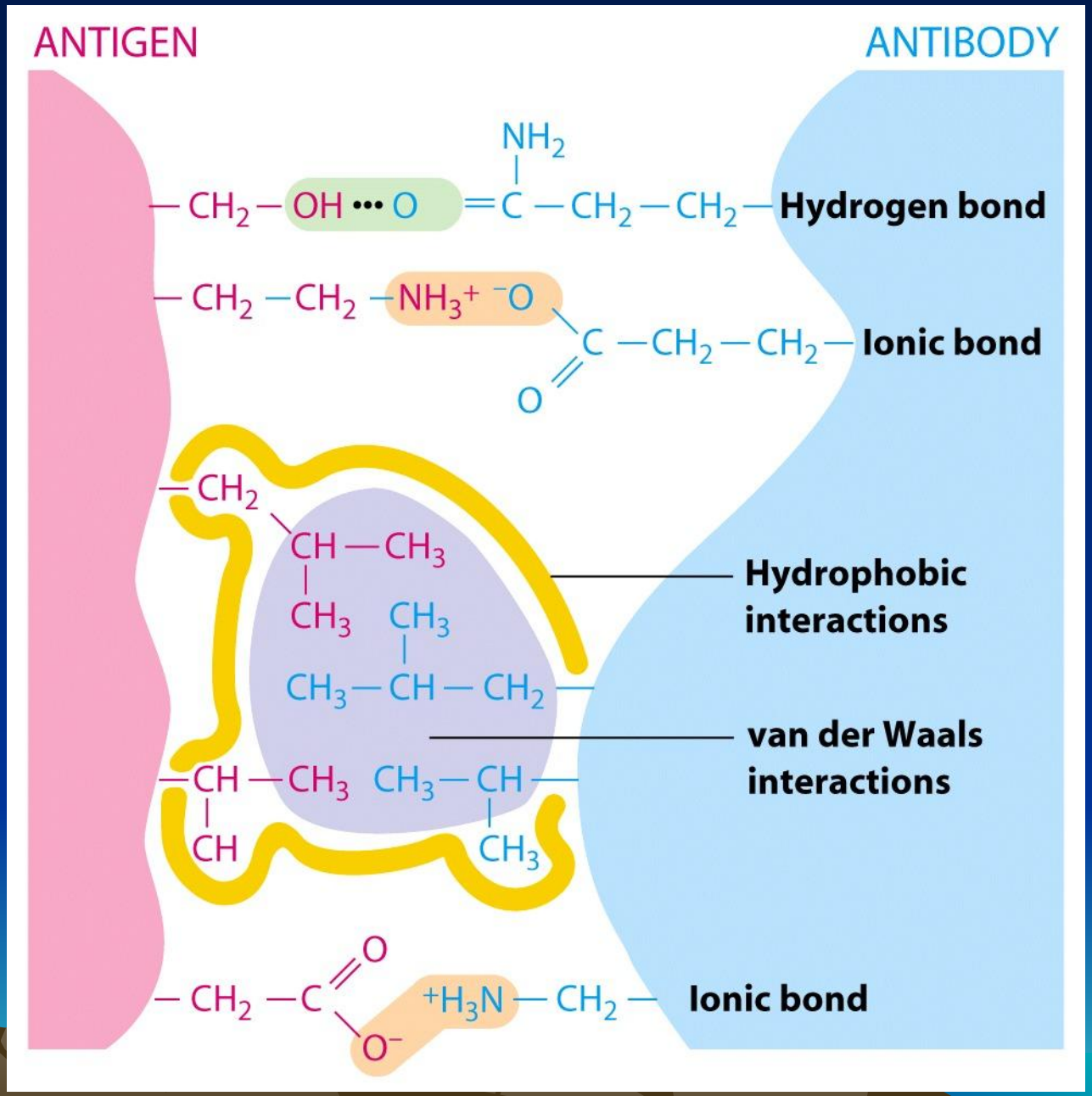
ANTIGEN
ANTIBODY
Hydrogen bond
Ionic bond
Hydrophobic interactions
van der Waals interactions
Ionic bond

TABLE 6-1 Forward and reverse rate constants (k_1 and k_{-1}) and association and dissociation constants (K_a and K_d) for three ligand-antibody interactions

Antibody	Ligand	k_1	k_{-1}	K_a	K_d
Anti-DNP	ϵ-DNP-L-lysine	8×10^7	1	1×10^8	1×10^{-8}
Anti-fluorescein	Fluorescein	4×10^8	5×10^{-3}	1×10^{11}	1×10^{-11}
Anti-bovine serum albumin (BSA)	Dansyl-BSA	3×10^5	2×10^{-3}	1.7×10^8	5.9×10^{-9}

SOURCE: Adapted from H. N. Eisen, 1990, *Immunology*, 3rd ed., Harper & Row Publishers.

TABLE 6-3 Sensitivity of various immunoassays

Assay	Sensitivity* (μg antibody/ml)
Precipitation reaction in fluids	20–200
Precipitation reactions in gels	
Mancini radial immunodiffusion	10–50
Ouchterlony double immunodiffusion	20–200
Immunoelectrophoresis	20–200
Rocket electrophoresis	2
Agglutination reactions	
Direct	0.3
Passive agglutination	0.006–0.06
Agglutination inhibition	0.006–0.06
Radioimmunoassay	0.0006–0.006
Enzyme-linked immunosorbent assay (ELISA)	<0.0001–0.01
ELISA using chemiluminescence	<0.0001–0.01†
Immunofluorescence	1.0
Flow cytometry	0.06–0.006

*The sensitivity depends upon the affinity of the antibody as well as the epitope density and distribution.

†Note that the sensitivity of chemiluminescence-based ELISA assays can be made to match that of RIA.

SOURCE: Adapted from N. R. Rose et al., eds., 1997, *Manual of Clinical Laboratory Immunology,* 5th ed., American Society for Microbiology, Washington, D.C.

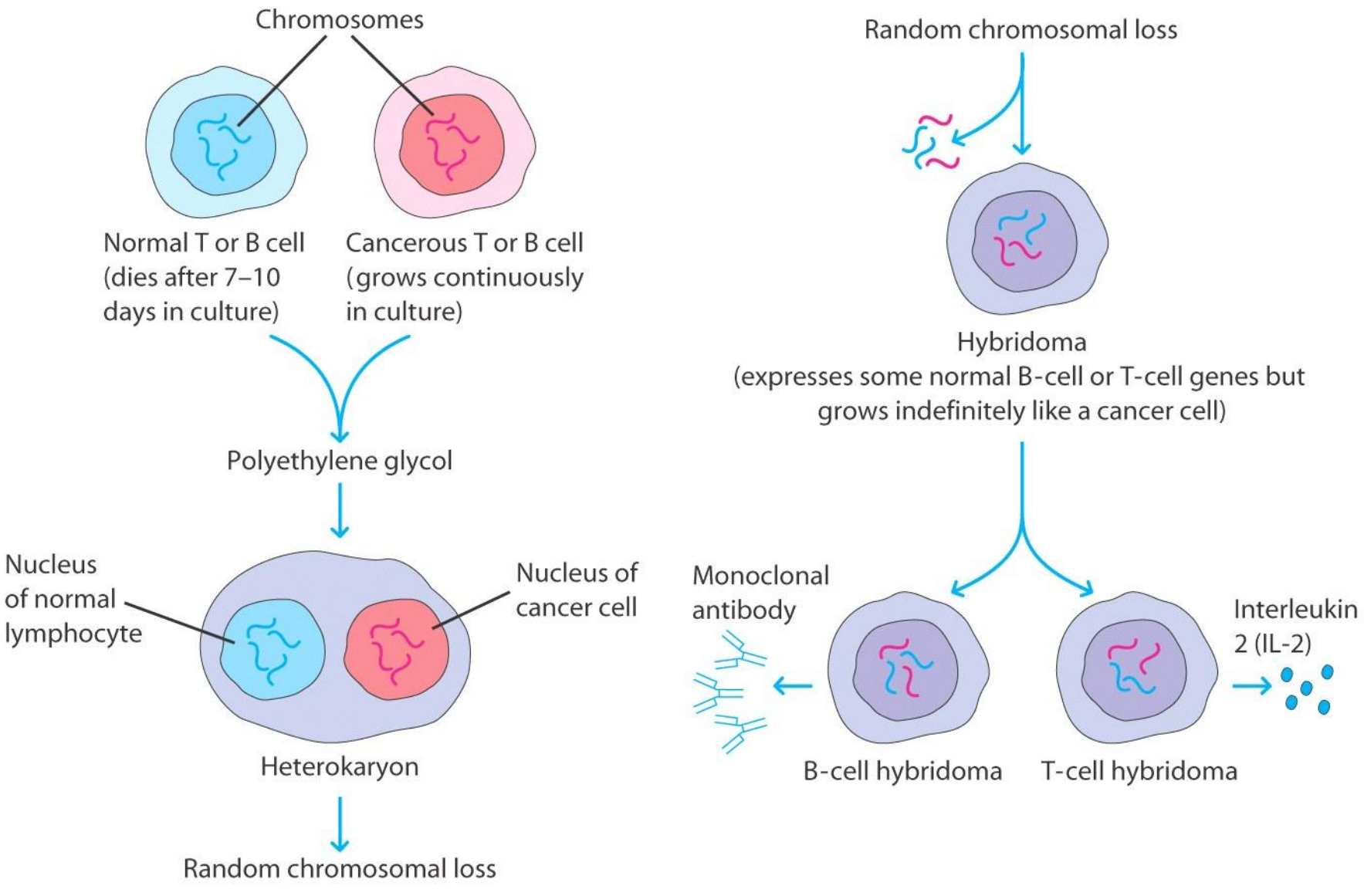
Chromosomes
Normal T or B cell (dies after 7–10 days in culture)
Cancerous T or B cell (grows continuously in culture)
Polyethylene glycol
Nucleus of normal lymphocyte
Nucleus of cancer cell
Heterokaryon
Random chromosomal loss
Random chromosomal loss
Hybridoma
(expresses some normal B-cell or T-cell genes but grows indefinitely like a cancer cell)
Monoclonal antibody
Interleukin 2 (IL-2)
B-cell hybridoma
T-cell hybridoma

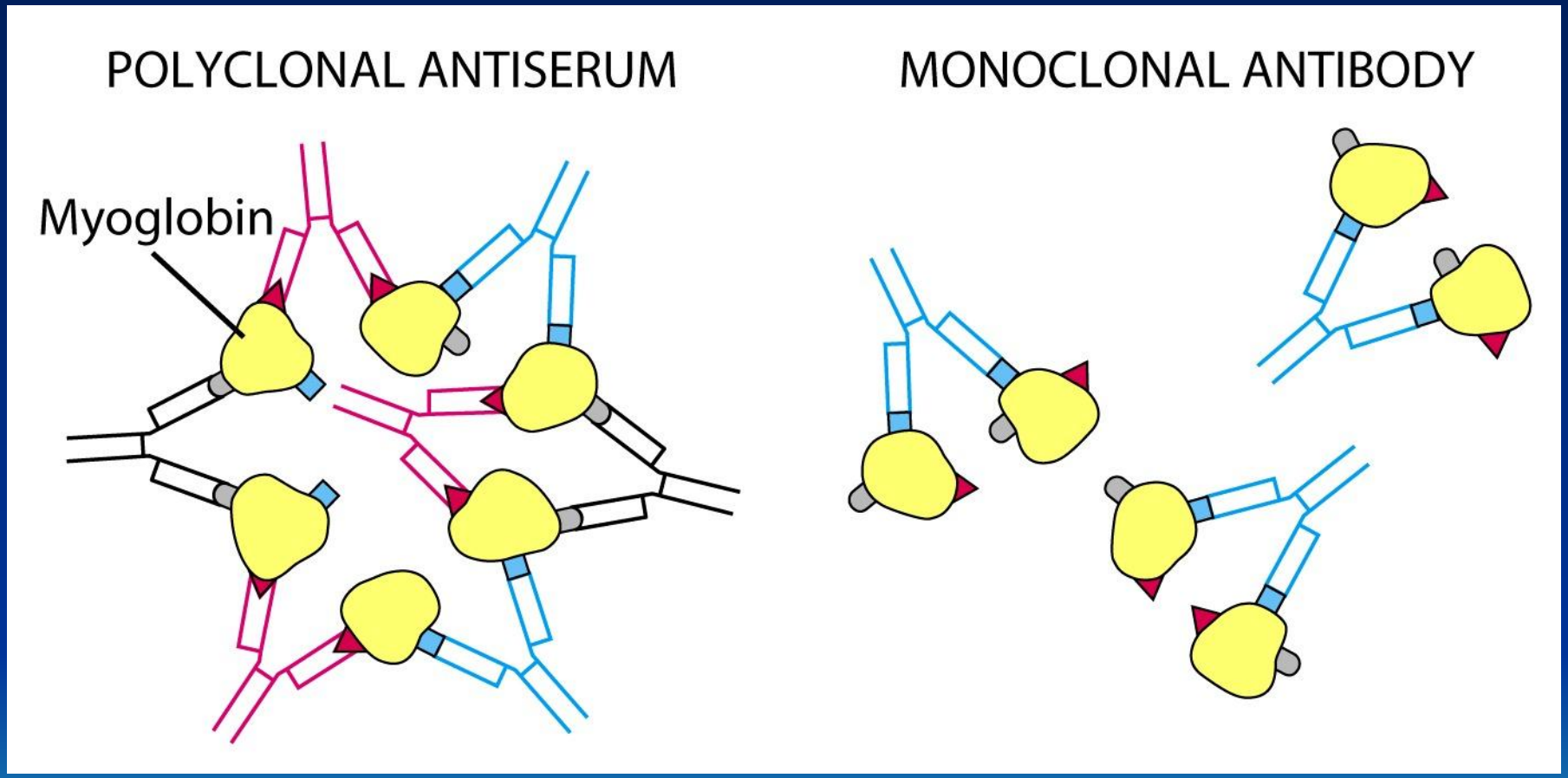
POLYCLONAL ANTISERUM
MONOCLONAL ANTIBODY
Myoglobin

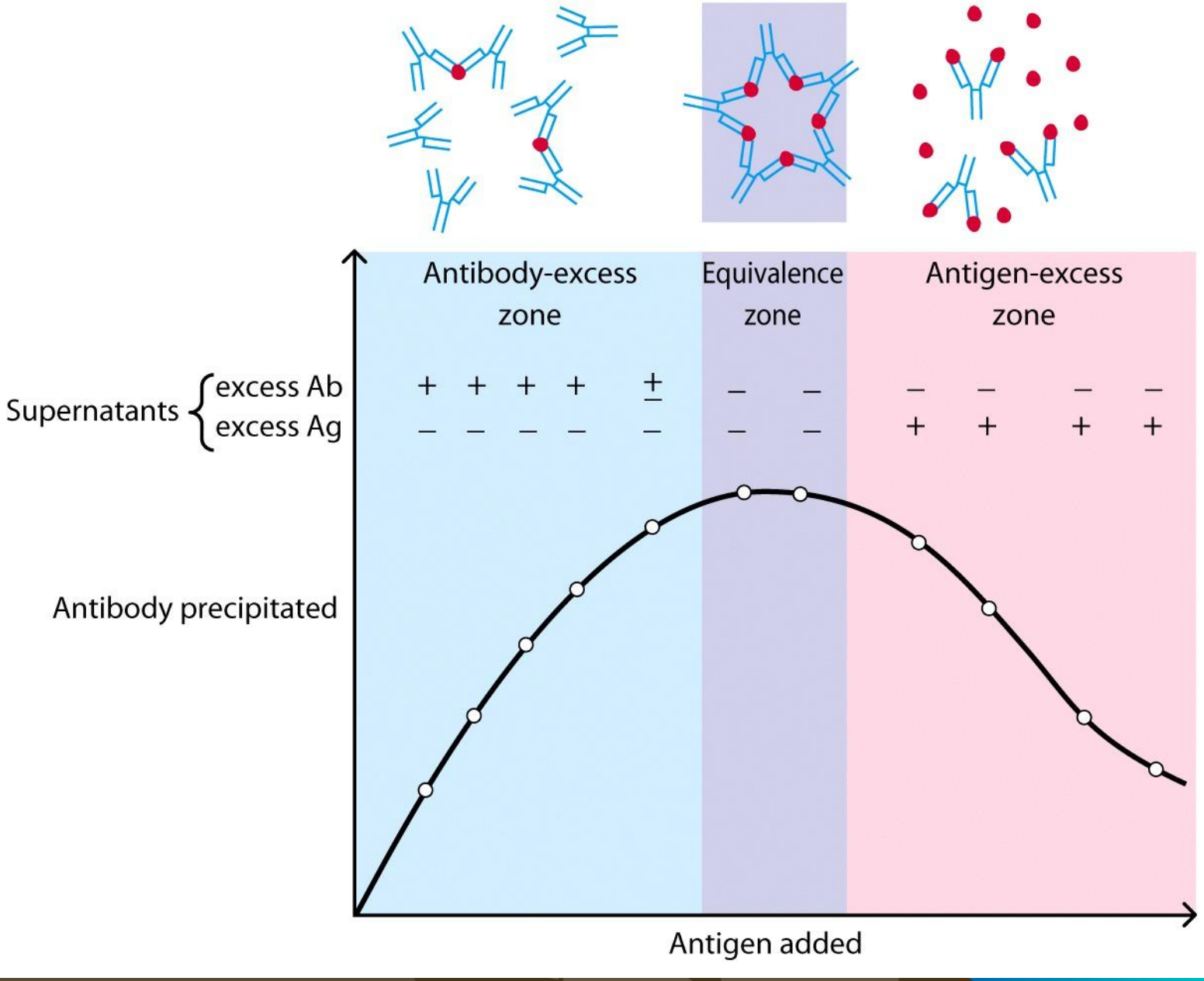
Antibody-excess zone
Equivalence zone
Antigen-excess zone
Supernatants
excess Ab
excess Ag
+ + + + ±
– – – – –
– – – – – –
– – – – + + + +
Antibody precipitated
Antigen added

RADIAL IMMUNODIFFUSION

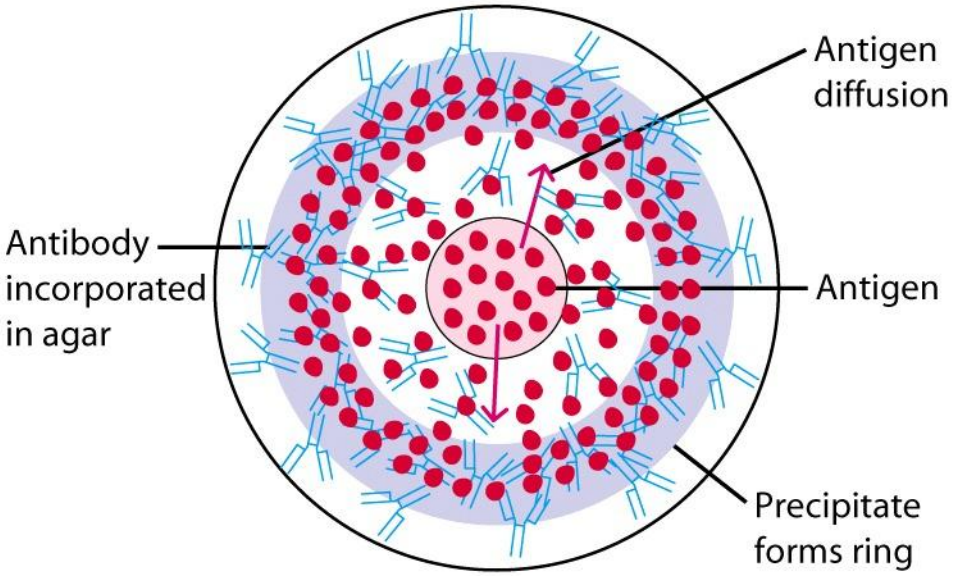

DOUBLE IMMUNODIFFUSION

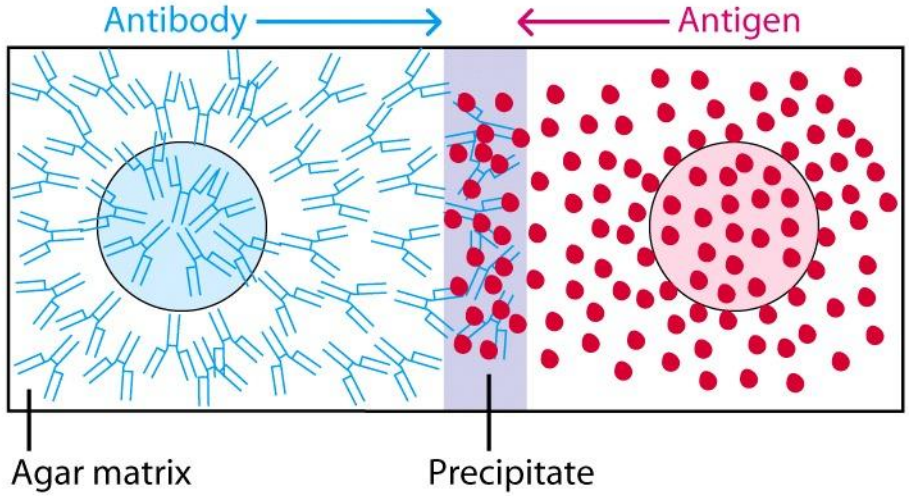

RADIAL IMMUNODIFFUSION

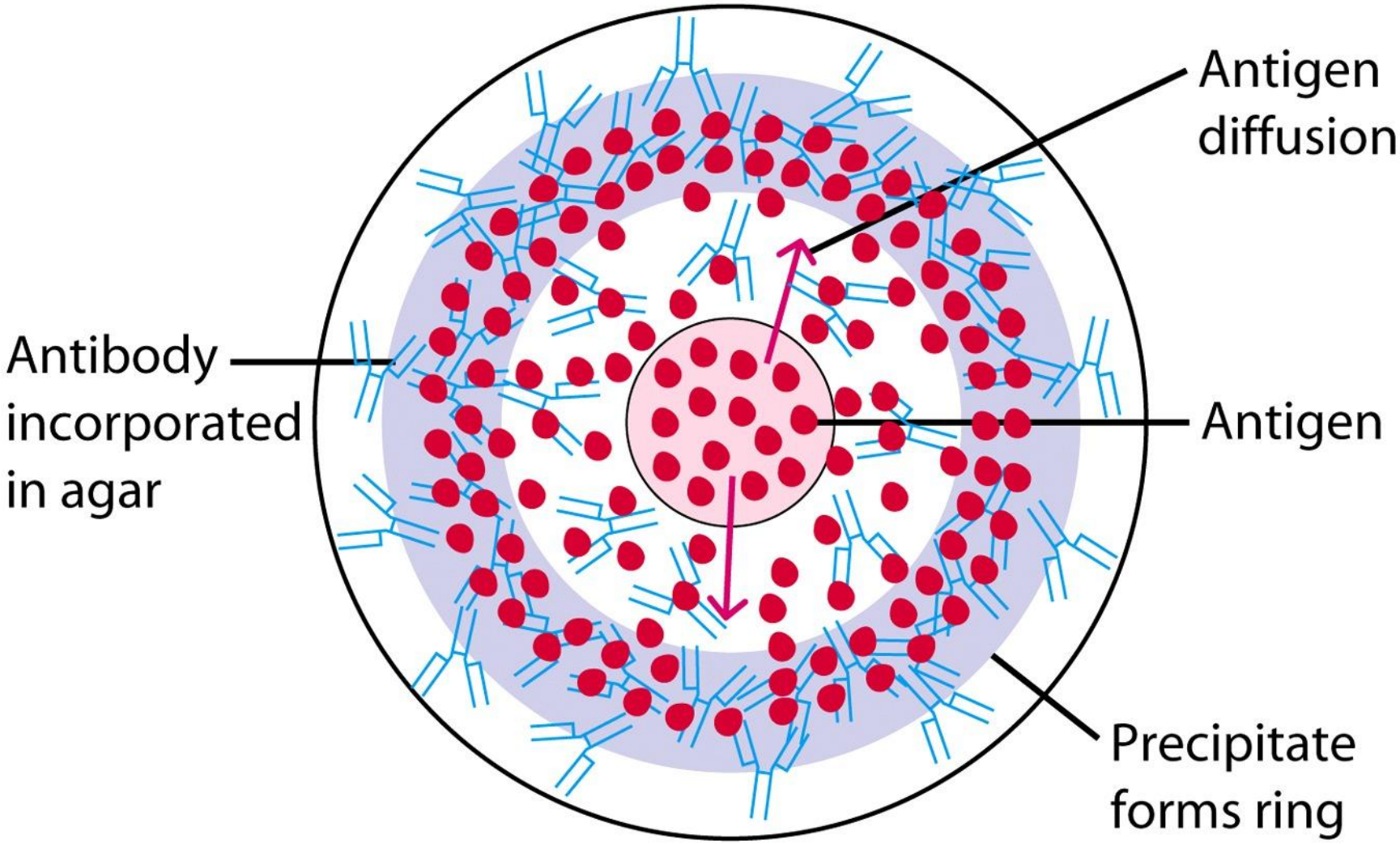

DOUBLE IMMUNODIFFUSION

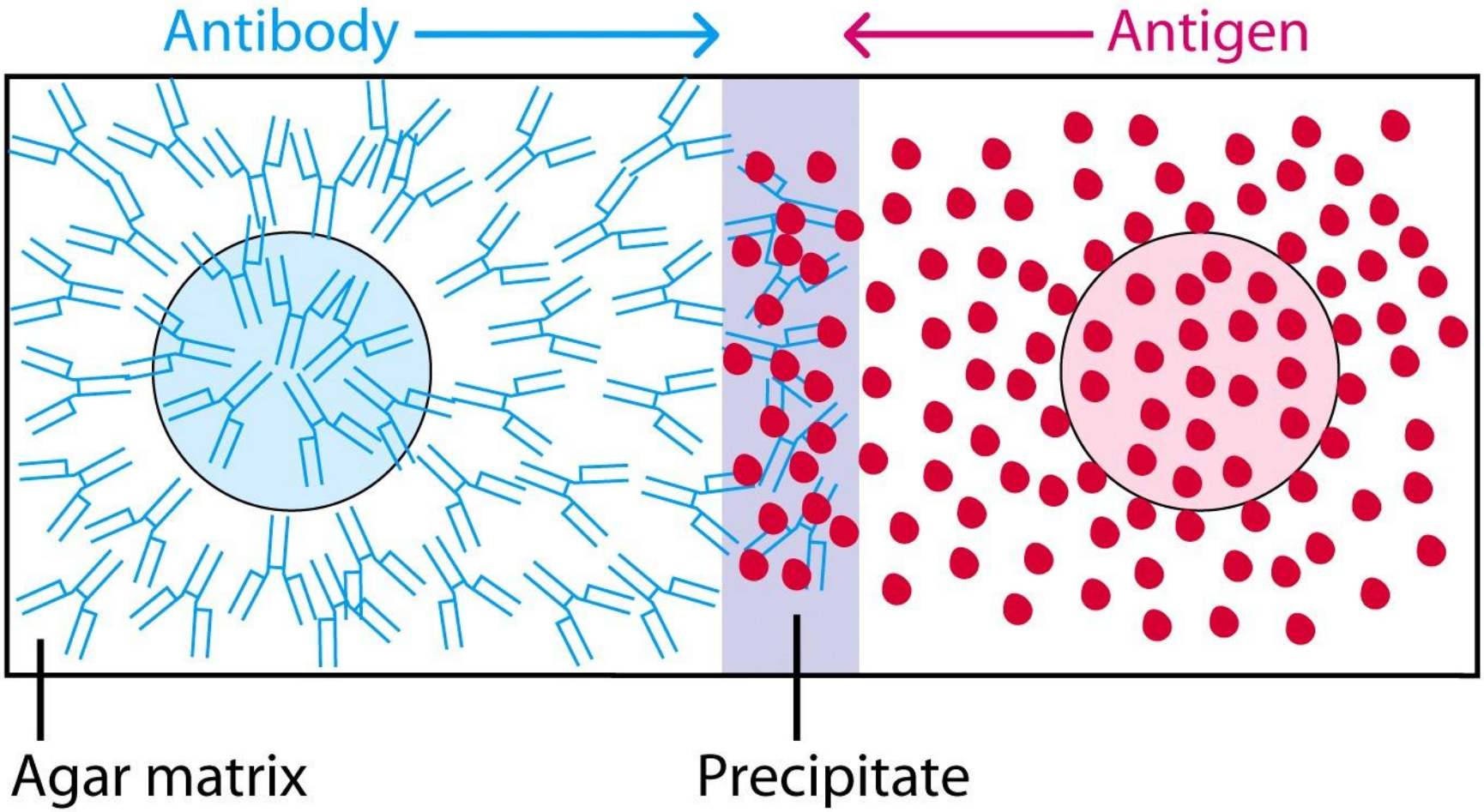

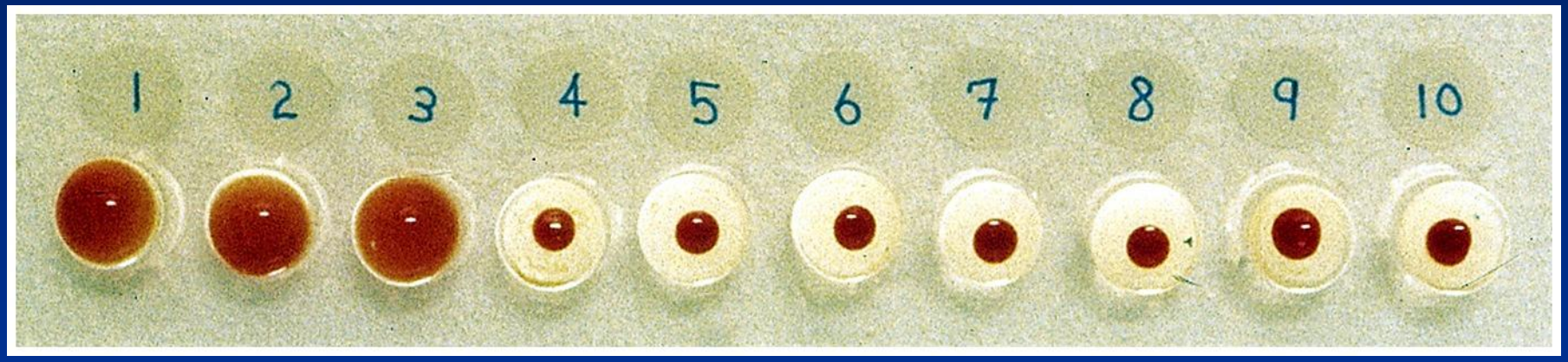
1
2
3
4
5
6
7
8
9
10

TABLE 6-2 ABO blood types

Blood type	Antigens on RBCs	Serum antibodies
A	A	Anti-B
B	B	Anti-A
AB	A and B	Neither
O	Neither	Anti-A and anti-B

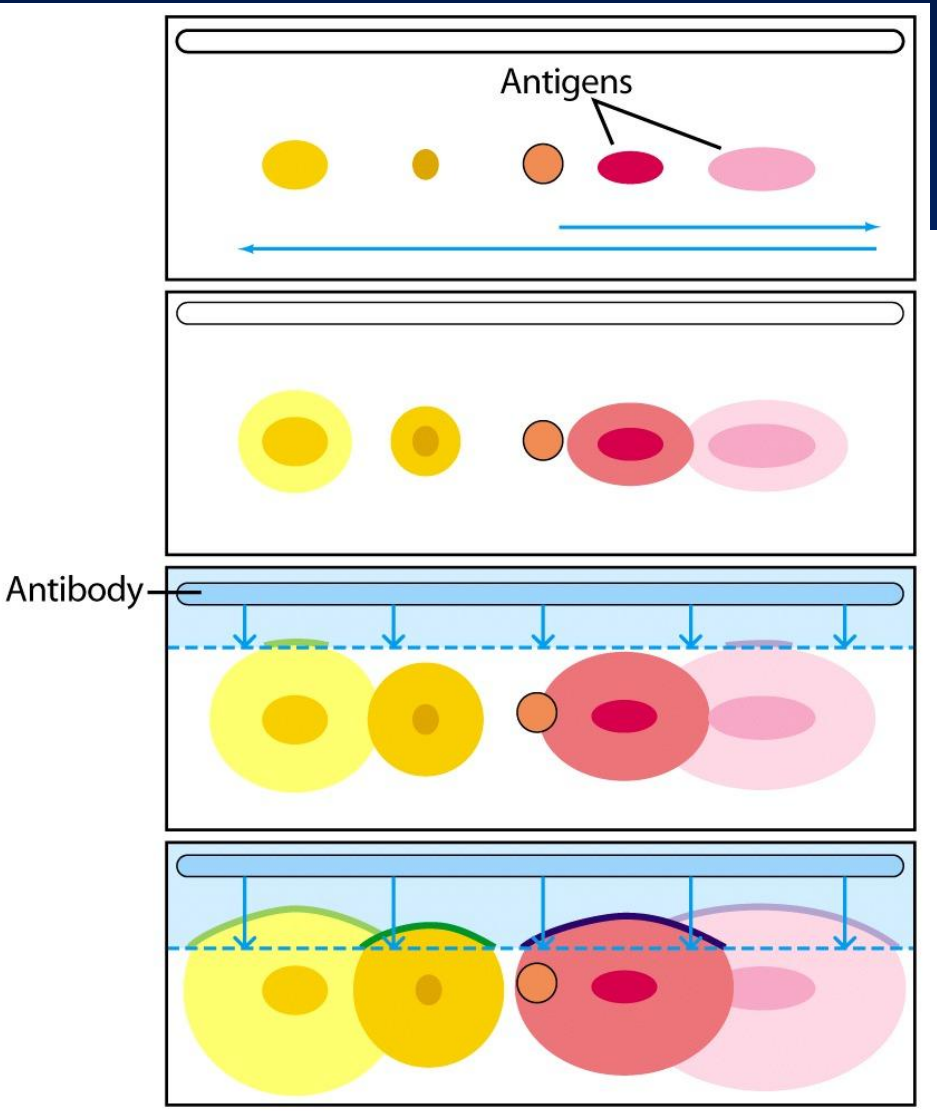
Antigens
Antibody

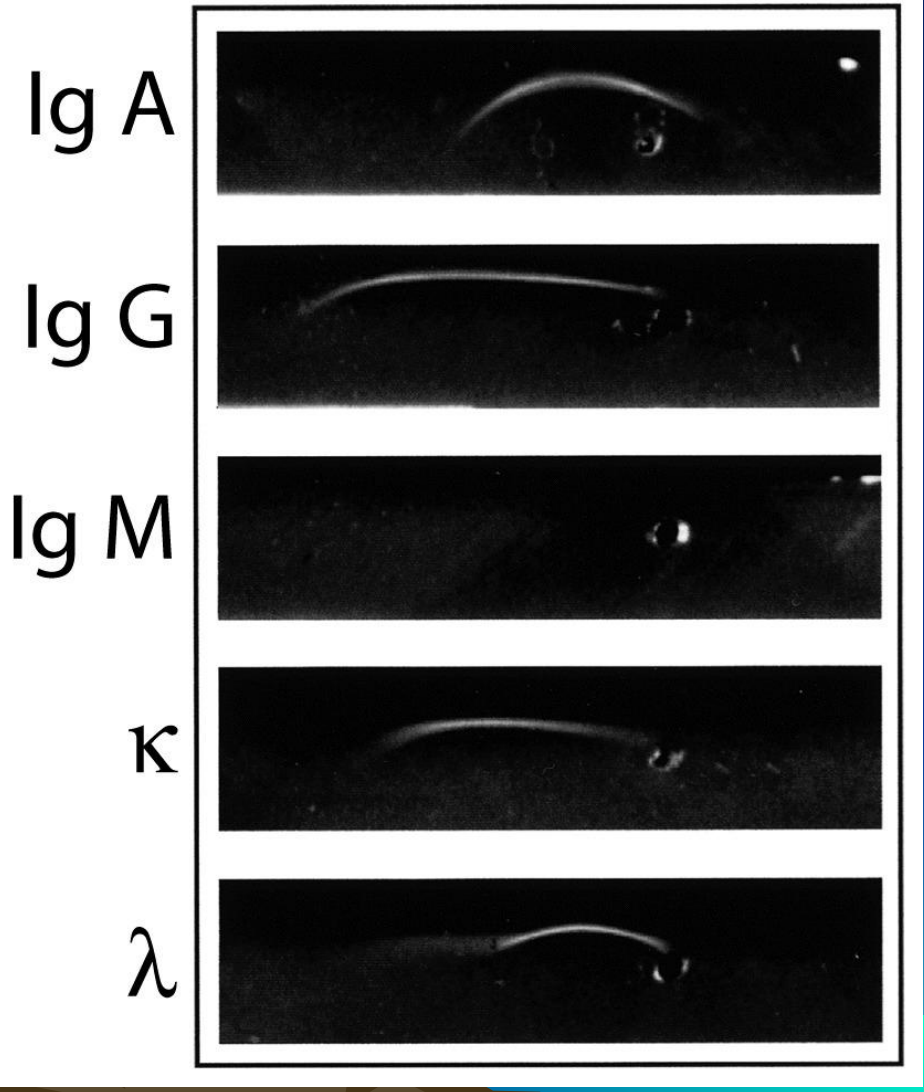
Ig A
Ig G
Ig M
κ
λ

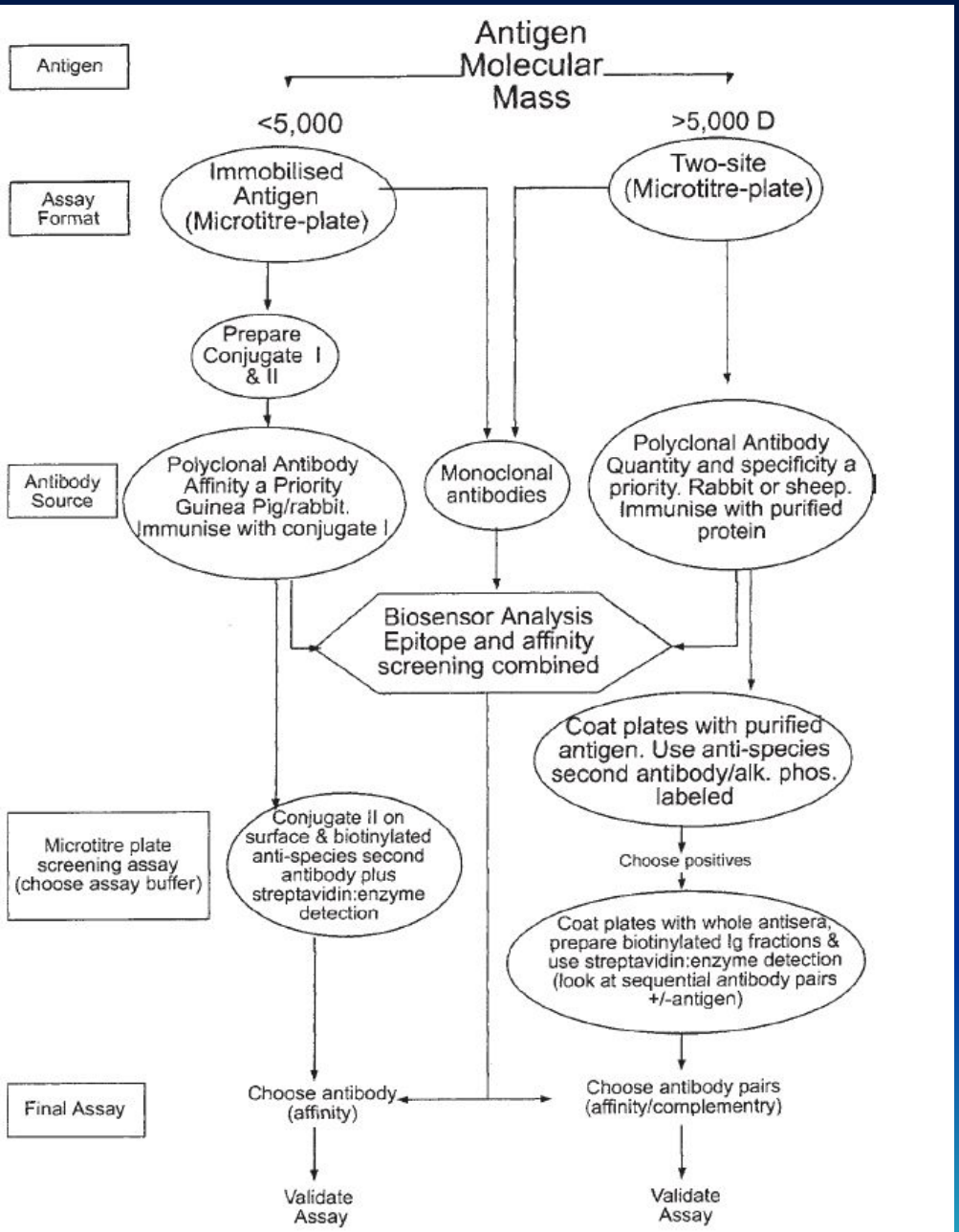

Fig. 1. Possible development pathways for immunoassays for a protein and hapten.

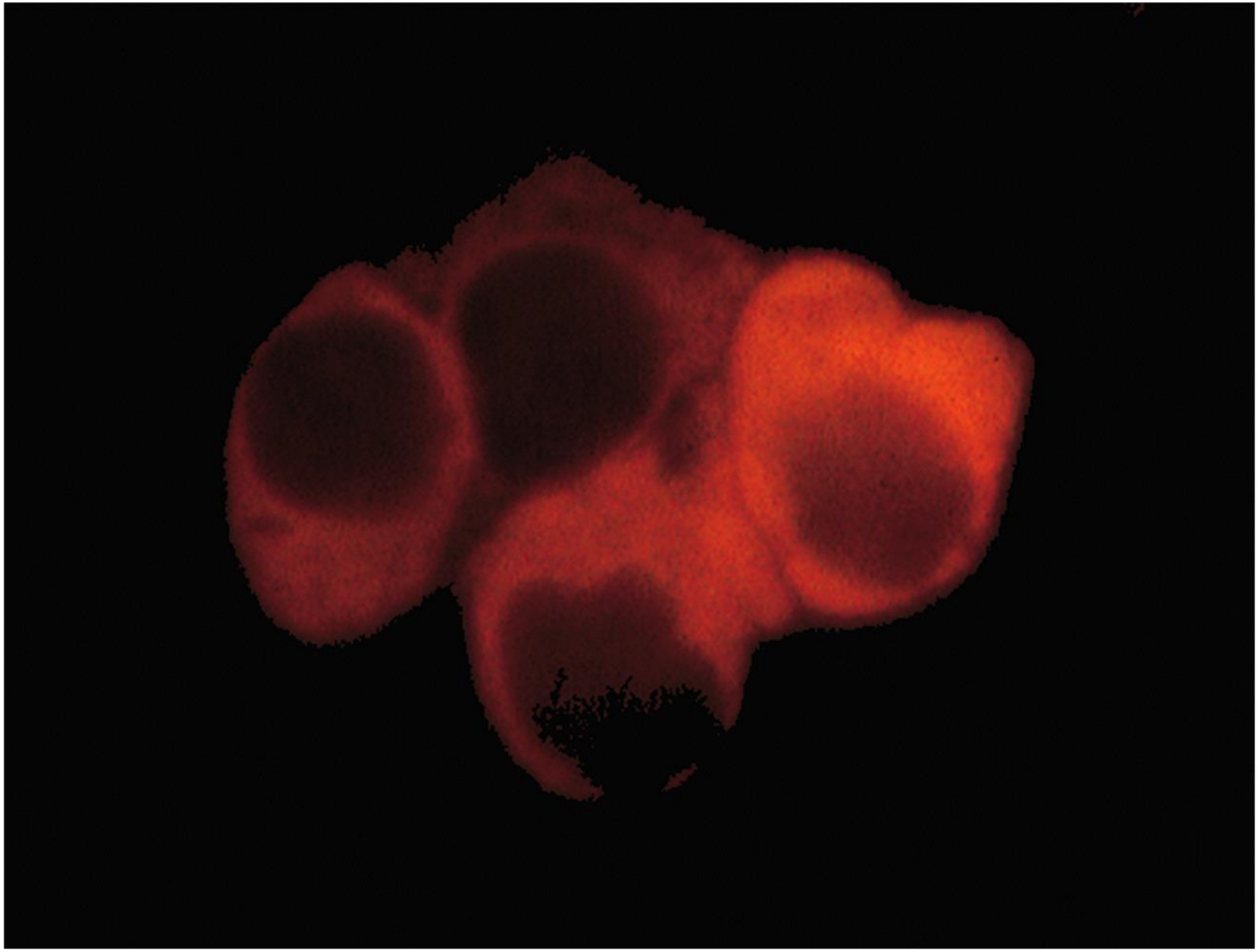

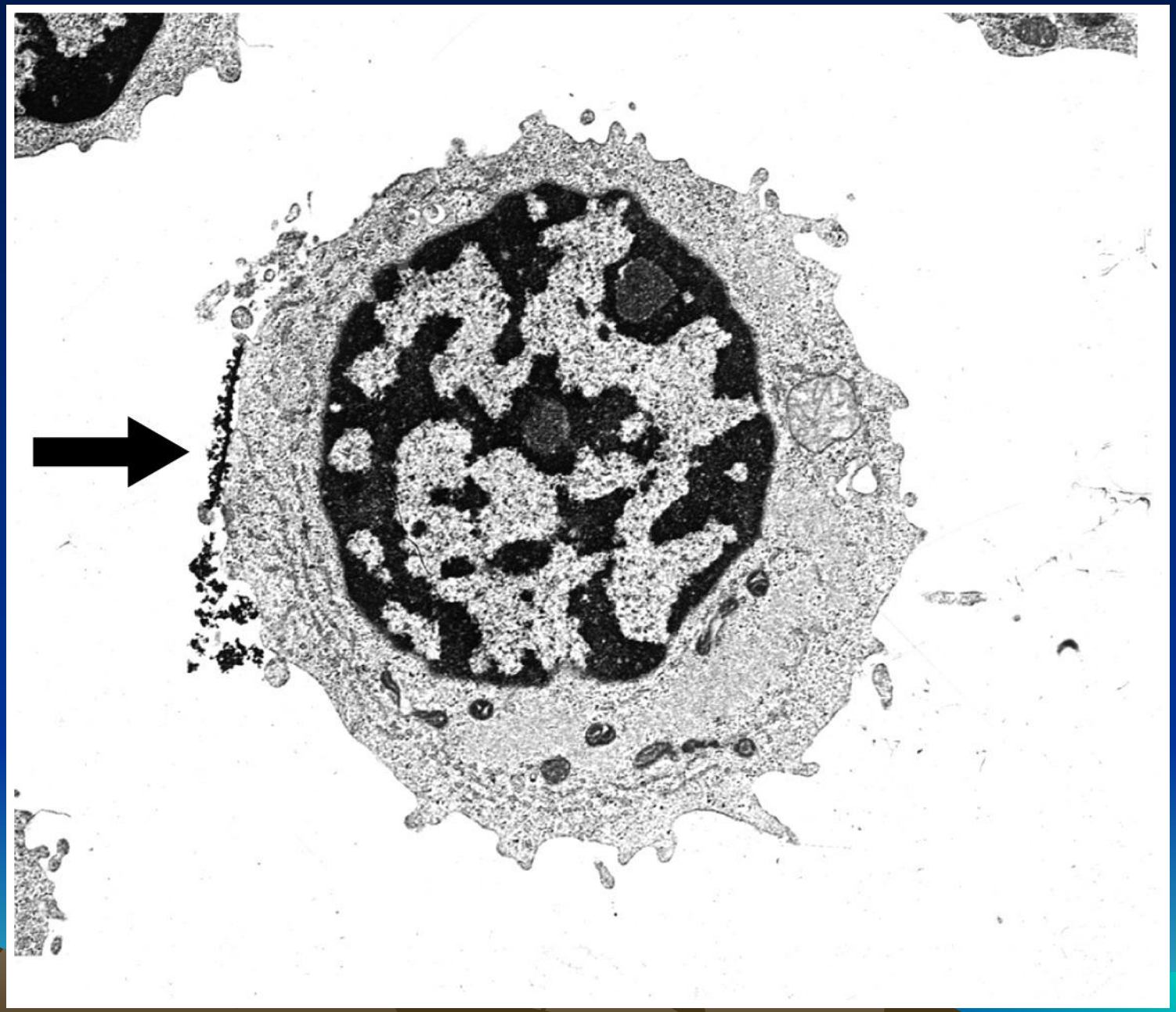

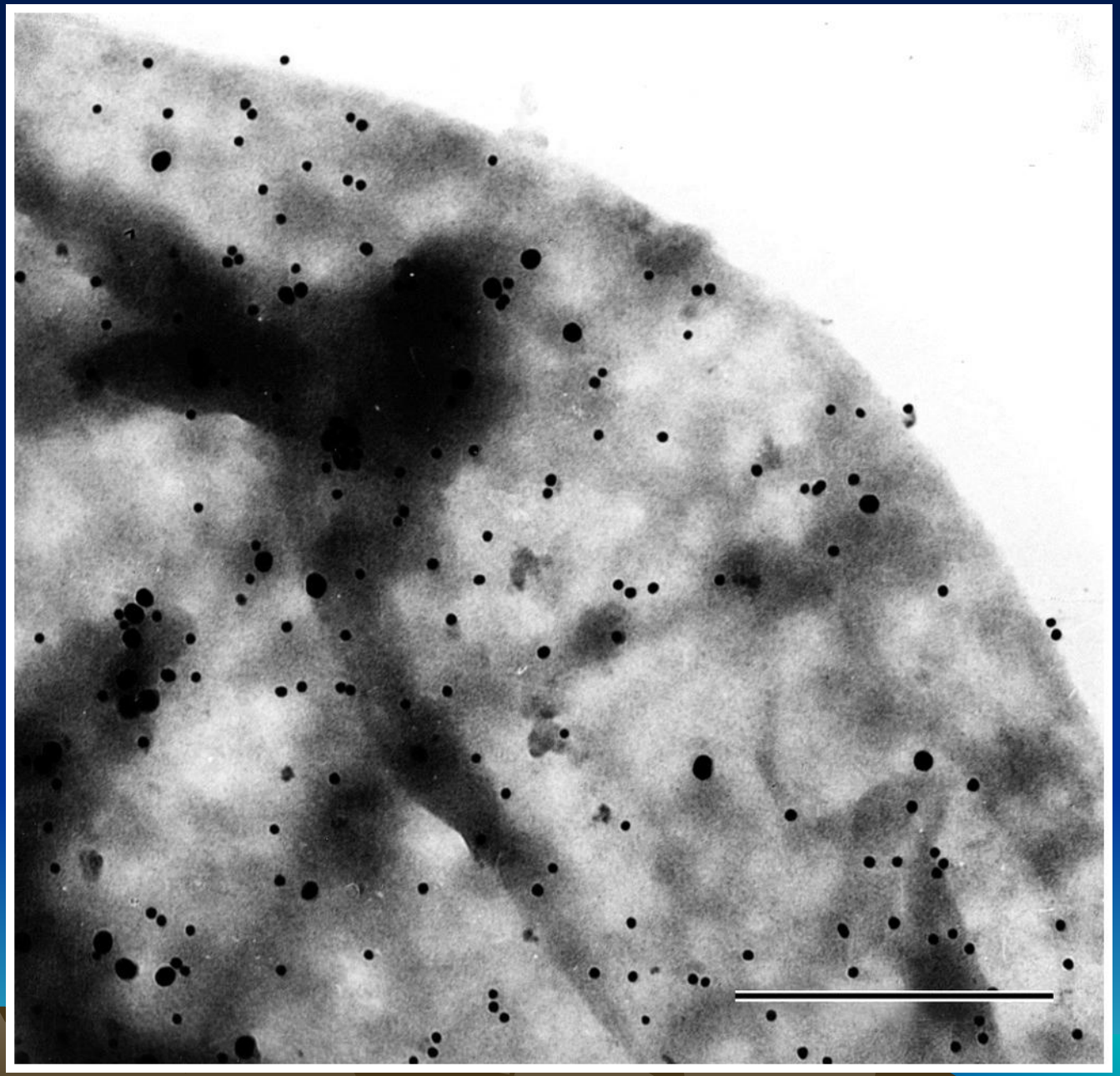

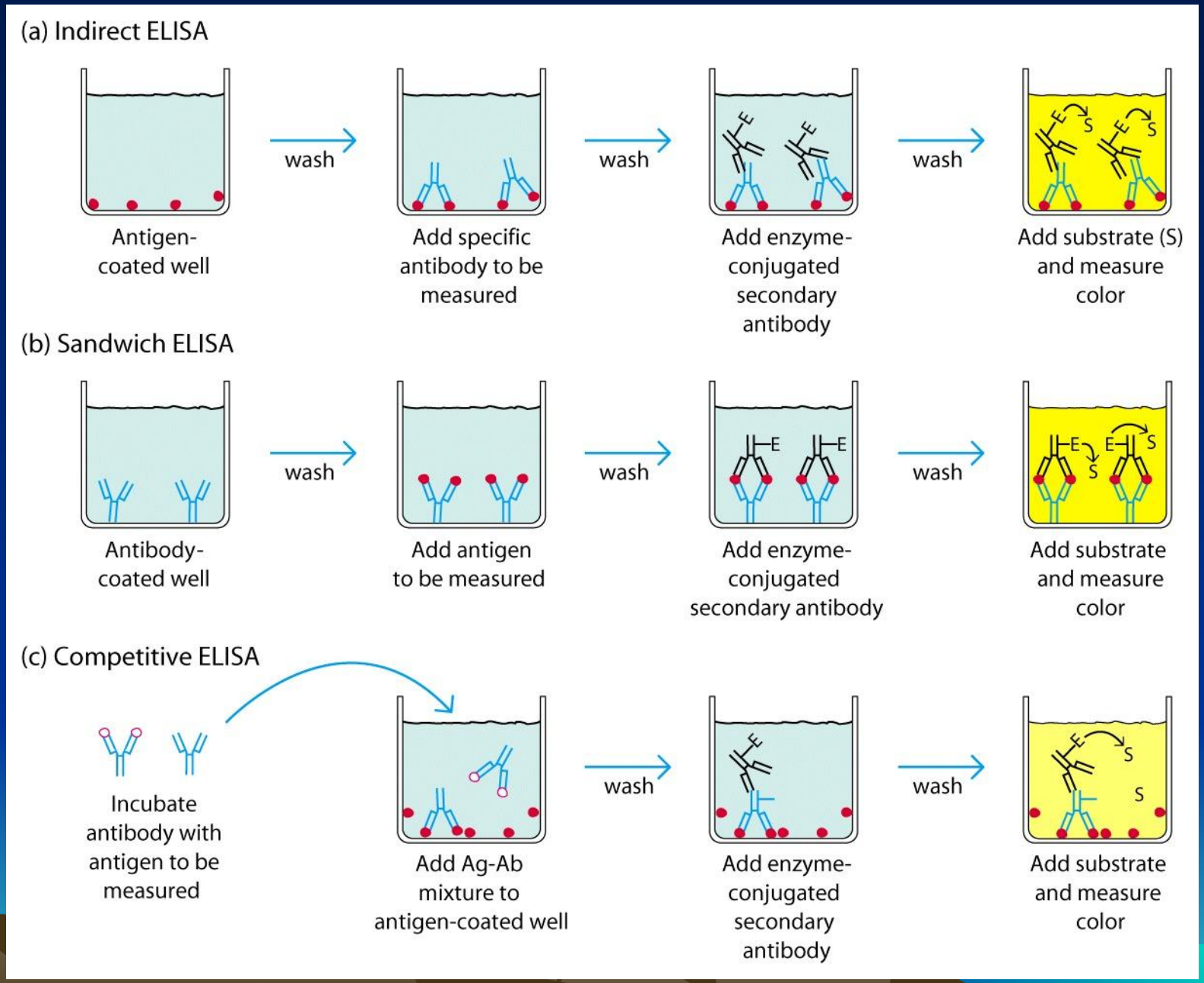
(a) Indirect ELISA
wash
wash
wash
Antigen-coated well
Add specific antibody to be measured
Add enzyme-conjugated secondary antibody
Add substrate (S) and measure color
(b) Sandwich ELISA
wash
wash
wash
Antibody-coated well
Add antigen to be measured
Add enzyme-conjugated secondary antibody
Add substrate and measure color
(c) Competitive ELISA
Incubate antibody with antigen to be measured
wash
wash
Add Ag-Ab mixture to antigen-coated well
Add enzyme-conjugated secondary antibody
Add substrate and measure color

KIT REAGENTS

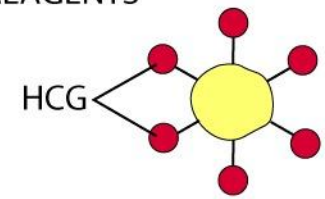

and

Hapten carrier–conjugate Anti–HCG antibody

TEST PROCEDURE

Urine + Anti–HCG —Incubate→ + HCG carrier conjugate → Observe for visible clumping

POSSIBLE REACTIONS

⊖ reaction: not pregnant

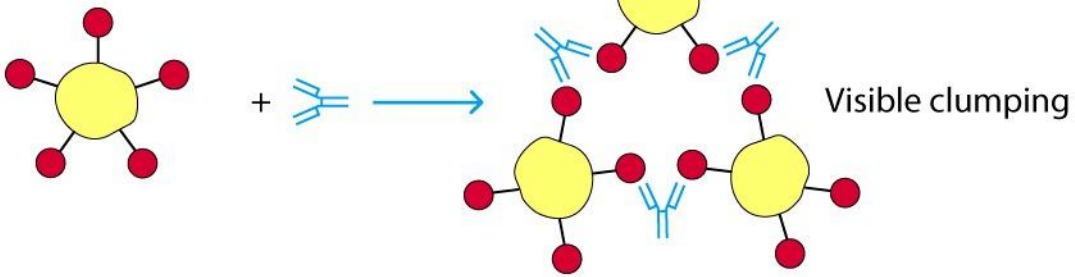

⊕ reaction: pregnant

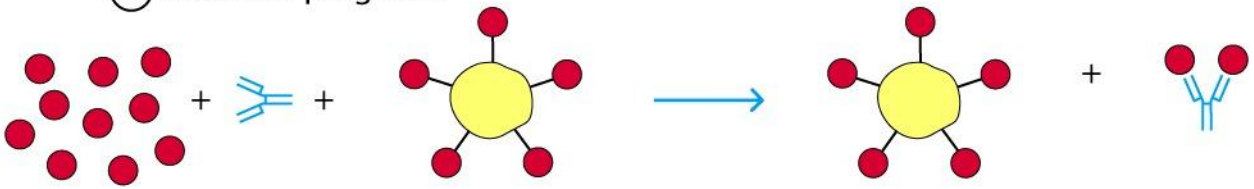

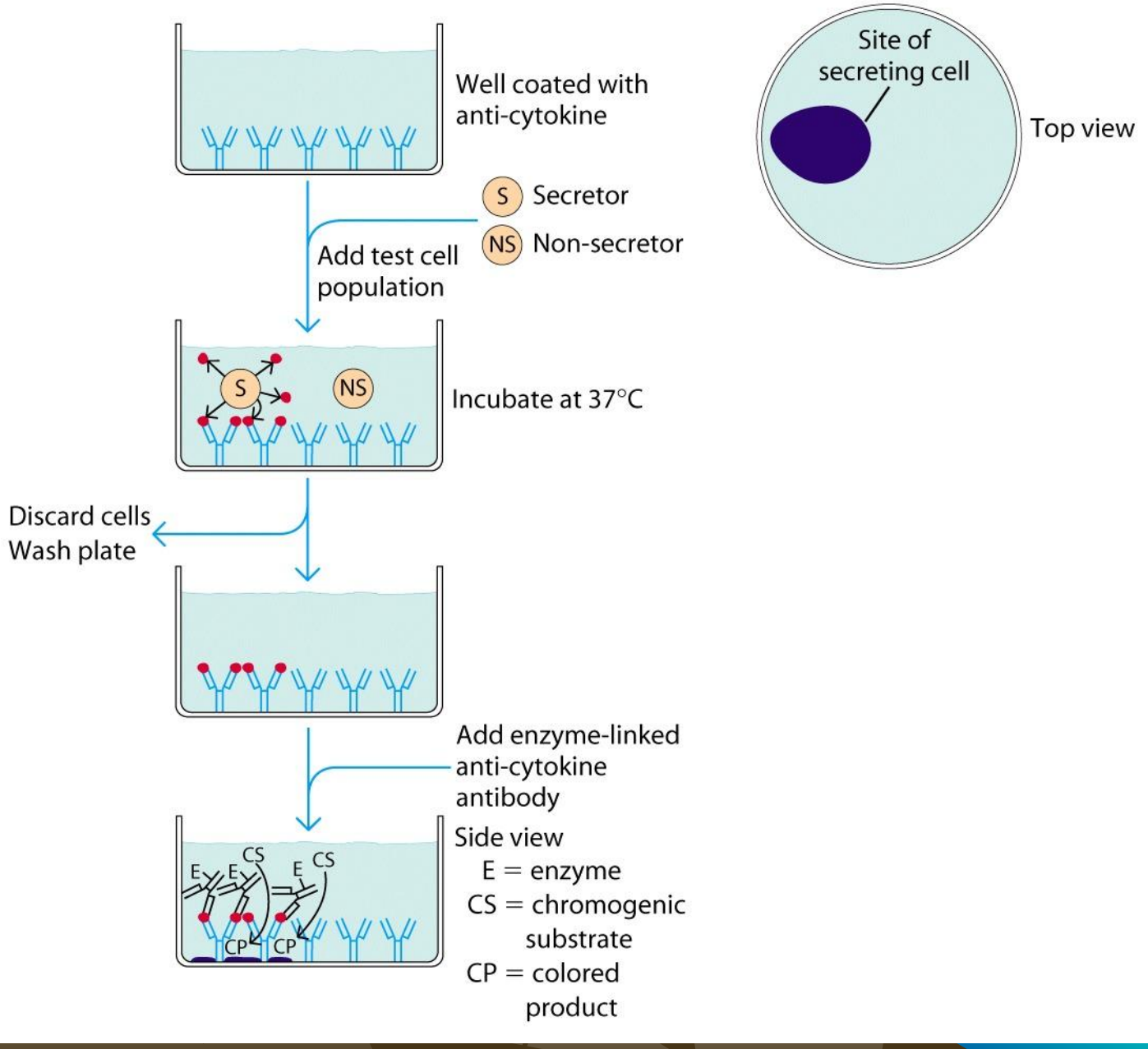
Well coated with anti-cytokine
S Secretor
NS Non-secretor
Add test cell population
S
NS
Incubate at 37°C
Discard cells
Wash plate
Add enzyme-linked anti-cytokine antibody
E
E
CS
E
CS
CP
CP
Side view
E = enzyme
CS = chromogenic substrate
CP = colored product
Site of secreting cell
Top view

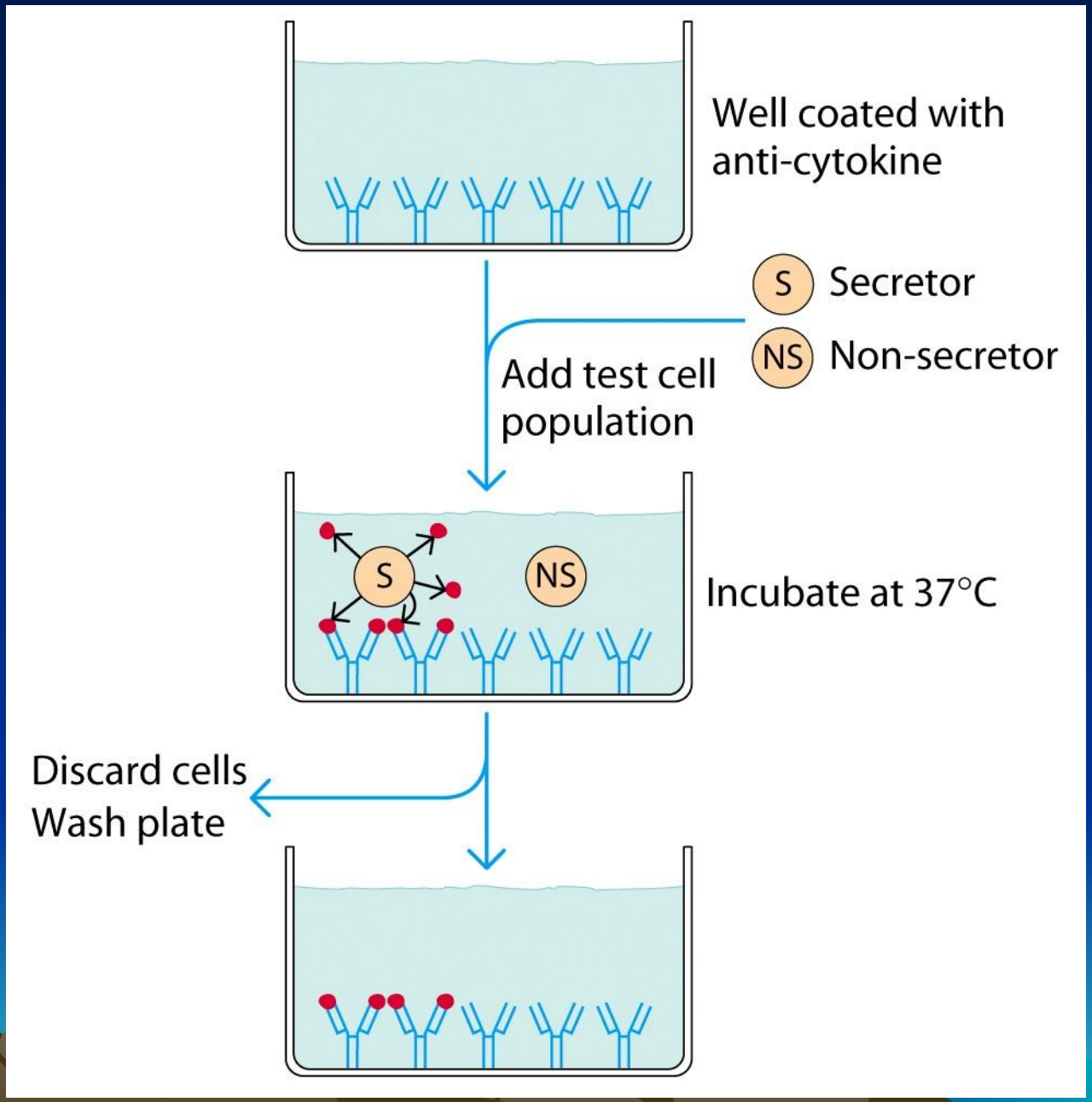
Well coated with anti-cytokine
S
Secretor
NS
Non-secretor
Add test cell population
S
NS
Incubate at 37°C
Discard cells
Wash plate

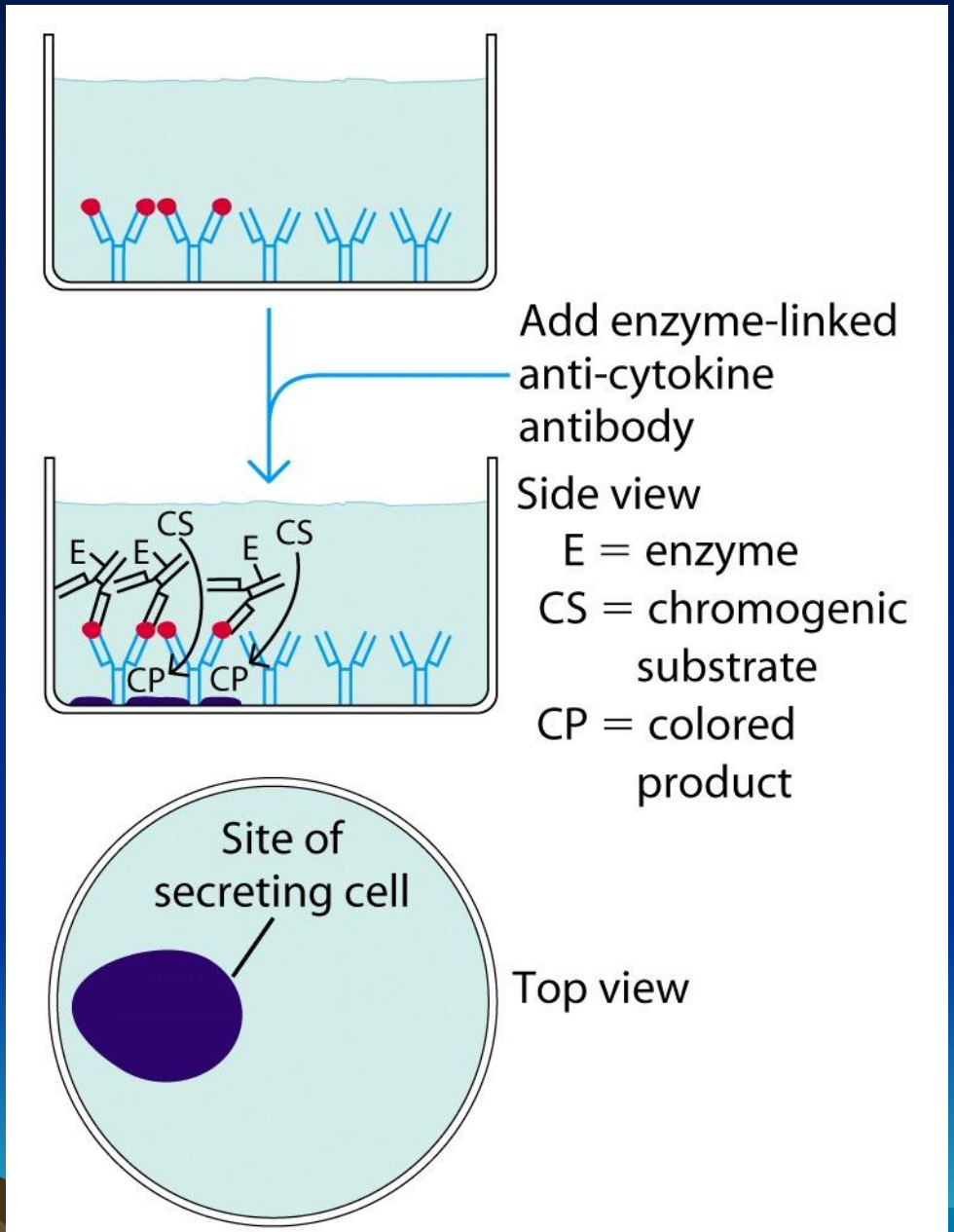
Add enzyme-linked anti-cytokine antibody
Side view
E = enzyme
CS = chromogenic substrate
CP = colored product
E
E
CS
E
CS
CP
CP
Site of secreting cell
Top view

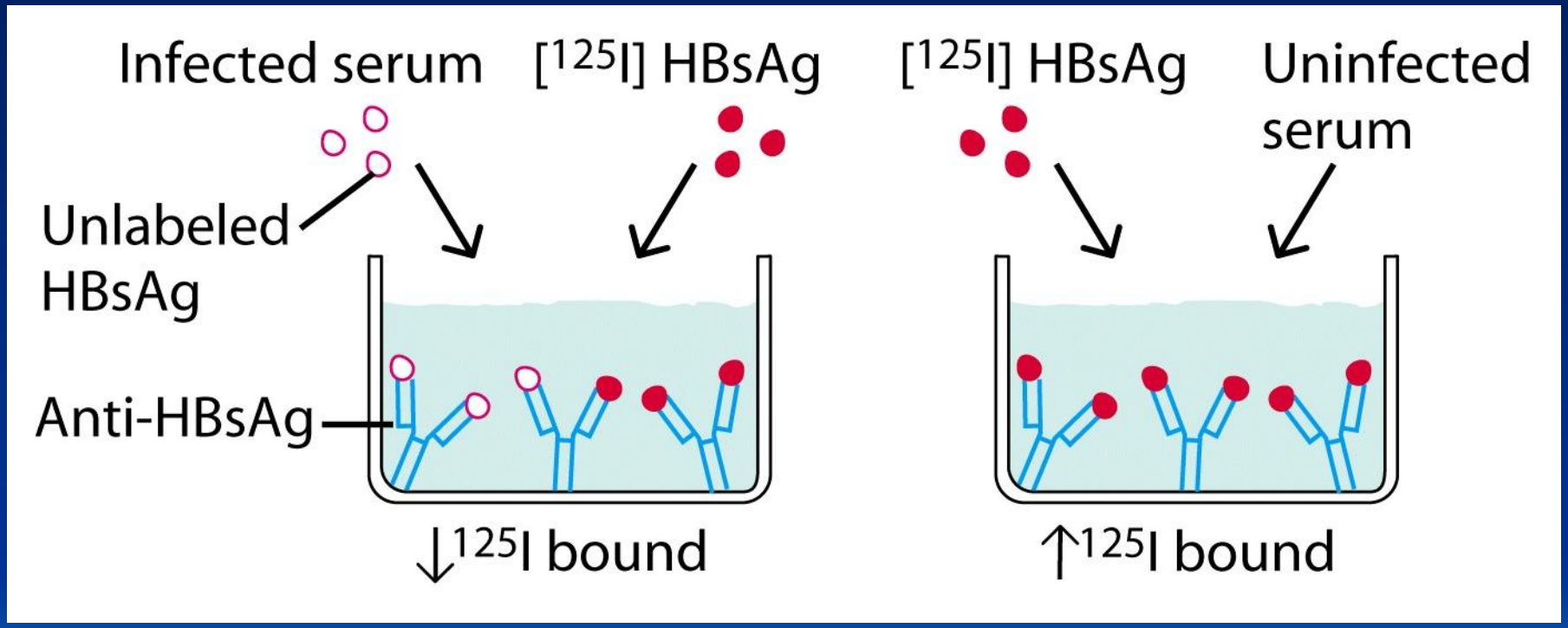
Infected serum
[125I] HBsAg
[125I] HBsAg
Uninfected serum
Unlabeled HBsAg
Anti-HBsAg
↓125I bound
↑125I bound

Control: No antibody present
(ligand equilibrates on both sides equally)

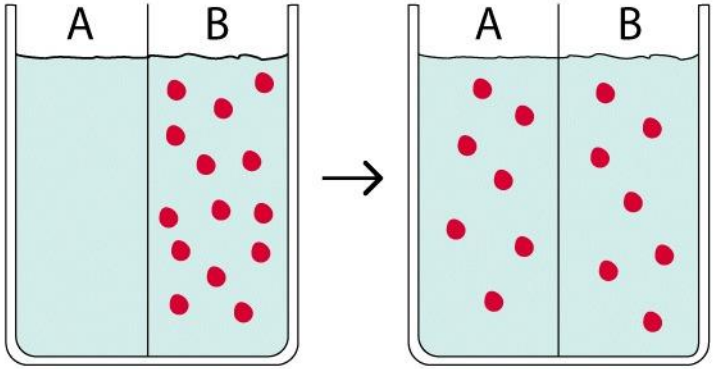

Experimental: Antibody in A
(at equilibrium more ligand in A due to Ab binding)

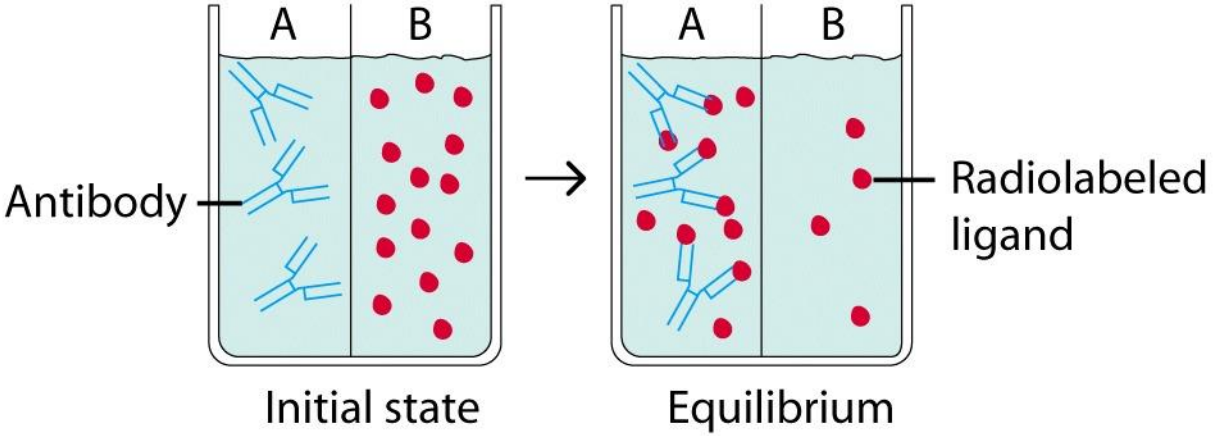

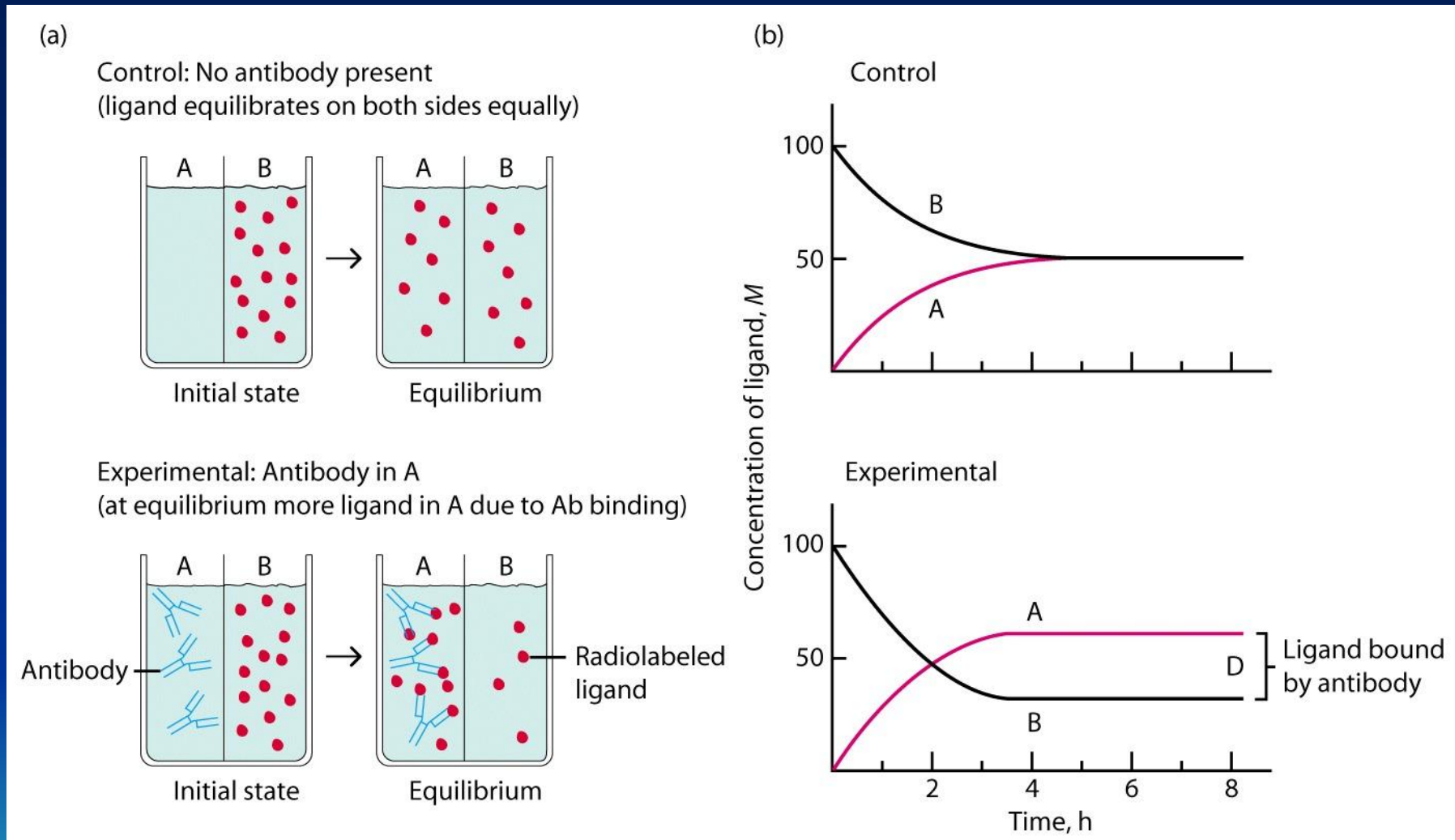
(a)
Control: No antibody present
(ligand equilibrates on both sides equally)
A
B
A
B
Initial state
Equilibrium
Experimental: Antibody in A
(at equilibrium more ligand in A due to Ab binding)
A
B
A
B
Antibody
Radiolabeled ligand
Initial state
Equilibrium
(b)
Control
100
50
B
A
Concentration of ligand, M
Experimental
100
50
A
D
B
Ligand bound by antibody
2
4
6
8
Time, h

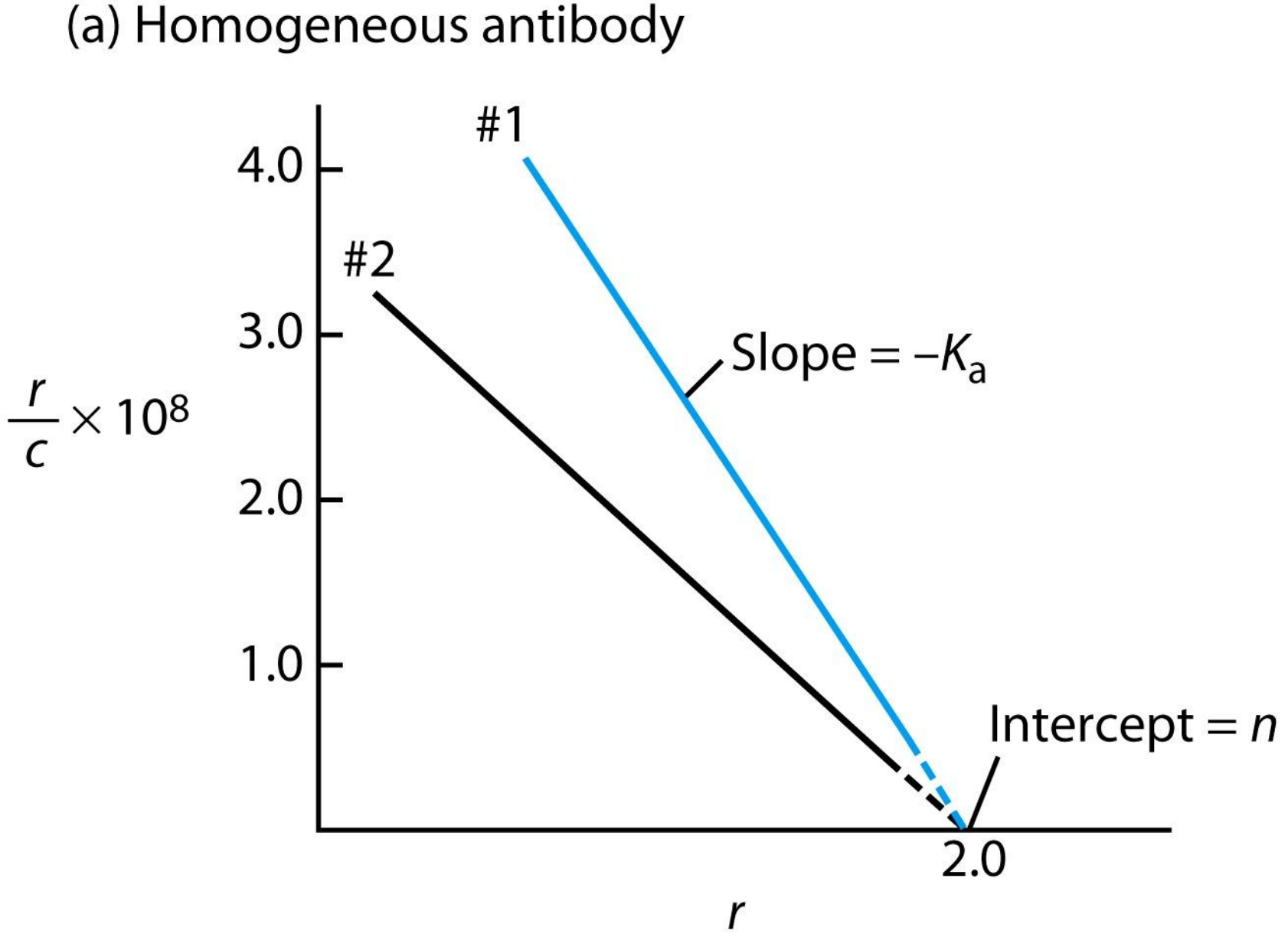
(a) Homogeneous antibody
#1
#2
4.0
3.0
2.0
1.0
$\frac{r}{c} \times 10^8$
Slope = $-K_a$
Intercept = n
2.0
r

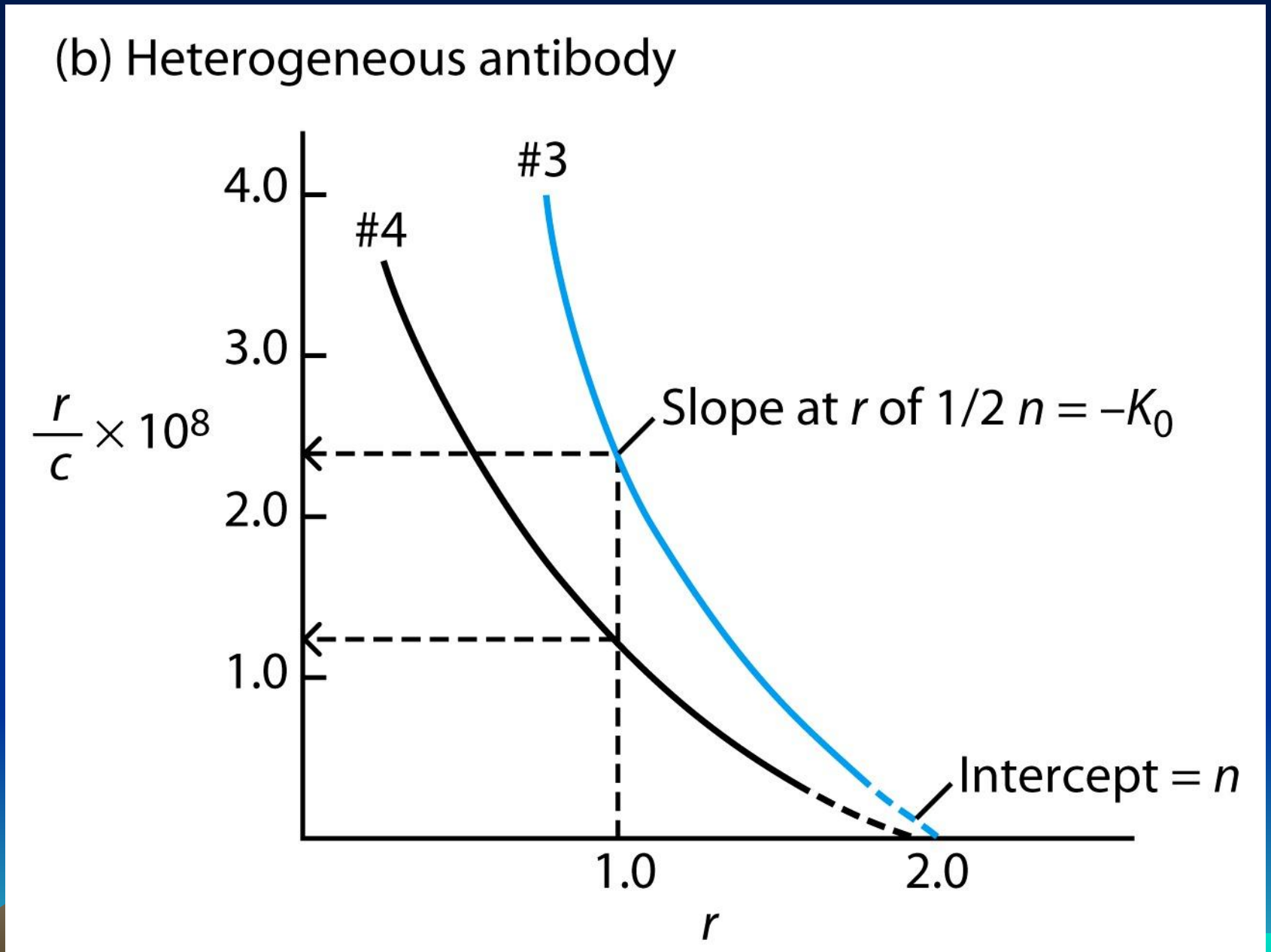
(b) Heterogeneous antibody
#3
#4
4.0
3.0
2.0
1.0
$\frac{r}{c} \times 10^8$
Slope at r of 1/2 $n = -K_0$
Intercept = n
1.0
2.0
r

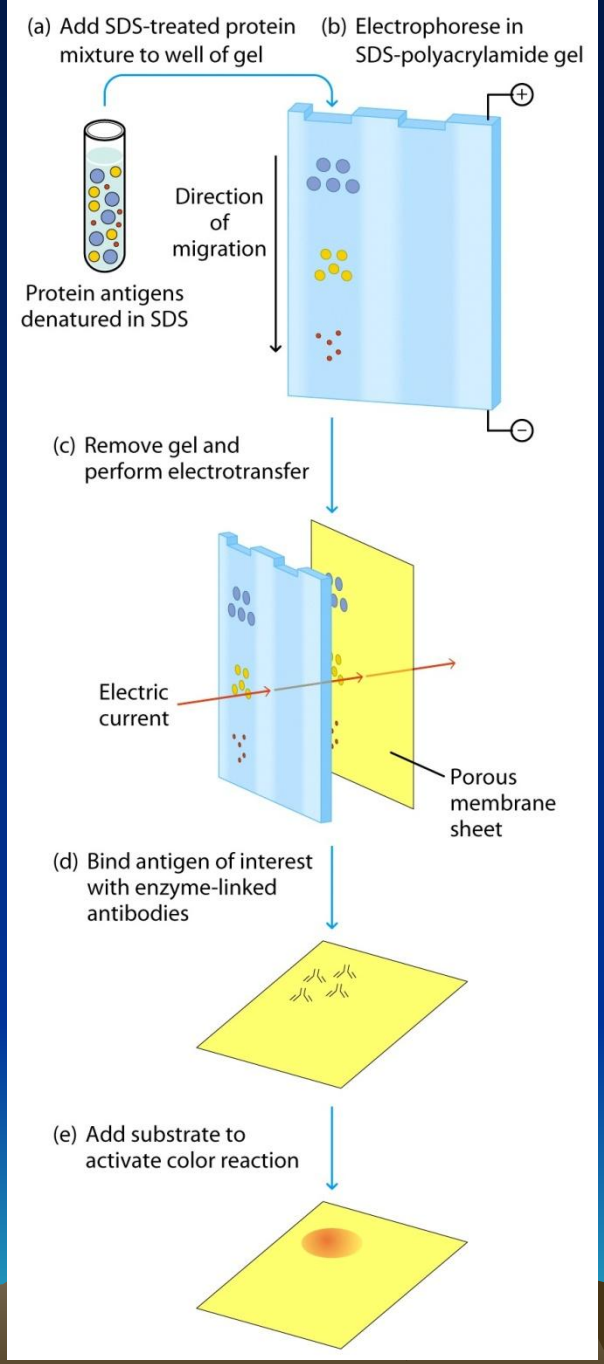
(a) Add SDS-treated protein mixture to well of gel
(b) Electrophorese in SDS-polyacrylamide gel
Direction of migration
Protein antigens denatured in SDS
(c) Remove gel and perform electrotransfer
Electric current
Porous membrane sheet
(d) Bind antigen of interest with enzyme-linked antibodies
(e) Add substrate to activate color reaction

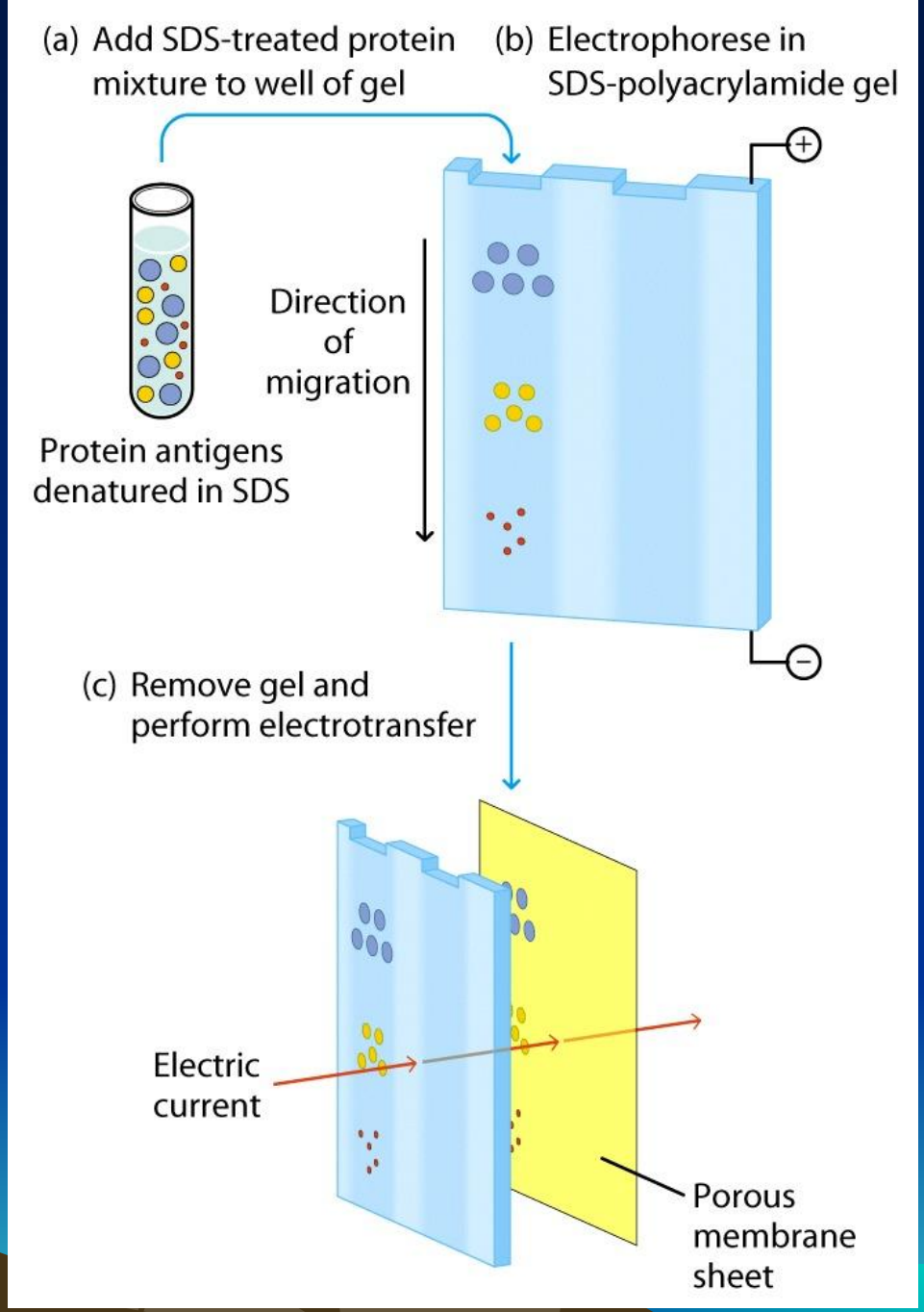
(a) Add SDS-treated protein mixture to well of gel
(b) Electrophorese in SDS-polyacrylamide gel
Direction of migration
Protein antigens denatured in SDS
(c) Remove gel and perform electrotransfer
Electric current
Porous membrane sheet

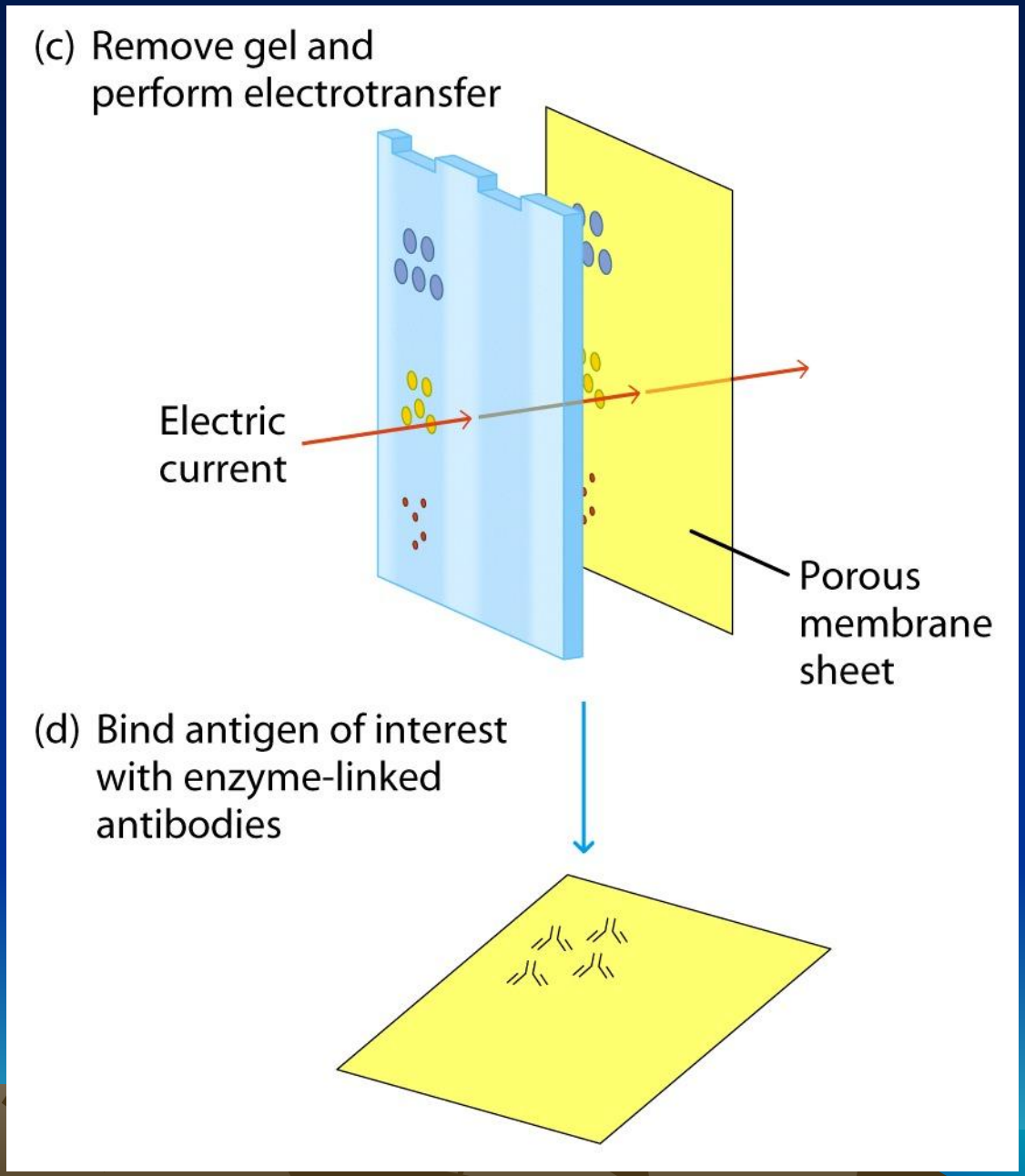
(c) Remove gel and perform electrotransfer
Electric current
Porous membrane sheet
(d) Bind antigen of interest with enzyme-linked antibodies

(d) Bind antigen of interest with enzyme-linked antibodies

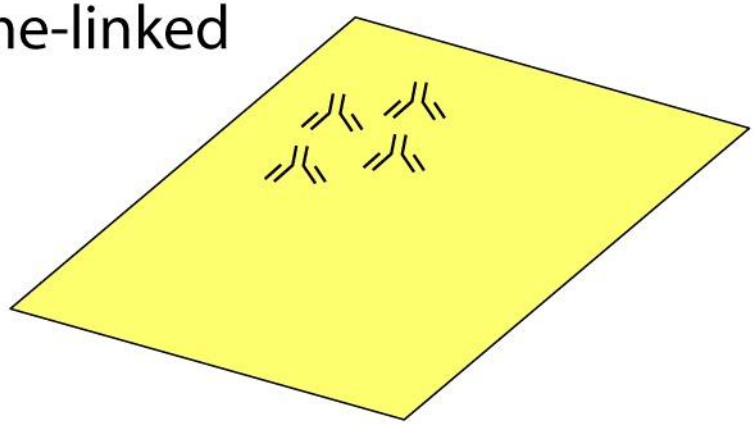

(e) Add substrate to activate color reaction

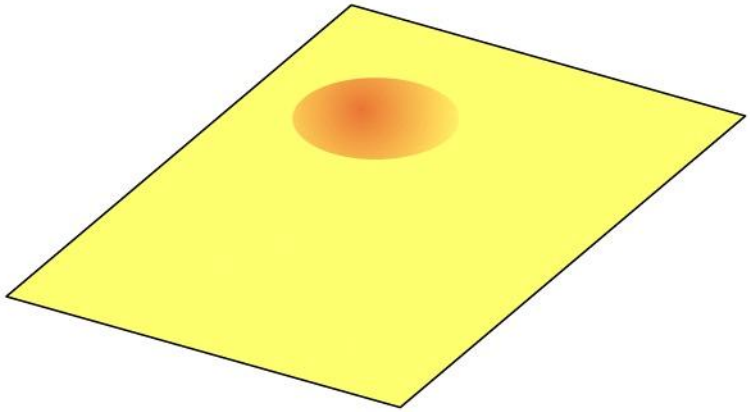

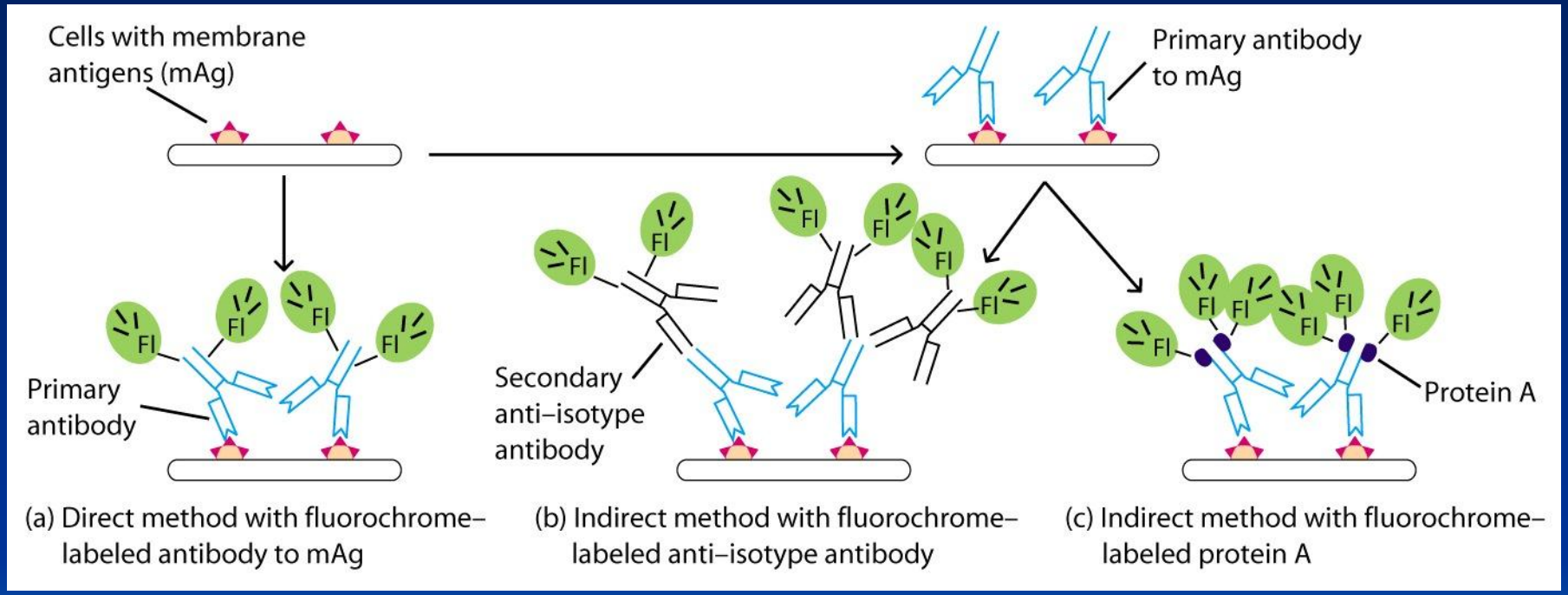
Cells with membrane antigens (mAg)
Primary antibody to mAg
Fl
Primary antibody
Secondary anti–isotype antibody
Protein A
(a) Direct method with fluorochrome–labeled antibody to mAg
(b) Indirect method with fluorochrome–labeled anti–isotype antibody
(c) Indirect method with fluorochrome–labeled protein A

Перенос антигенов в буферном растворе

Влажный или полусухой перенос антигенов на мембрану

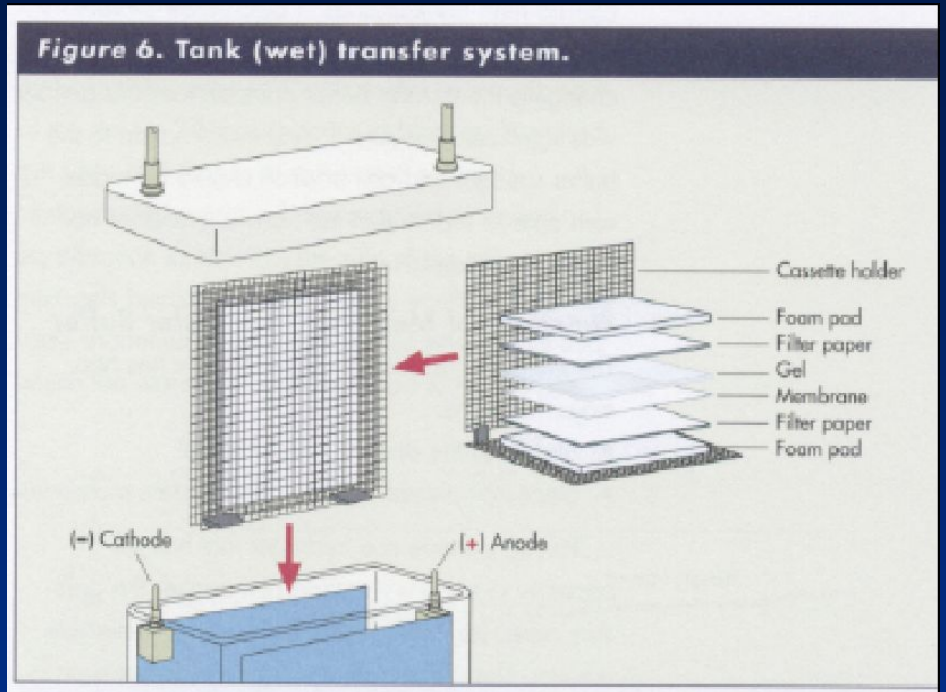

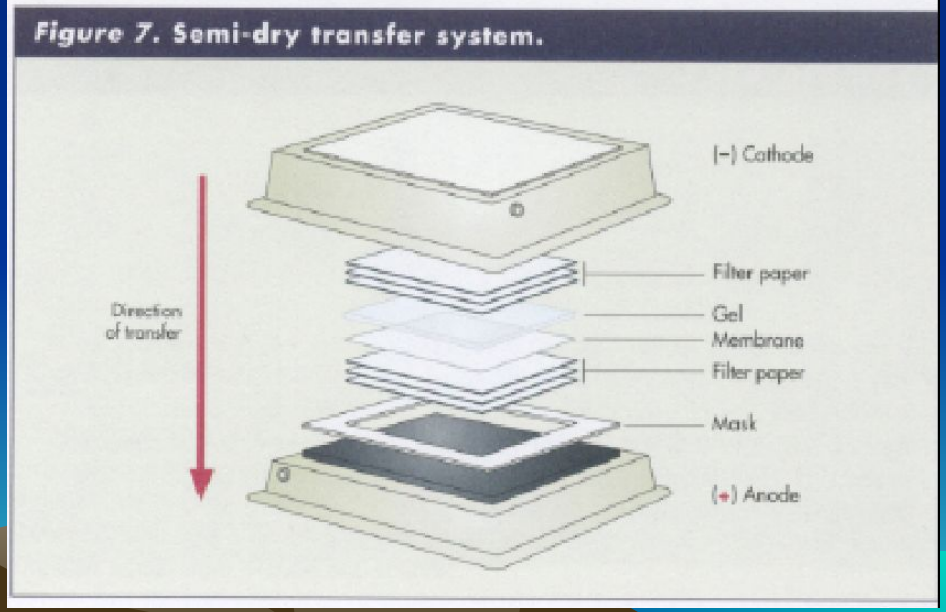

How it Works

- Traditional western blotting takes a variety of formats and reagent conditions to accomplish. It's a passive process!
- SNAP i.d. actively drives reagents through the membrane to increase the quality of the blots and increase the speed of immunodetection!
- **It's a combination of reagent flows and concentrations**

Standard 'rocking' of reagents

Vs.

Actively drive reagents with vacuum flow

How it Works – reagent flows

Reagents penetrate more of the membrane 3D structure where the proteins are blotted.

Result = Increase quality of the blot in a SNAP!

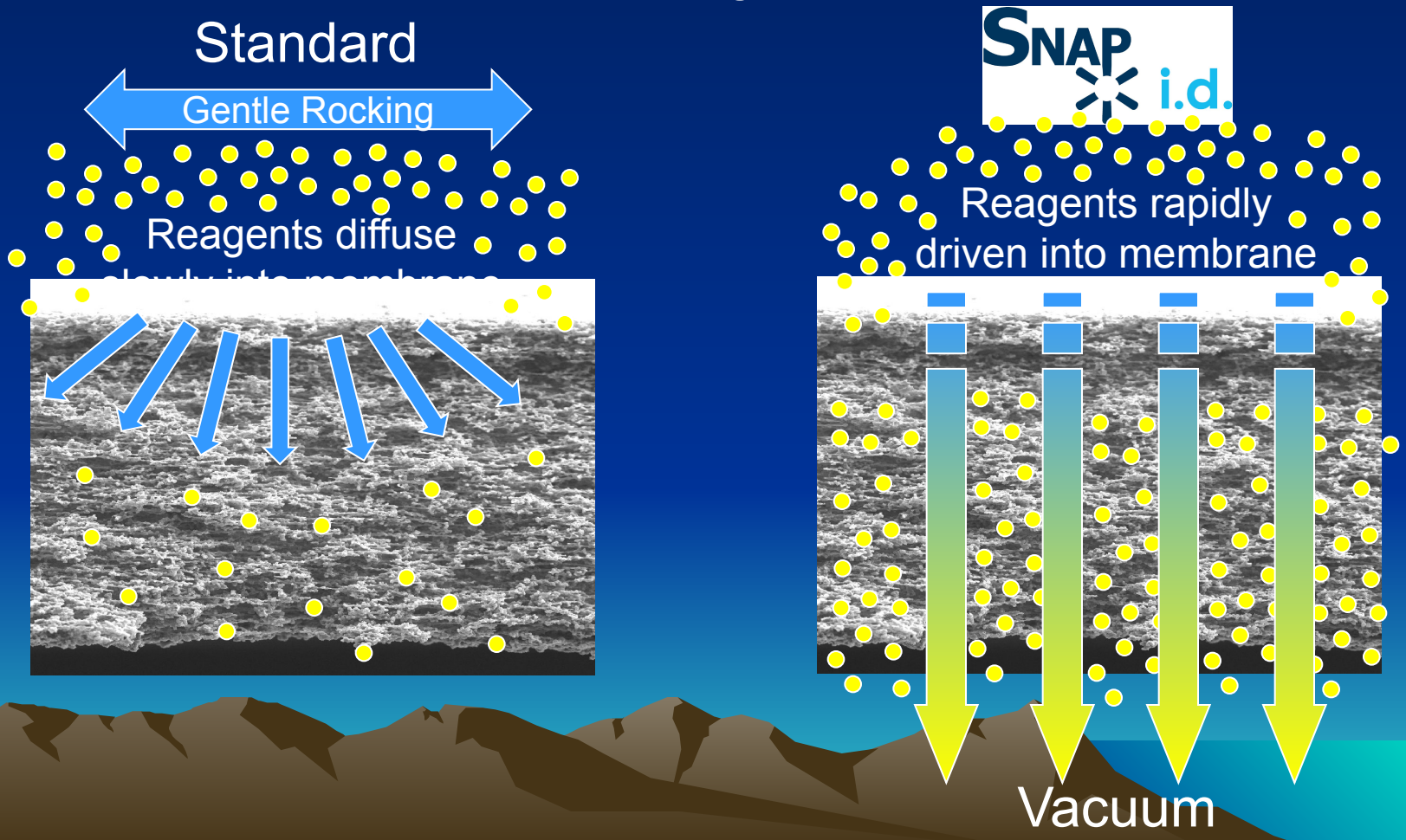

Standard vs. SNAP i.d. - concentrations

Concentrations

- Blocking concentrations are limited to prevent clogging of blot holder
- Antibody concentrations are increased to speed up reaction kinetics

Step	Standard Protocol	SNAP i.d.
Blocking	5% NFDM	**0.5%** NFDM
Primary Antibody	1X	**3X** in 1/3 volume (same quantity)
Washing (3x)	1X	1X
Secondary Antibody	1X	**3X** in 1/3 volume (same quantity)
Washing (3x)	1X	1X

Compatible Blocking Reagents and Recommended Concentrations

Blocker	Compatible	Recommended Concentration
Non-fat/low fat dry milk	yes, ≤ 0.5%	0.5%
Casein, N-Z-Amine AS (Sigma)	yes, ≤ 5%	1%
Bovine Serum Albumin (BSA)	yes, ≤ 5%	1%
PVP-40 (Polyvinylpyrrolidone)	yes, ≤ 1%	1%
Immunoblot Blocking Reagent (Millipore cat. no. 20-200)	yes, ≤ 0.5%	0.5%
BLOT-QuickBlocker™ Reagent (Millipore cat. no. B2080)	yes, ≤ 0.5%	0.5%, pre-filter
ChemiBLOCKER™ Reagent (Millipore cat. no. 2170)	yes	≤ 50%
SEA BLOCK Blocking Buffer (Pierce)	yes	undiluted
SuperBlock® Blocking Buffer (Pierce)	yes	undiluted
Gelatin	not compatible	N/A

From page 8 of the SNAP i.d. User Guide

How it Works – reagent flows

Blocking

- Efficient coverage of membrane which yields higher sensitivity
  - Can use 1/10th-1/100th less concentrated blocking solution to minimize overblocking
- Actively driven vacuum flow coats inner surfaces of membrane in 20 sec

Standard

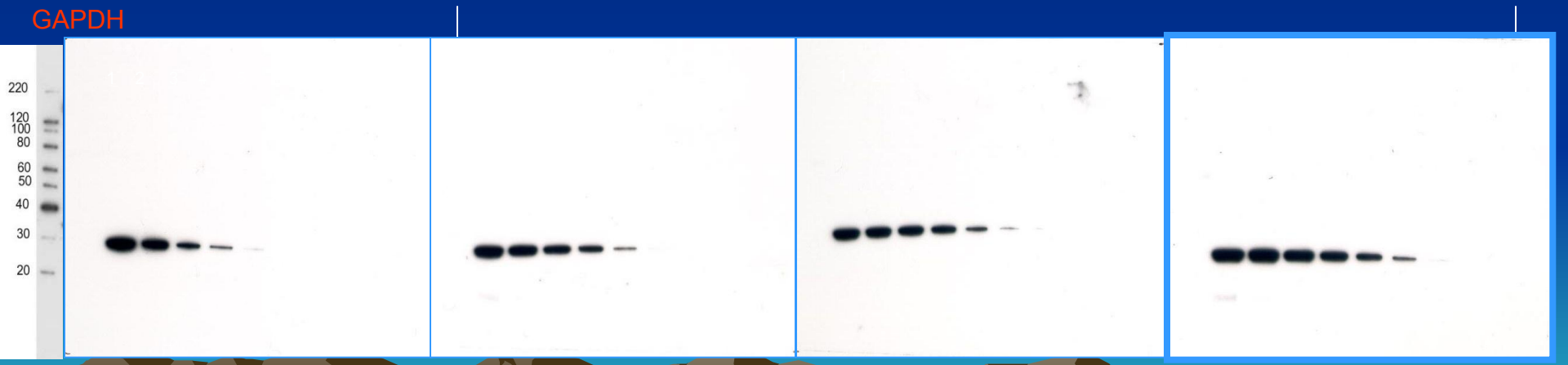

How it Works: Time savings

Western Blotting Protocol

SNAP i.d.™

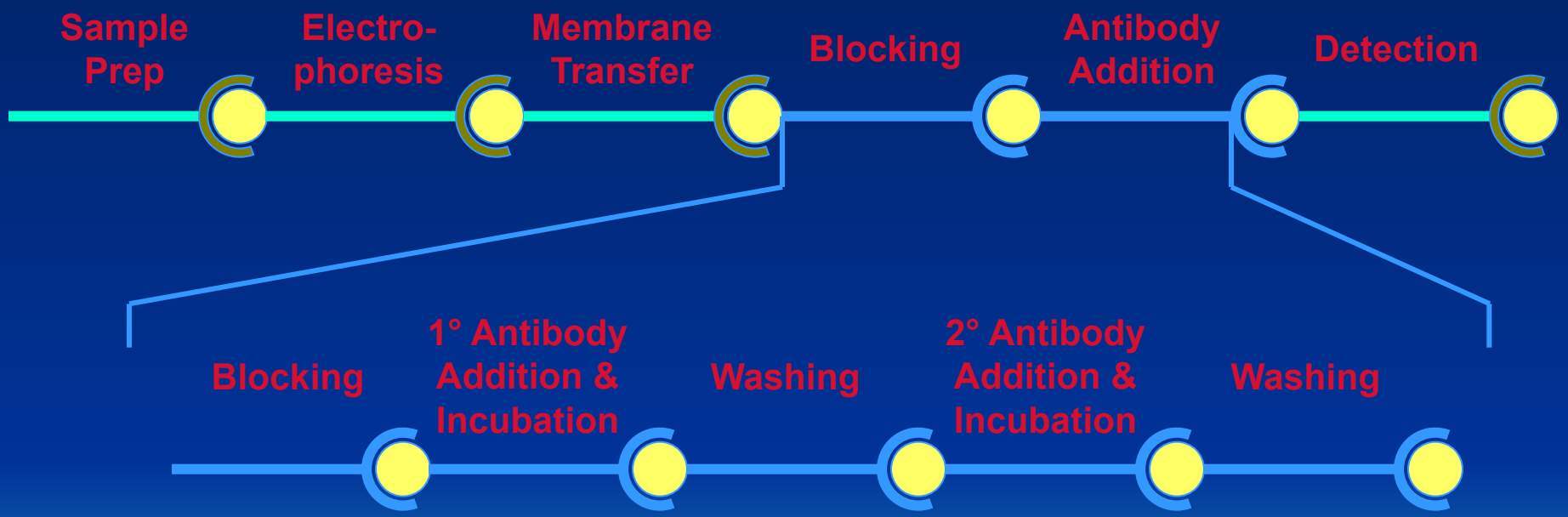

Standard	1 Hr	1 Hr-overnight	15 min	1 Hr	15 min	4 Hrs Vs. 22 min
SNAP i.d.	20 sec	10 min	1 min	10 min	1 min	

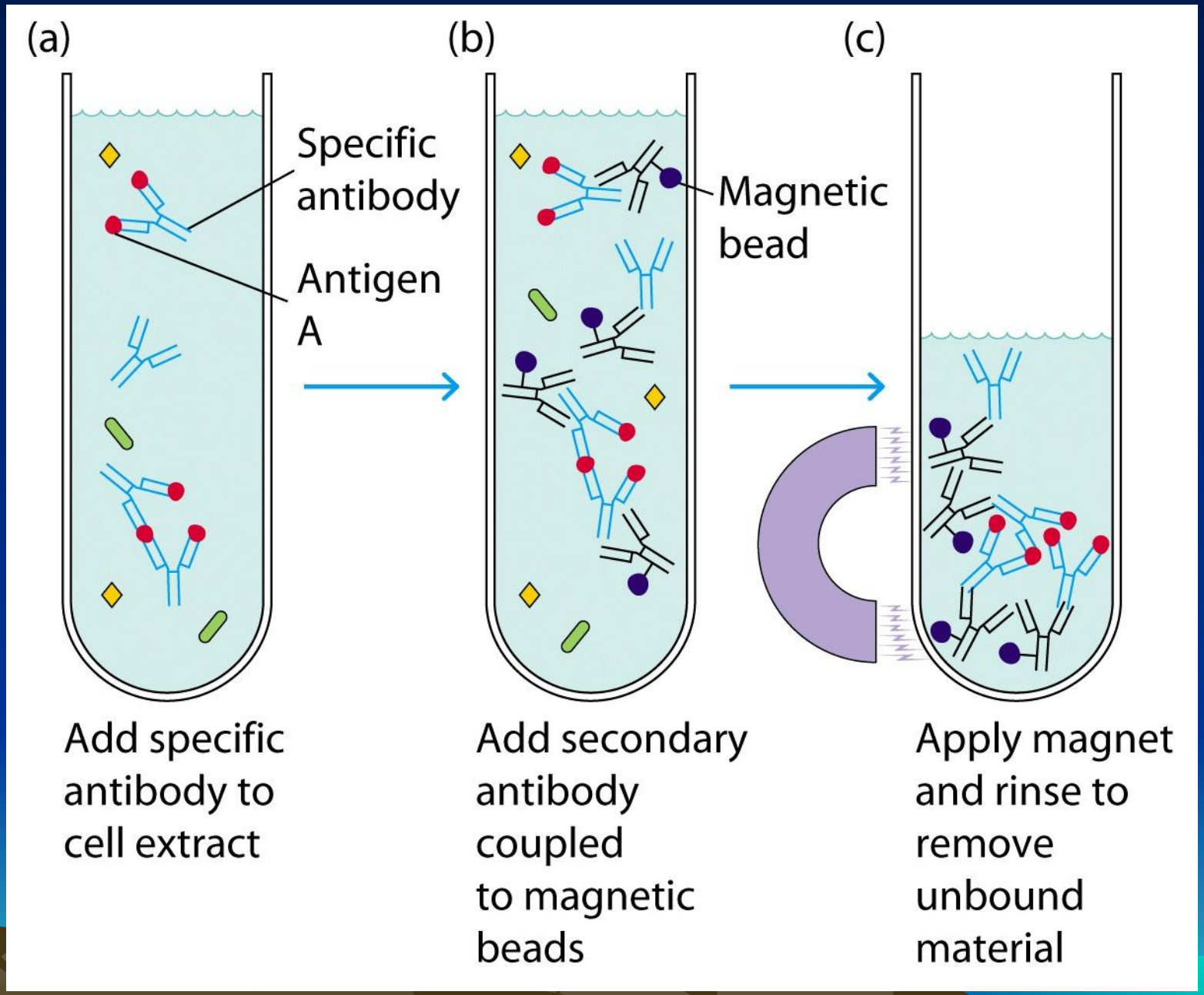
(a)
(b)
(c)
Specific antibody
Antigen A
Magnetic bead
Add specific antibody to cell extract
Add secondary antibody coupled to magnetic beads
Apply magnet and rinse to remove unbound material

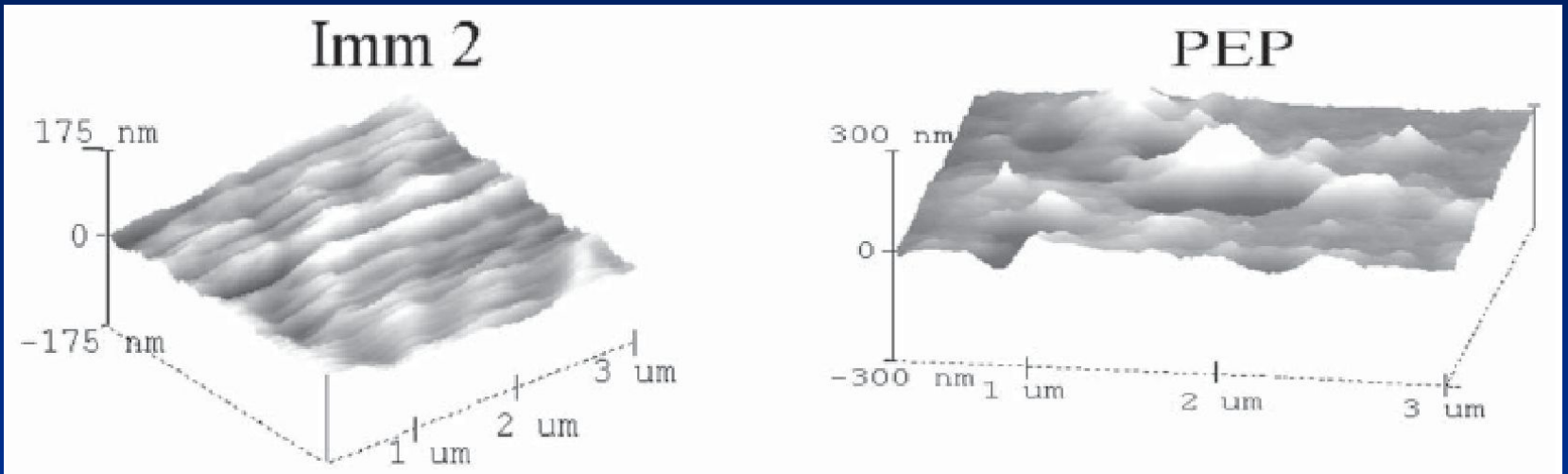

Fig. 8. The surface topography of PEP (right) and Imm 2 (left). Images are for 3 μm squares obtained by atomic force microscopy in the Tapping Mode. Note that the maximum surface height depicted (Z axis) is 175 nm for Imm 2 but 300 nm for PEP. From Butler et al. *(4)*.

Table 2
Adsorption-Induced Conformational Change

Protein	Phenomenon	Authors
Albumin	Conformational change after adsorption on glass	Bull, 1956 *(32)*
IgG	Concentration-dependent allosteric conformers after adsorption on polystyrene	Oreskes and Singer, 1961 *(38)*
IgG	Molecule unfolding and changes in antigenicity when adsorbed on polystyrene	Kochwa et al., 1967 *(39)*
IgG	Thermodynamic evidence for conformational change	Nyilas et al., 1974 *(40)*
Monoclonal Ab	Altered specificity after adsorption	Kennel, 1982 *(41)*
Tryptophan synthase	Altered enzymic and antigenic activity after adsorption	Friquet et al., 1984 *(42)*
Lactic dehydrogenase	Conformational alteration after dehydrogenase adsorption on polystyrene	Holland and Katchalski-Katzir, 1986 *(43)*
Monoclonal Ab	Loss of activity after adsorption on polystyrene	Suter and Butler, 1986 *(44)*
IgG, IgA	Loss of antigenicity after adsorption to polystyrene	Dierks et al., 1986 *(12)*
Ferritin	Cluster formation on silica wafers	Nygren, 1988 *(19)*
Antifluorescein	Functional monoclonal antifluorescein adsorbed on polystyrene is clustered	Butler et al., 1992 *(7)*
Antifluorescein	Adsorbed MAbs lose 90% of their activity on polystyrene	Butler et al., 1993 *(15)*
Antitheophylline	MAb adsorbed on polystyrene loses 90% of its activity	Plant et al., 1991 *(37)*
Antiferritin	Adsorbed functional antiferritin is clustered on the surface of polystyrene	Davis et al., 1994 *(8)*
Bovine IgG1	Antigenicity of IgG1 or Gu-HCl denatured IgG1 is similar and much less than IgG1 immobilized through a streptavidin linkage	Butler et al., 1977 *(16)*
Bovine IgG1	Superficial layer of IgG1 adsorbed in multilayers is most antigenic	Butler et al., 1977 *(16)*
Myoglobin	Adsorption of myoglobin effects reactivity of conformation-specific monoclonal antibody	Darst et al., 1988 *(45)*

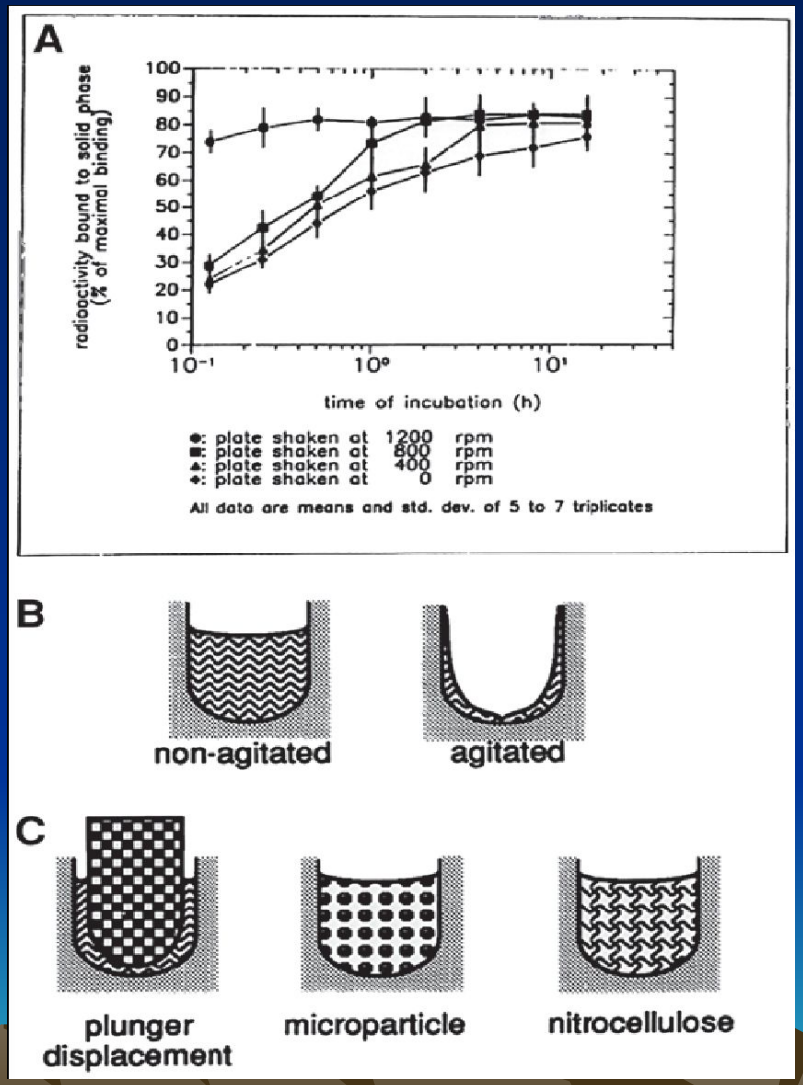

Fig. 1. The diffusion dependence of solid-phase immunoassay and methods used to reduce its influence. (A) The effect of vortexing (shaking) microtiters wells on establishment of equilibrium (from ref. *13*). (B) Illustration of the physical effect of vortexing microtiter wells (rotary agitation) on the distribution of the fluid phase relative to the solid phase. The fluid phase is depicted by wavy lines. (C) Alternative methods of confining the reaction volume to within close proximity to the solid phase bearing the immobilized reactant.

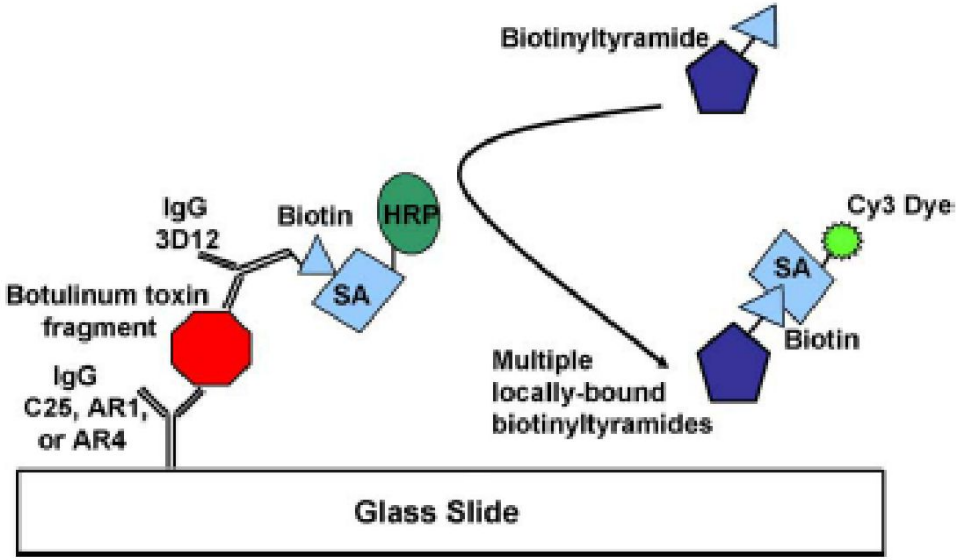

Fig. 1. ELISA microarray immunochemical assay using the reaction of horse radish peroxidase (HRP) with tyramide for signal amplification.

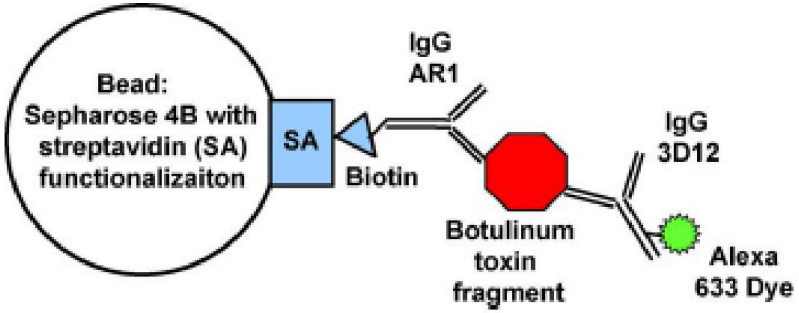

Fig. 2. Sandwich assay developed for the renewable microcolumn sensor detection of botulinum toxin. It consists of a streptavidin-coated Sepharose 4B bead that is functionalized with a biotinylated AR1. This material is used to pack a microliter-sized column capable of binding the surrogate botulinum toxin fragment. Once bound to the column the toxin fragment binds a secondary antibody (3D12) labeled with a fluorescent reporter.

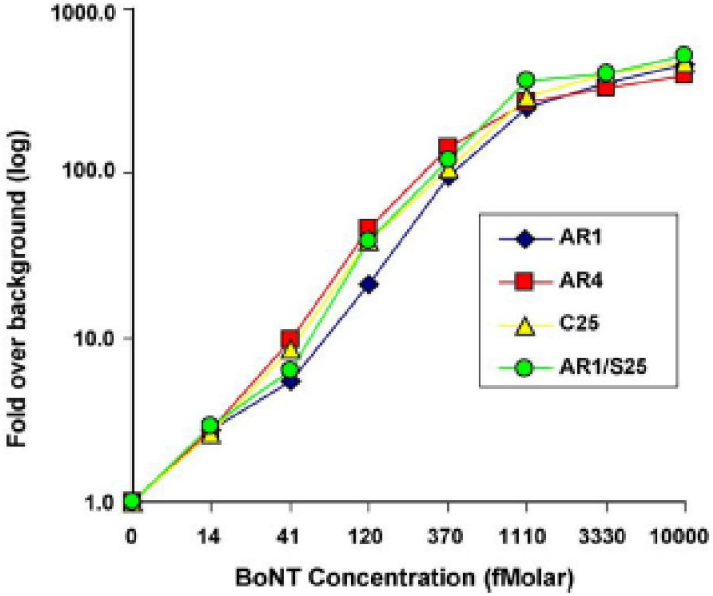

Fig. 5. Detection of BoNT/A-Hc fragment in plasma with the ELISA microarray. Calibration curves for the detection of BoNT/A-Hc fragment in plasma using detection antibody incubation time of 2 h.

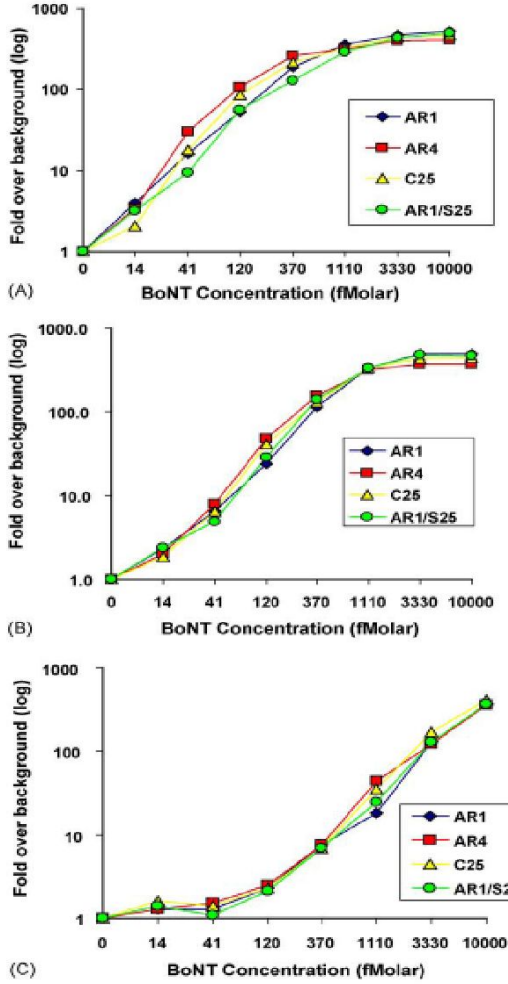

Fig. 4. Calibration curves for the detection of BoNT/A-Hc fragment in buffer using an ELISA protein microarray. Assays were performed as described in Section 2 with the four capture antibodies used as shown in the figure legends. Each point represents the average of five microarray spots. (A) Standard assay incubation times were used. (B) Decreased detection antibody incubation time. (C) Decreased antigen incubation time, as indicated in the text.

$14\ \mathrm{fM}\ (1.4\ \mathrm{pg\ mL^{-1}})$

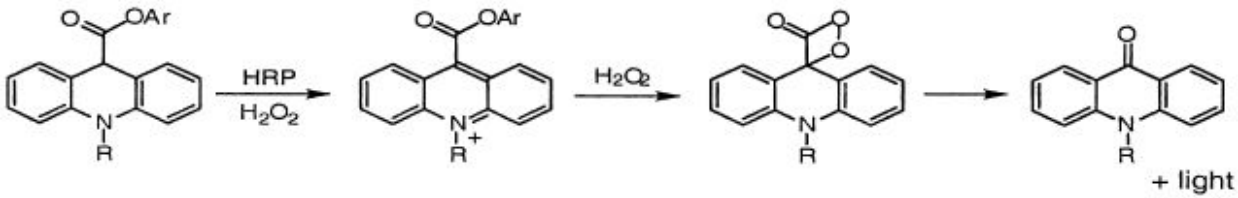

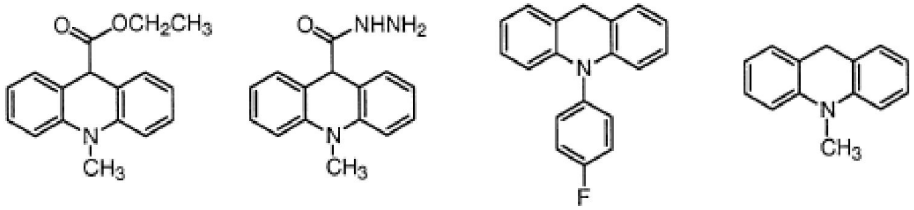

3 4 5 6

Table 1
Comparison of reported limits of detection (LOD) of HRP with fluorescent substrates

Reference	Substrate	Reported LOD	LOD (moles of HRP)
[13]	Tyramine	0.1 mU	2.3×10^{-14} mol
[13]	Homovanillic acid	0.5 mU	1.1×10^{-13} mol
[4]	MHPMC	0.5 μmol	5×10^{-19} mol
[2]	*p*-Hydroxyphenylpropionic acid	7.8 μU	6.5×10^{-16} mol
[2]	Tyrosol	15.6 μU	1.3×10^{-15} mol
[2]	Tyramine	0.5 mU	4.2×10^{-14} mol
[2]	Homovanillic acid	1 mU	8.3×10^{-14} mol
[14]	*o*-Phenylenediamine	0.56 μU ml^{-1} (2 ml)	1.1×10^{-16} mol
[15]	Amino aluminum phthalocyanine	0.6 pM (10 ml)	6×10^{-15} mol
[5]	DCM-OPA	~20 pM (5 ml)	1×10^{-13} mol
	Lumigen PS-1	10^{-14} M	$< 10^{-18}$ mol
	Compound 4	4.6×10^{-14} M	4.6×10^{-19} mol

MHPMC, *N*-methyl-*N*-(4-hydroxyphenyl)methyl carbamate; DCM-OPA, *N*,*N*′-dicyanomethyl *o*-phenylenediamine.

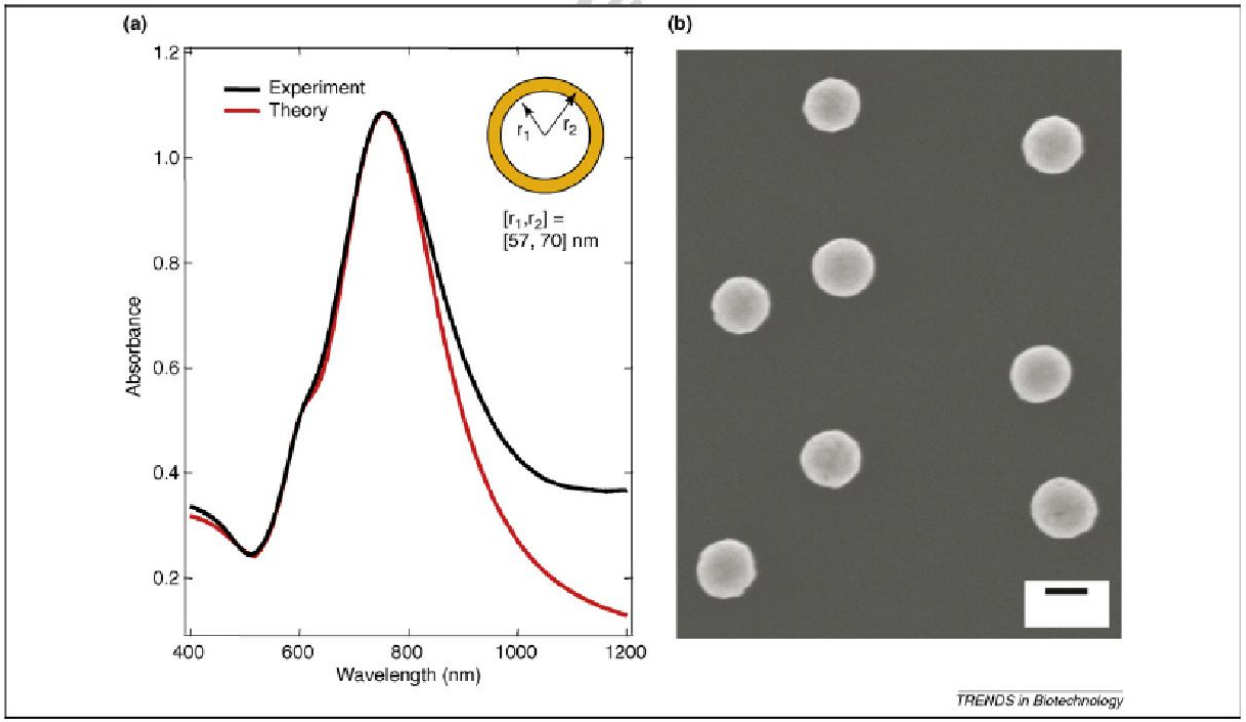

Figure 1. Gold–silica nanoshells tuned to NIR wavelengths. Gold nanoshells are synthesized using SiO_2 cores (~114 nm diameter) with surface seeding using 1–3 nm gold particles on cores, followed by controlled surface fill-in with gold by reductive deposition from a gold salt solution. **(a)** The experimental and theoretical extinction spectra of nanoshells with $[r_1, r_2]$ = [57,70] nm (inset). The radii define the inner and outer diameters of the shell and hence its thickness, leading to the generation of gold nanoshells with an absorption maximum in the NIR (~780 nm). **(b)** Scanning electron micrograph of synthesized gold nanoshells. Bar = 100 nm.

Table 2. Nanostructures for diagnostic applications

***In vitro* diagnostic**		
Nanostructure	**Application**	**Refs**
Nanochannel		
Glass	DNA sequencing	[a]
Nanocrystal		
CdS, CuS, PbS	Single-nucleotide polymorphism	[48]
Fluorescein diacetate	IgG	[49]
Nanoparticle		
Eu^{III}-chelate-doped polystyrene	PSA	[50]
Au	Prion protein	[51]
2-methacryloyloxyethyl phosphorylcholine	C-reactive protein	[52]
Polystyrene	Single-base mutation	[53]
Silica	Calf thymus DNA	[54]
Ag on Au	IgG	[55]
Tris (2,2′-bipyridyl) dichloroRu (II) hexahydrate-doped silica	IgG, DNA	[56]
Nanopore		
Silicon nitride	DNA sequencing	[57]
Nanoprism		
Ag	–	[58]
Au	–	[59]
Nanorod		
Au/Ag/Ni/Pd/Pt	IgG	[60]
Nanotube		
Carbon	DNA	[61]
Nanowire		
Si	Influenza A	[62]
Au	*E. coli*	[63]
Polypyrrole	DNA	[64]
***In vivo* diagnostic**		
Nanostructure	**Application**	**Refs**
Liposome		
Gadolinium	MRI imaging	[65,66]
Dual-fluorescence or iron oxide	Optical and MRI imaging	[67]
Dendrimer		
Gadolinium	MRI imaging	[41,42]
Nanoparticle		
Dextran-coated iron oxide	MRI imaging	[45]
Quantum dots	Near-infrared imaging	[46,47,68]
Gold	Optical detection	[69]
Nanoshell		
Gold	Optical detection	[70]
Nanotube		
Ultrashort Gd packed nanotubes	MRI imaging	[71]

[a] http://www.ece.cmu.edu/~mems/pubs/show.php?pub_id=160

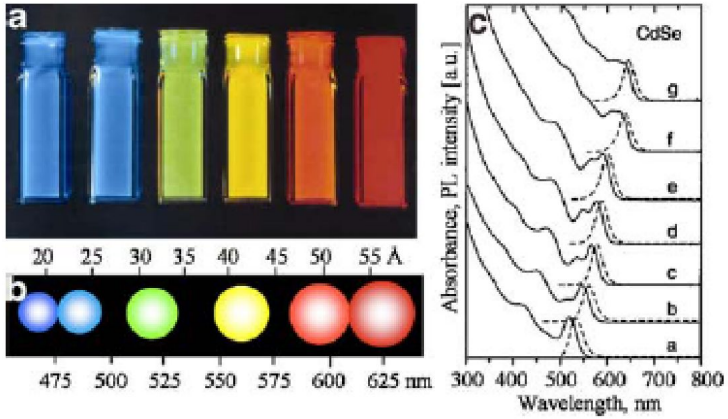

Fig. 1 (a) Size-dependent PL color and (b) schematic presentation of size, color, and PL wavelength of CdSe–ZnS QDs. (c) Absorption (solid lines) and PL (broken lines) spectra of CdSe QDs with various sizes. Reprinted with permission from Refs. [7] (a) and [30] (b). Copyright (1997, 2001) American Chemical Society

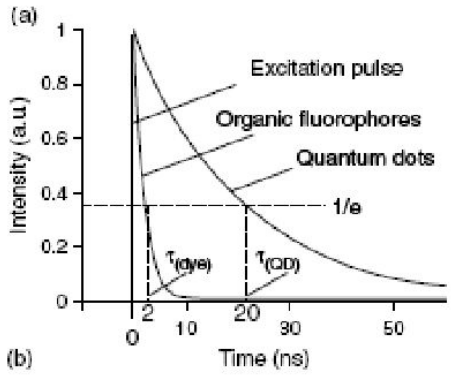

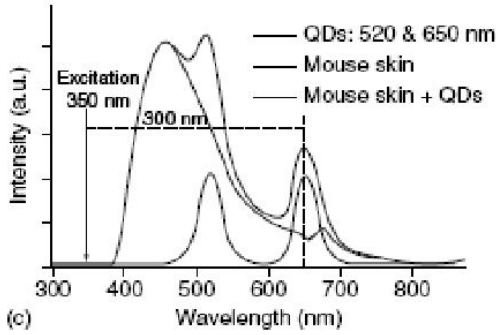

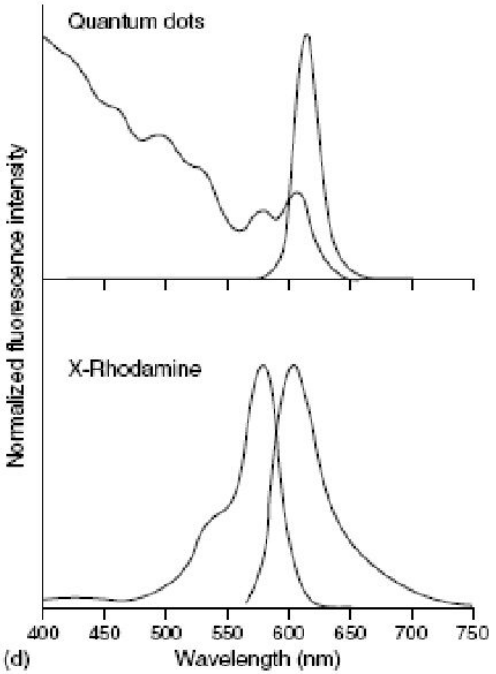

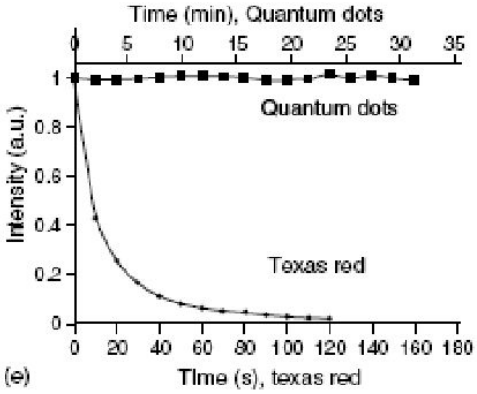

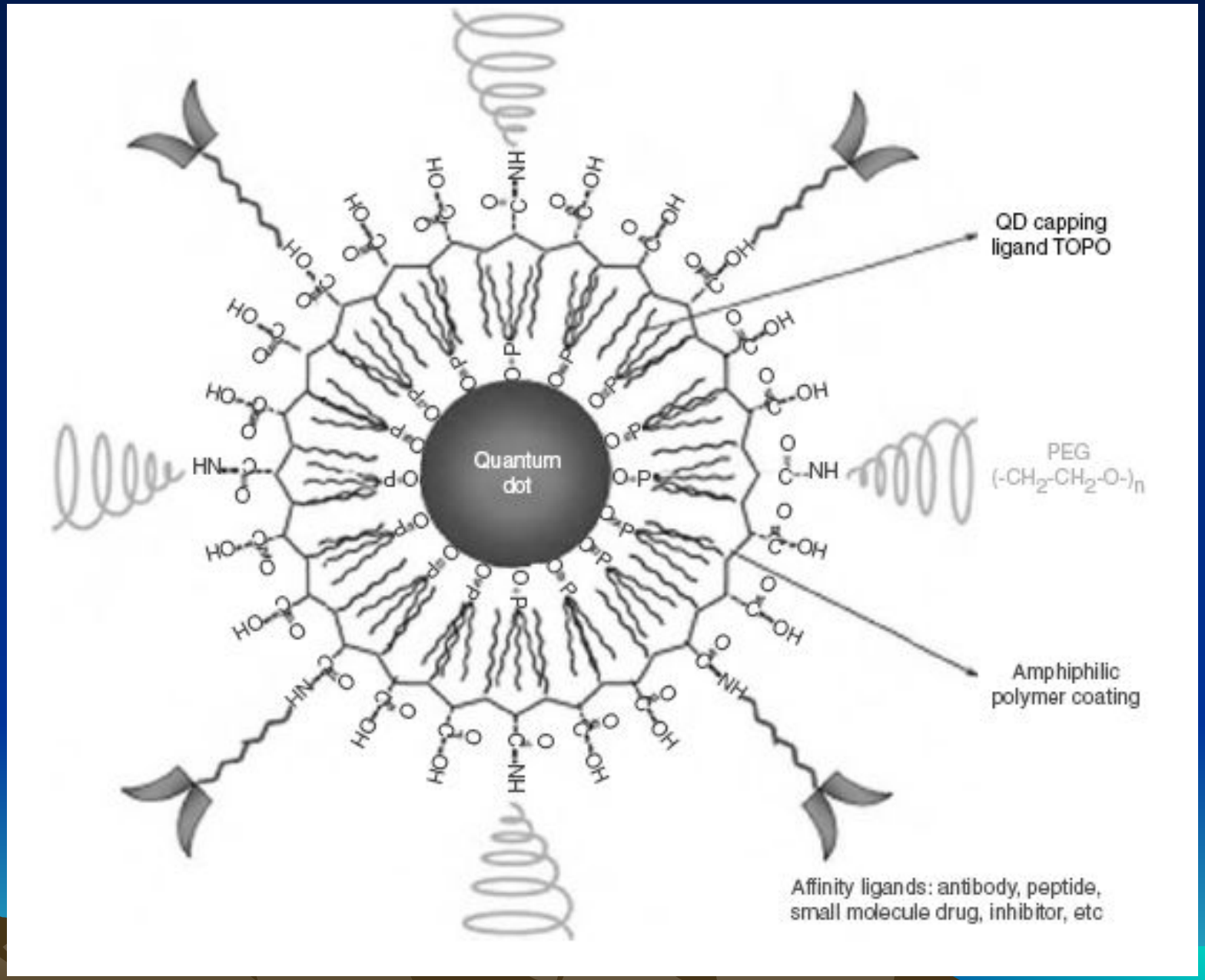
QD capping ligand TOPO
Quantum dot
PEG
(-CH2-CH2-O-)n
Amphiphilic polymer coating
Affinity ligands: antibody, peptide, small molecule drug, inhibitor, etc

Методы коньюгации – иммобилизации антител на квантовых наночастицах

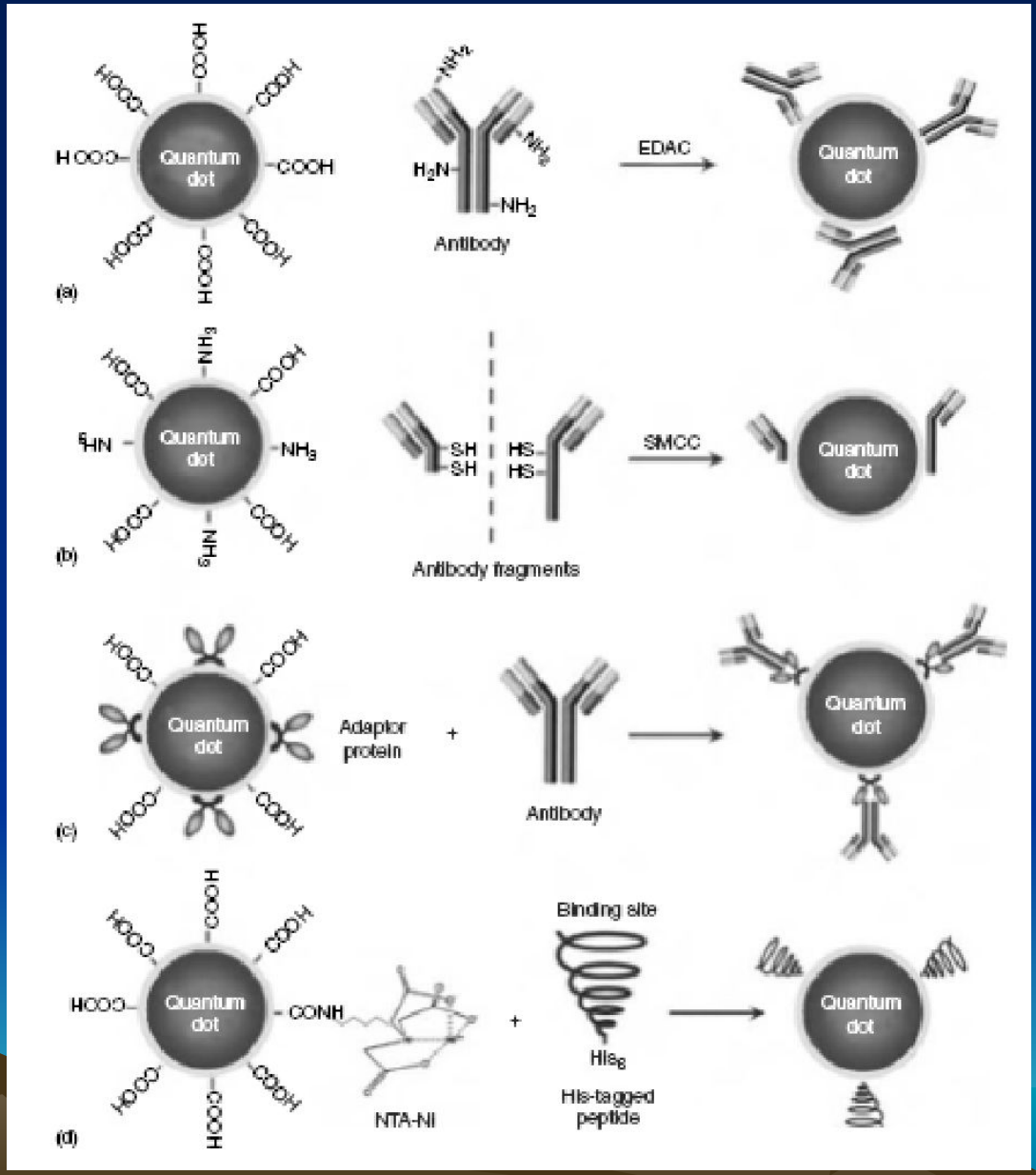

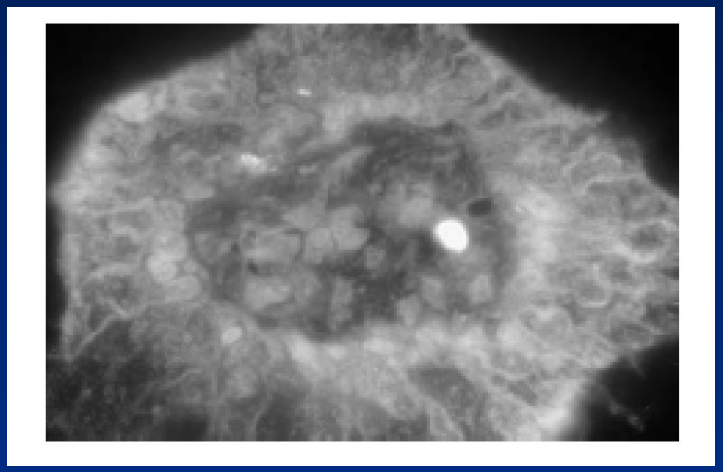

Иммунофлюоресцентный анализ среза ткани
с использованием антител,
меченных квантовыми наночастицами

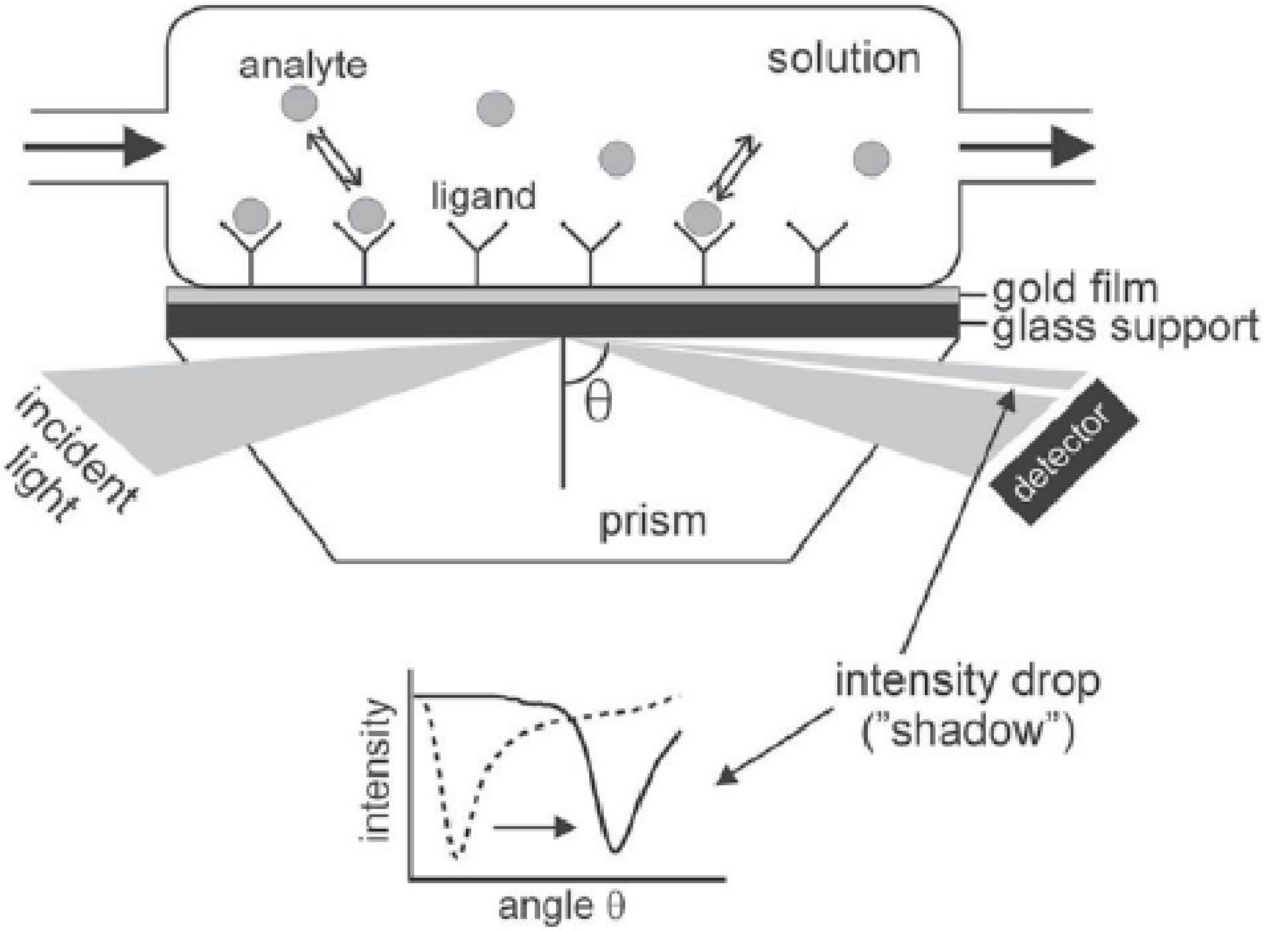

Fig. 1. Schematic view of a surface plasmon resonance (SPR) detector as utilized in a Biacore system. SPR arises when light is totally internally reflected from a metal-coated interface between two media of different refractive index (a glass prism and solution). If the incident light is focused on the surface in a wedge, the drop in intensity at the resonance angle appears as a "shadow" in the reflected light wedge, which is detected by a position-sensitive diode array detector. When an interaction between an immobilized ligand (e.g., an antibody, Y) and an analyte in solution (filled circles) occurs, the "shadow" is shifted on the detector, i.e., the angle θ changes.

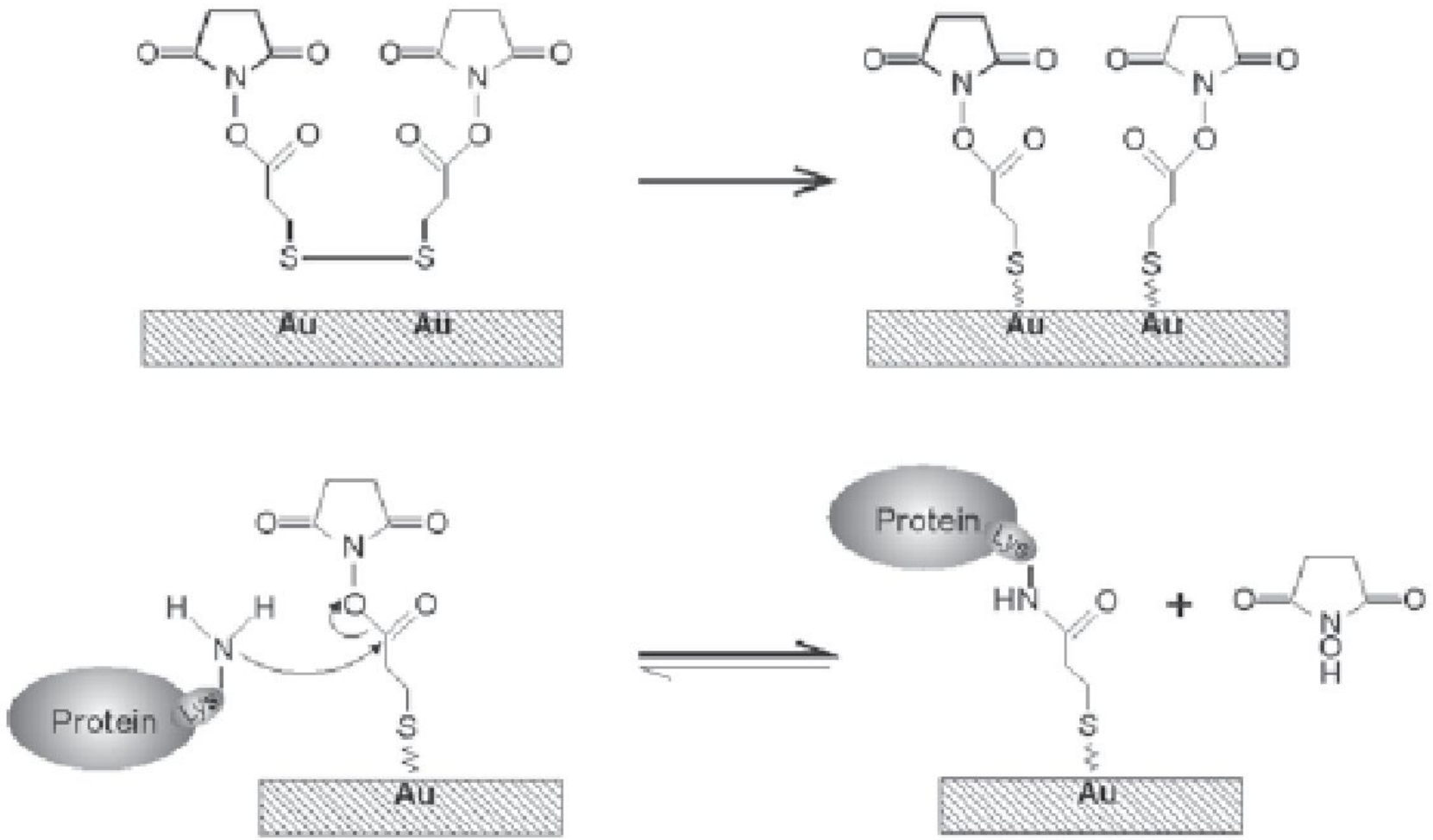

Fig. 2. Immobilization of proteins to a gold surface using 3,3'-dithiodipropionic acid-di(N-succinimidylester) (DSP).

Магнитные Наночастицы покрытые стрептавидином

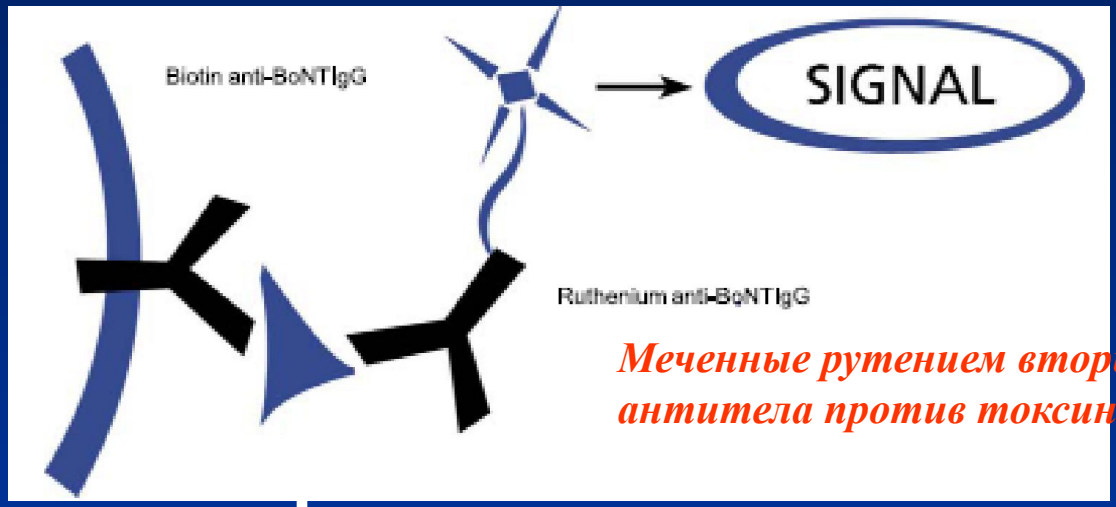

Меченные рутением вторые антитела против токсина

Биотинилированные антитела против токсина

Чиповая технология

с использованием сандвич варианта ИФА и стрептавидин биотиновой ститемы

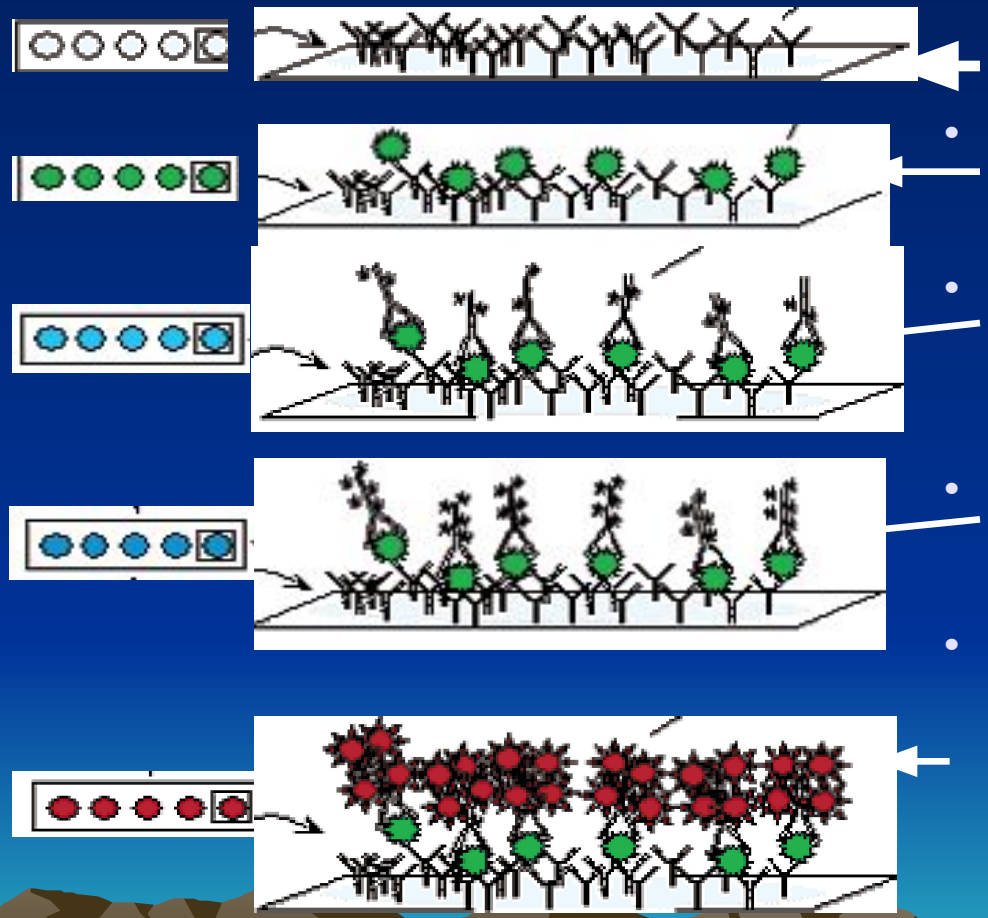

- Иммобилизация первых антител на чип, предпочтительнее ориентированная посадка антител
- Захват антигена (зеленые шарики) антителами
- Вторые специфические антитела, меченные биотином, взаимодействуют с антигеном
- Создание стрептавидин-биотиновых комплексов
- Образование комплекса - стрептавидин-тирамид или струптавиди Cy3, которые детектируются спектрофотометрически

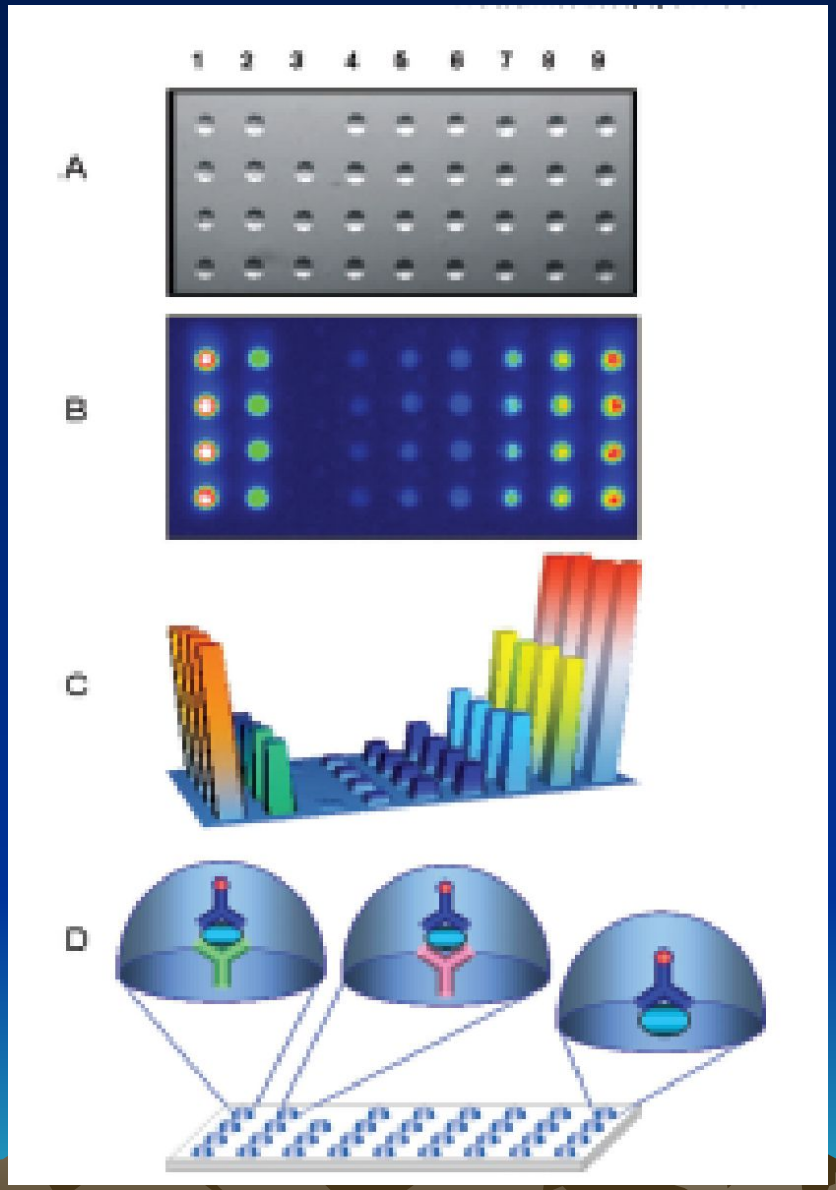
1 2 3 4 5 6 7 8 9
A
B
C
D

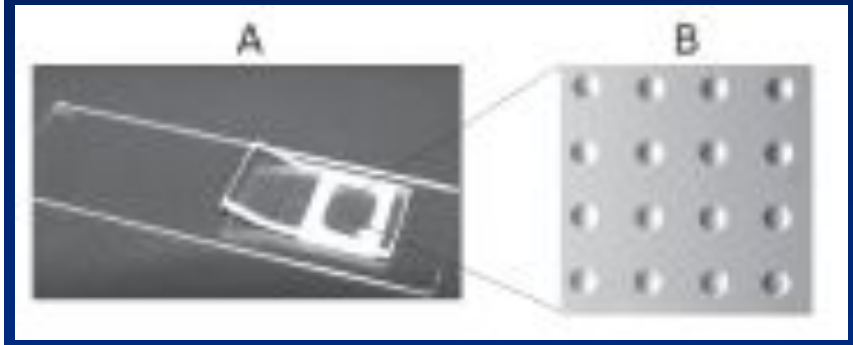
A
B

Структура нейротоксинов клостридий и молекулярные мишени

Претеолитическое расщепление

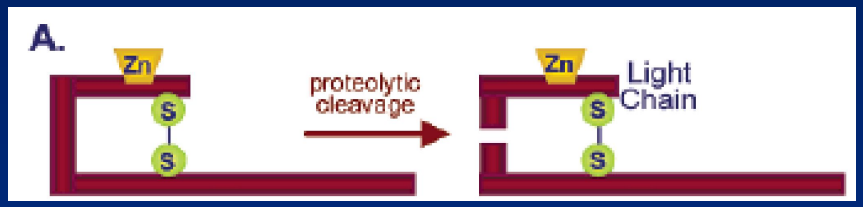

Молекула токсина предшественника

Двуцепочная молекула токсина в активной форме

Созревание токсина и переход его в активную форму

Молекулы - мишени бактериальных нейротоксинов клостридий

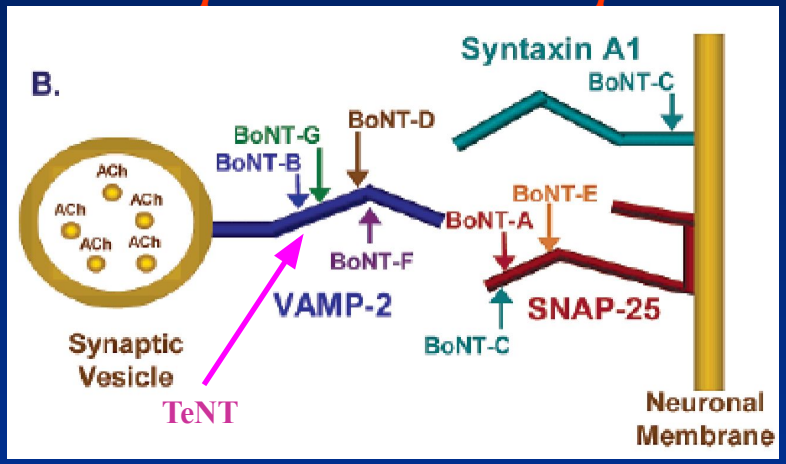

Синаптические визикулы

Нейрональная мембрана

Стрелками обозначены места расщепления эндопротеиназой токсина мембранных белков синаптических мембран.

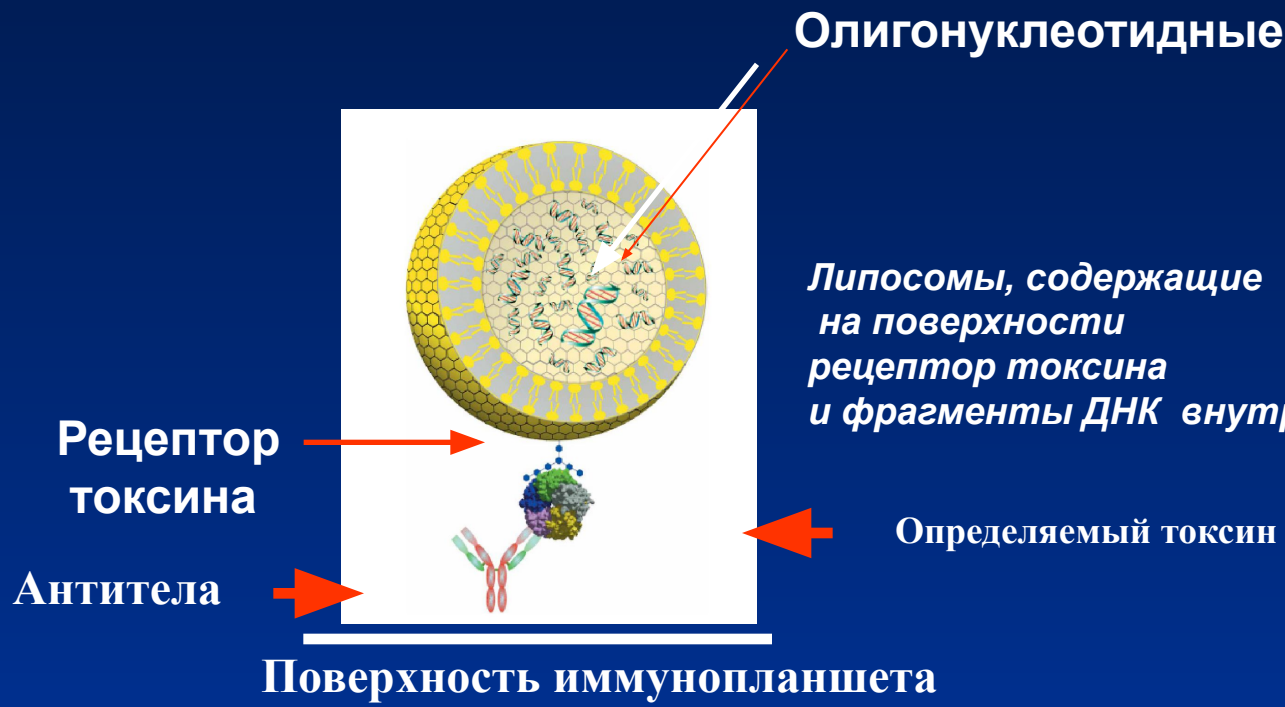

Липосомы-ПЦР иммуноанализ биотоксинов

Схема иммунохроматографического анализа

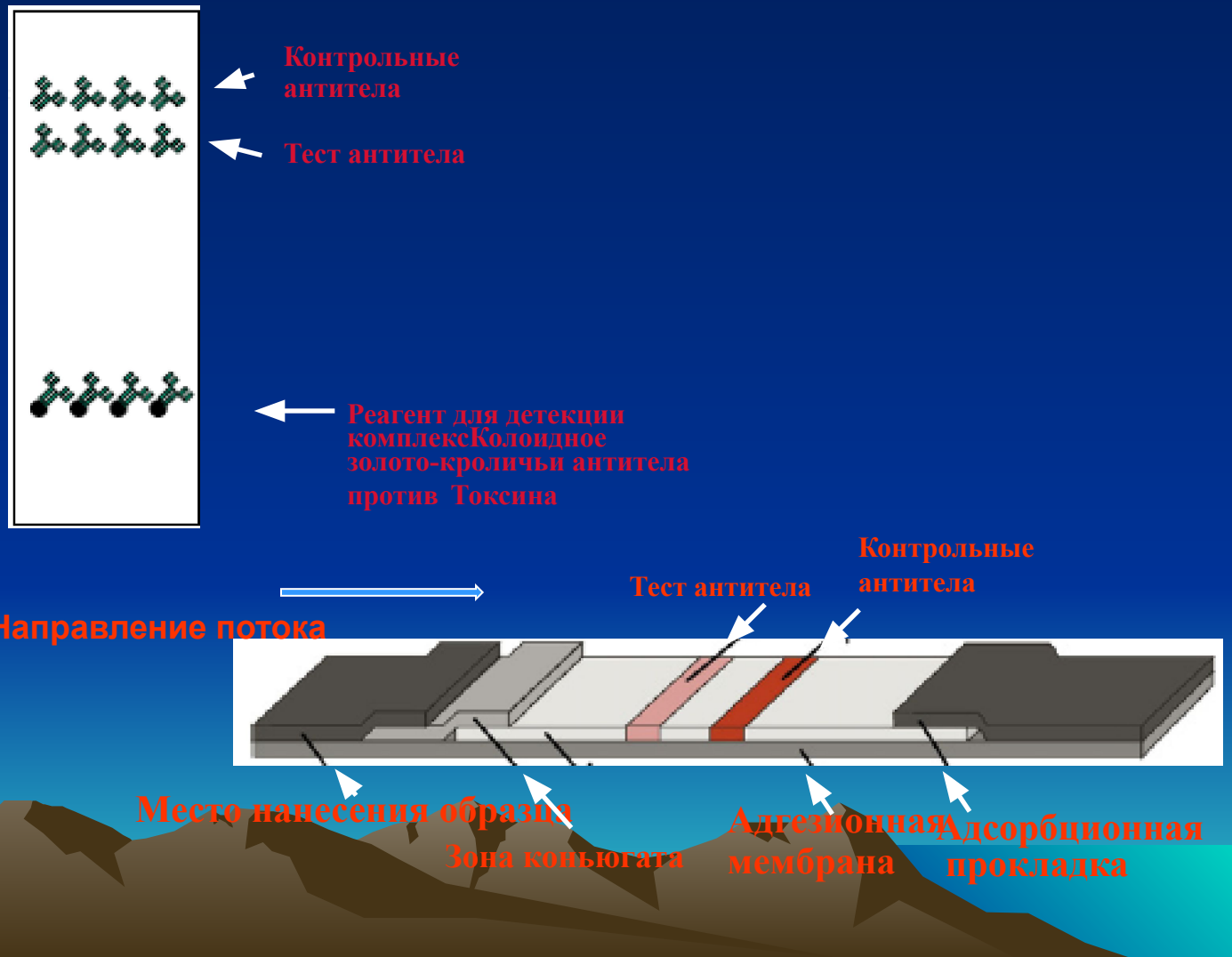

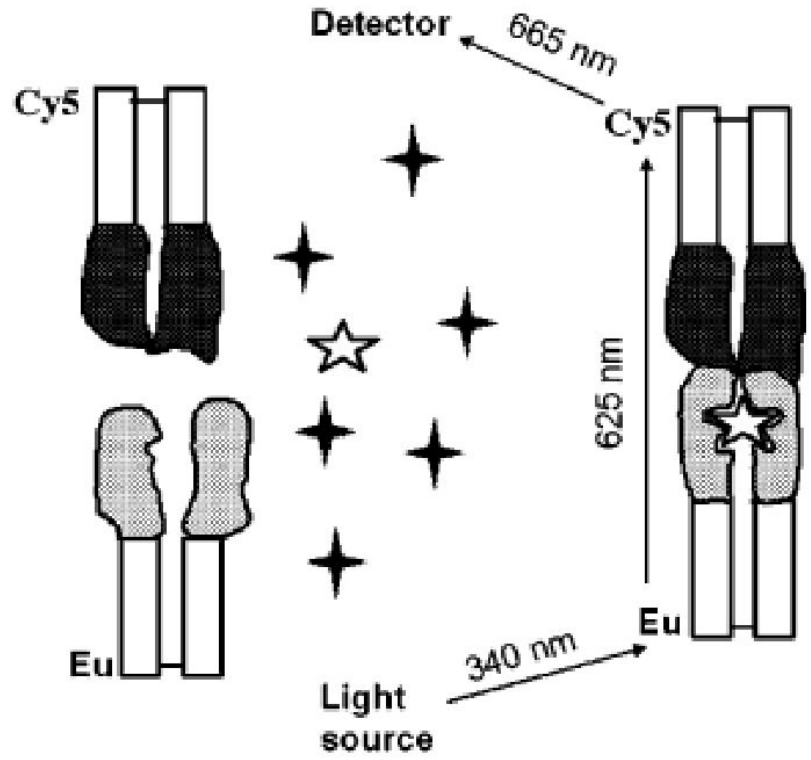

Figure 1. Schematic illustration of the principle of the one-step, noncompetitive FRET immunoassay for morphine. Eu-labeled anti-morphine and Cy5-labeled anti-IC Fab fragments are added into a saliva sample. FRET occurs only when two fluorophores are close to each other; i.e., anti-IC Fab is specifically bound to IC. The star represents the analyte, and dotted patterns represent variable regions of the Fab fragment.

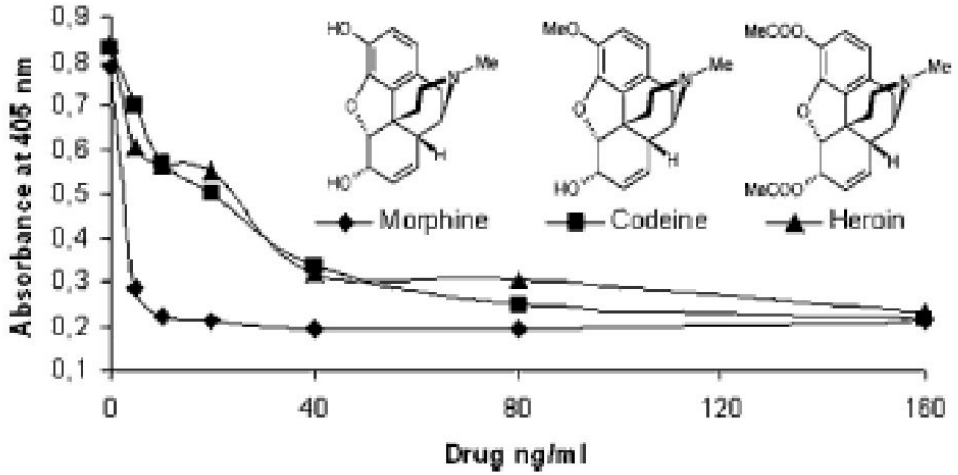

Figure 3. Cross-reactivity of the anti-morphine M1 Fab to codeine and heroin in a competitive ELISA. M1 Fab with various amounts of morphine, codeine, or heroin in PBS was added into morphine–BSA coated wells. After washings the bound Fab was detected with alkaline phosphatase conjugated anti-Fab antibody.

	xMAP® (мультиплексный анализ)	Классический ИФА
Число 96-луночных плашек		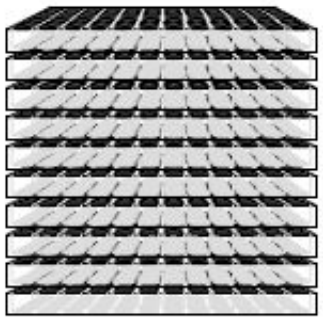
Время эксперимента	3-5 часов	10 часов
Расход антител	100 мкг	1 мг
Расход образца	0,05 мл	4 мл
Внутренний контроль	ДА	НЕТ
Динамический диапазон	3,5 log	2,5 log
Нижний порог детекции	~1 пкг/мл	~1 пкг/мл

MILLIPORE

100 вариантов окраски сфер

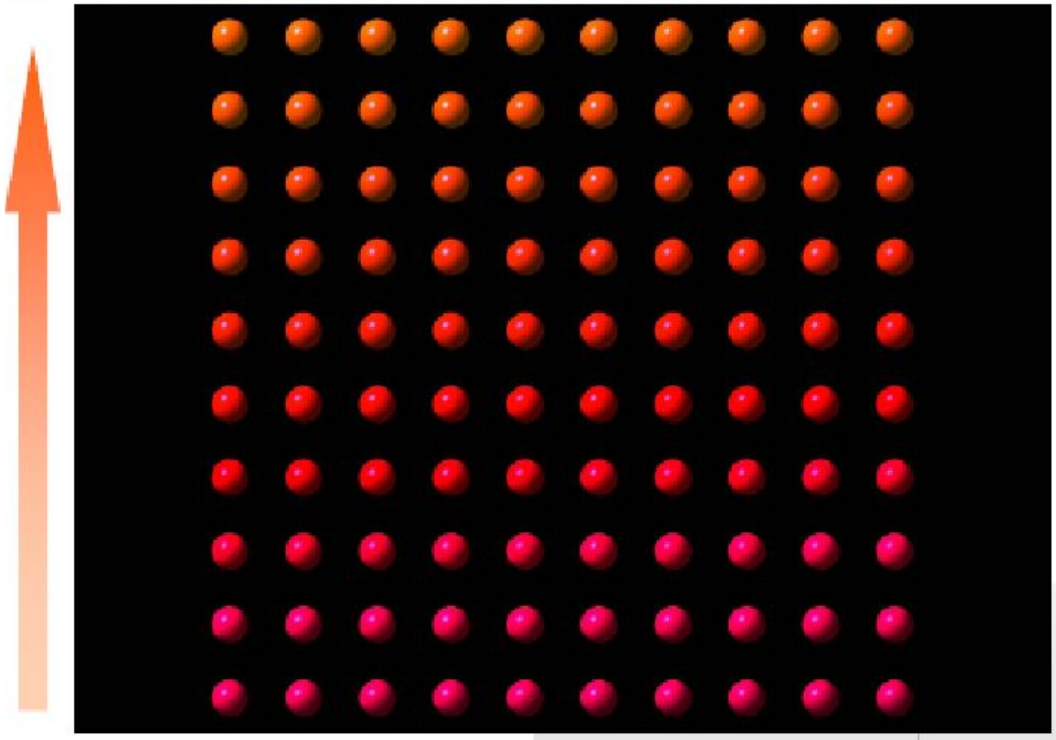

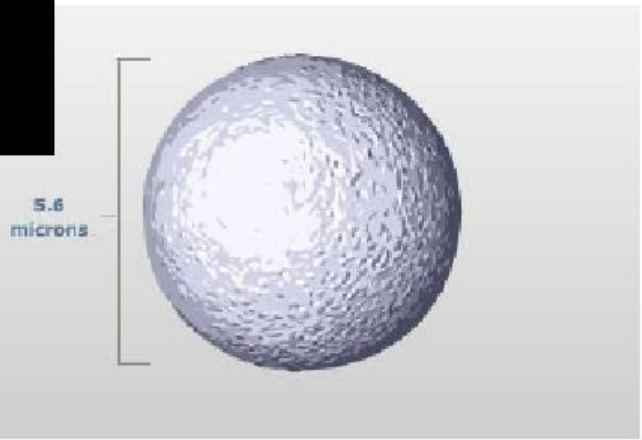

MILLIPORE

Процесс детекции

Мультиплексный анализ – технология Люминекс

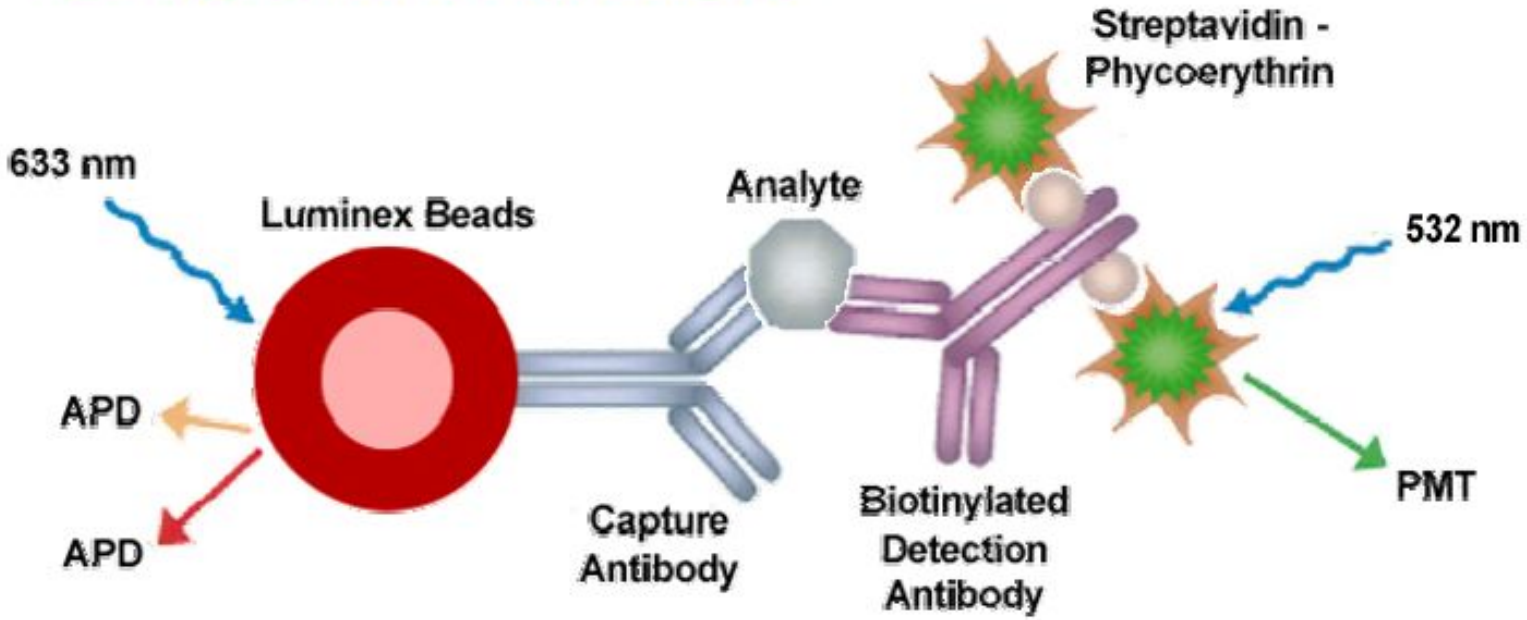

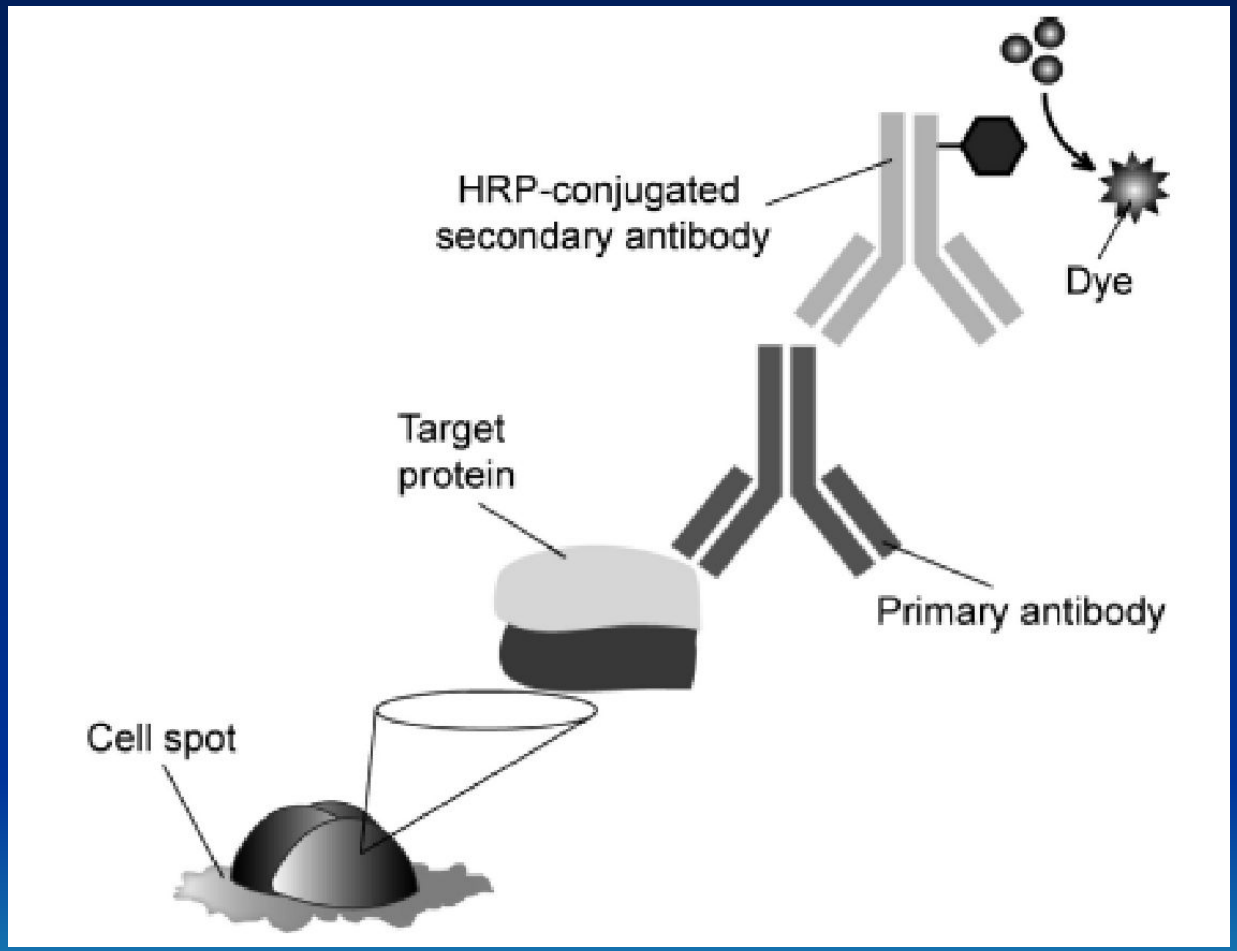
HRP-conjugated
secondary antibody
Dye
Target
protein
Primary antibody
Cell spot

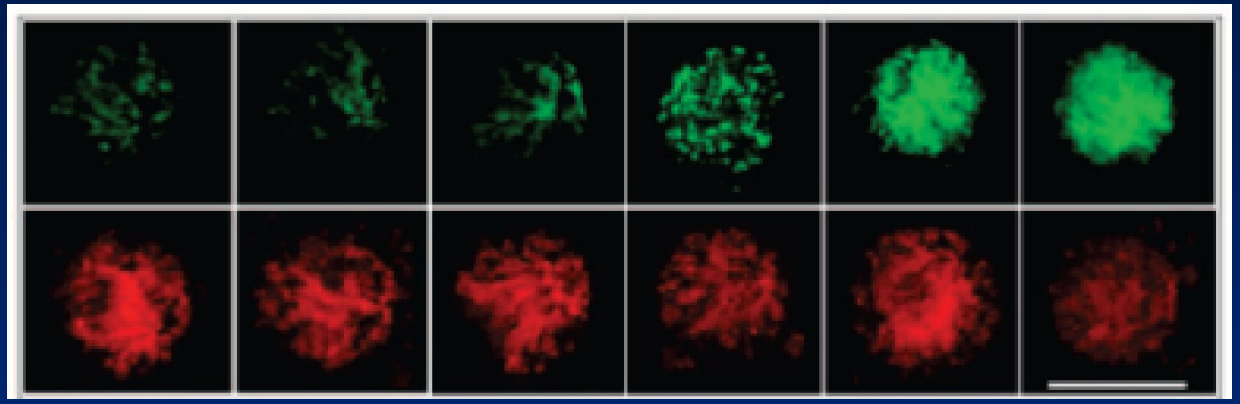

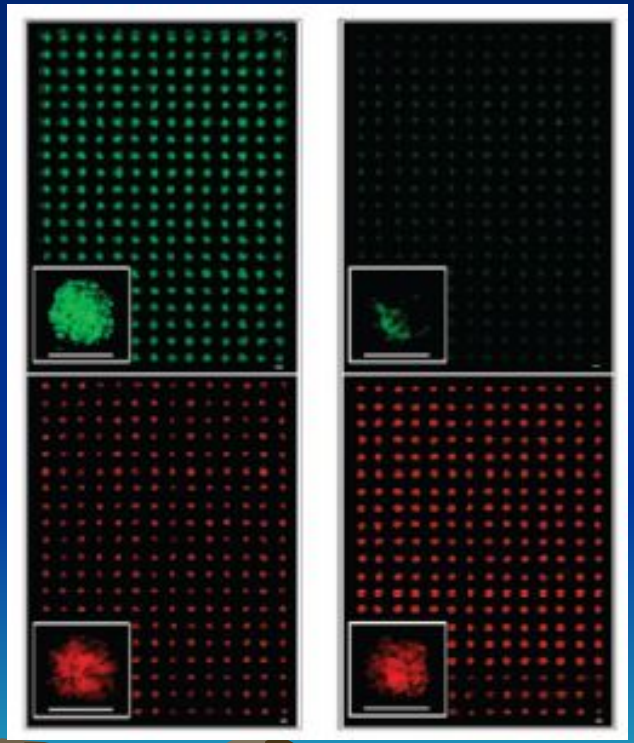

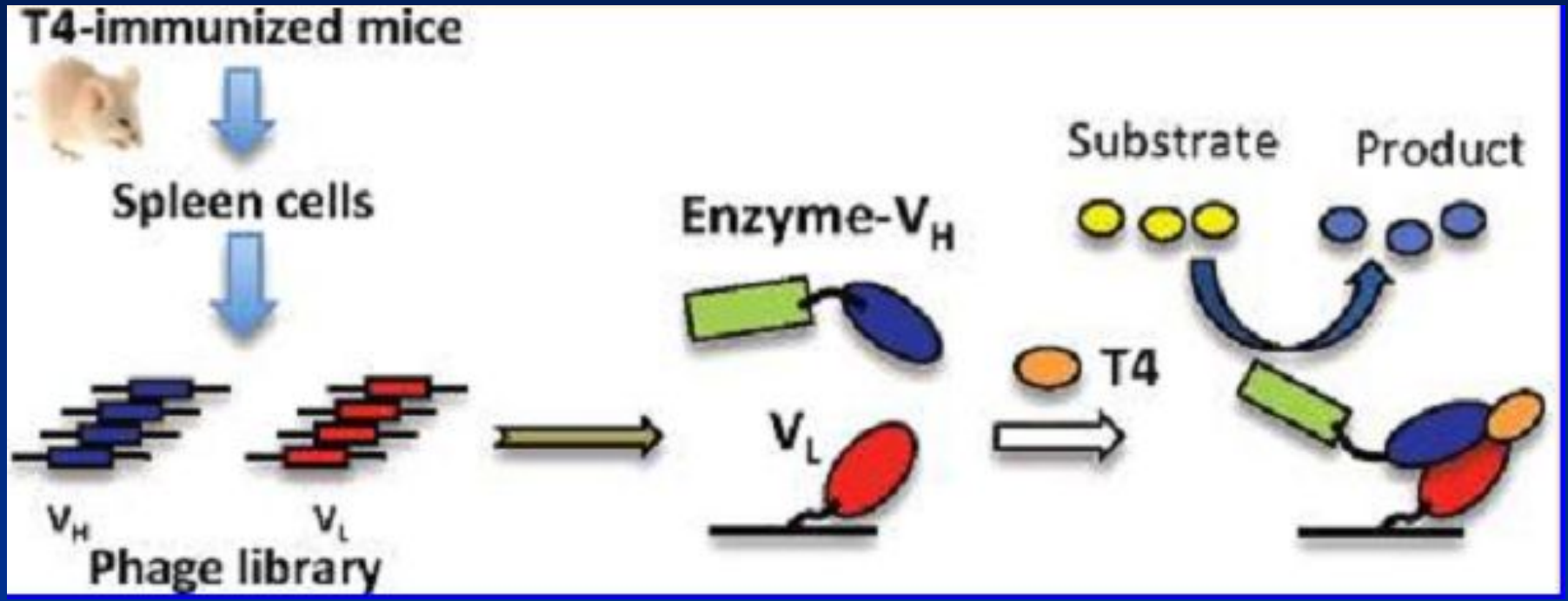
T4-immunized mice
Spleen cells
V_H
V_L
Phage library
Enzyme-V_H
V_L
T4
Substrate
Product

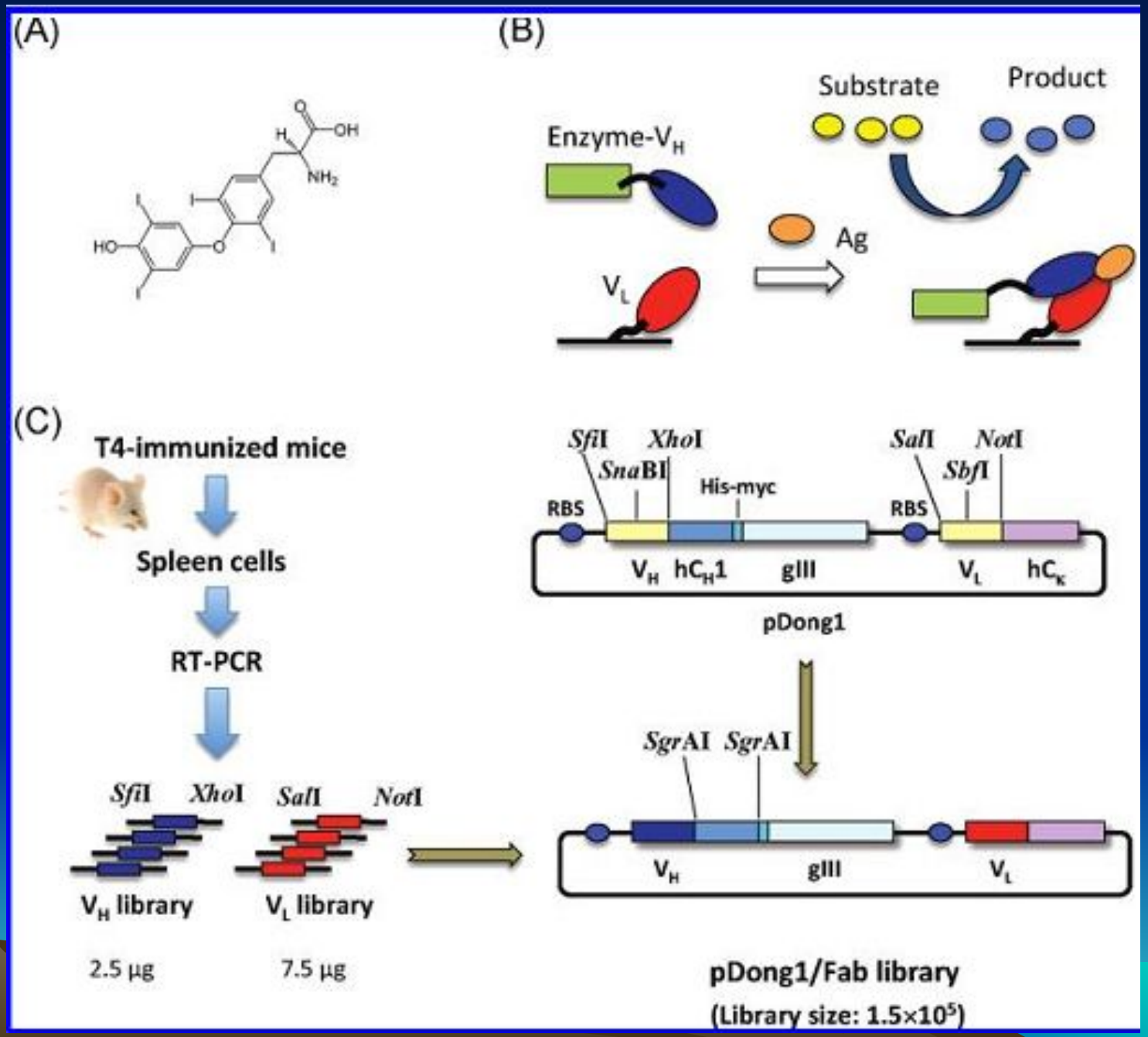
(A)
(B)
Substrate
Product
Enzyme-V_H
Ag
V_L
(C)
T4-immunized mice
Spleen cells
RT-PCR
SfiI
XhoI
SnaBI
His-myc
RBS
SalI
NotI
SbfI
RBS
V_H hC_H1 gIII V_L hC_K
pDong1
SfiI
XhoI
SalI
NotI
V_H library
V_L library
2.5 μg
7.5 μg
SgrAI
SgrAI
V_H gIII V_L
pDong1/Fab library
(Library size: 1.5×10^5)

Table 2
Adsorption-Induced Conformational Change

Protein	Phenomenon	Authors
Albumin	Conformational change after adsorption on glass	Bull, 1956 *(32)*
IgG	Concentration-dependent allosteric conformers after adsorption on polystyrene	Oreskes and Singer, 1961 *(38)*
IgG	Molecule unfolding and changes in antigenicity when adsorbed on polystyrene	Kochwa et al., 1967 *(39)*
IgG	Thermodynamic evidence for conformational change	Nyilas et al., 1974 *(40)*
Monoclonal Ab	Altered specificity after adsorption	Kennel, 1982 *(41)*
Tryptophan synthase	Altered enzymic and antigenic activity after adsorption	Friquet et al., 1984 *(42)*
Lactic dehydrogenase	Conformational alteration after dehydrogenase adsorption on polystyrene	Holland and Katchalski-Katzir, 1986 *(43)*
Monoclonal Ab	Loss of activity after adsorption on polystyrene	Suter and Butler, 1986 *(44)*
IgG, IgA	Loss of antigenicity after adsorption to polystyrene	Dierks et al., 1986 *(12)*
Ferritin	Cluster formation on silica wafers	Nygren, 1988 *(19)*
Antifluorescein	Functional monoclonal antifluorescein adsorbed on polystyrene is clustered	Butler et al., 1992 *(7)*
Antifluorescein	Adsorbed MAbs lose 90% of their activity on polystyrene	Butler et al., 1993 *(15)*
Antitheophylline	MAb adsorbed on polystyrene loses 90% of its activity	Plant et al., 1991 *(37)*
Antiferritin	Adsorbed functional antiferritin is clustered on the surface of polystyrene	Davis et al., 1994 *(8)*
Bovine IgG1	Antigenicity of IgG1 or Gu-HCl denatured IgG1 is similar and much less than IgG1 immobilized through a streptavidin linkage	Butler et al., 1977 *(16)*
Bovine IgG1	Superficial layer of IgG1 adsorbed in multilayers is most antigenic	Butler et al., 1977 *(16)*
Myoglobin	Adsorption of myoglobin effects reactivity of conformation-specific monoclonal antibody	Darst et al., 1988 *(45)*

Enzymatic coupling of SpA
to strictly define antibody orientation

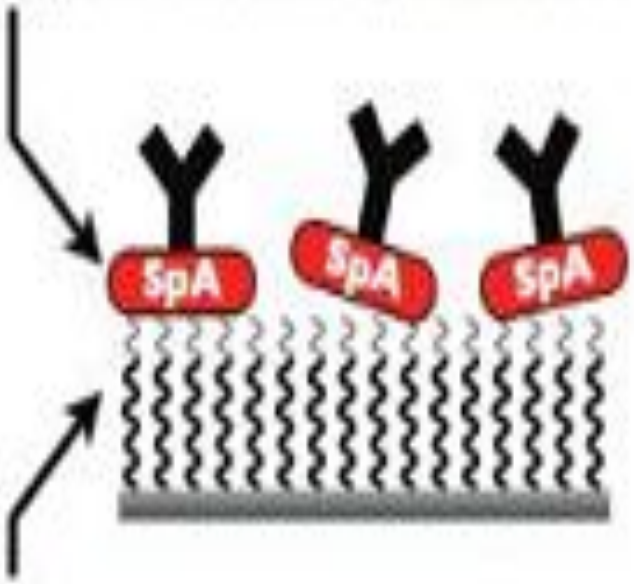

Phospholipid polymer brush
to reduce unnecessary loss of bioactivity

Improved binding capacity
(1.8 antigens/antibody)

Retained binding affinity
($K_d \sim 10^{-10}$ /M)

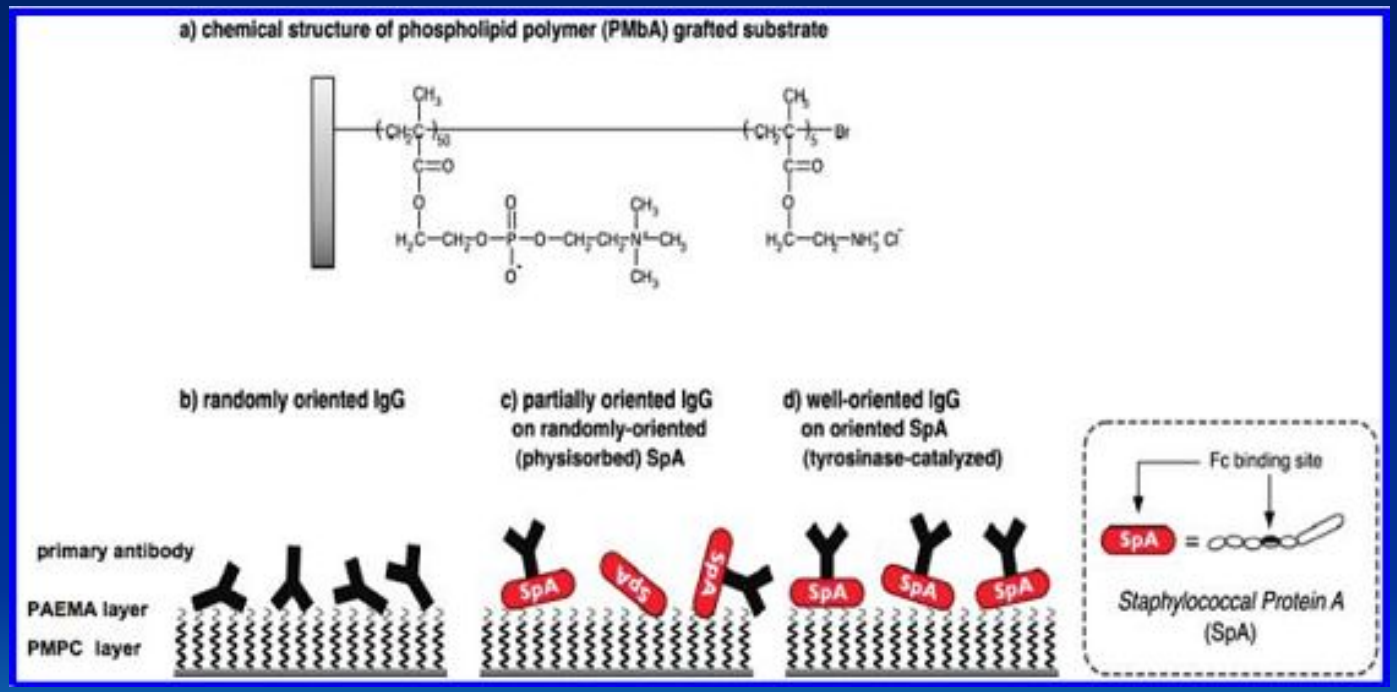
a) chemical structure of phospholipid polymer (PMbA) grafted substrate
b) randomly oriented IgG
c) partially oriented IgG on randomly-oriented (physisorbed) SpA
d) well-oriented IgG on oriented SpA (tyrosinase-catalyzed)
primary antibody
PAEMA layer
PMPC layer
SpA
Fc binding site
Staphylococcal Protein A (SpA)

Table 1. Cooperative Index (n) and Dissociation Constant (K_d) of Antigen−Antibody Reaction

	cooperative index (n)	dissociation constant (K_d) (mol/L)
without SpA	0.99	2.0×10^{-7}
with SpA only	1.01	1.2×10^{-7}
with SpA and tyrosinase	1.23	8.6×10^{-10}

Conjugated to the amino group carrying platform using tyrosinase.

To assess the orientation of immobilized antibodies, antigen binding capacity was measured with four di ere antantigen shaving molecular weight sranging from 66 to 330kDa. Forsmall antigens like albumin and CRP, highly oriented antibodies recorded as much as 1.8 (0.1 antigens per each immobilized antibody suggesting that at least 80% of immobilized antibodies reacted with two antigens. The multivalent binding analysis revealed that the oriented antibodies showed exceptionally strong a?nity for -10 antigens (Kd =8.6 10 mol/L). This value was 100-fold stronger than values for the partially oriented and randomly oriented antibodies and is comparable to the reported Kd values of the active antibodies. Bystrictlycontrolling orientation on an Antibiofoulingphospholipid platform, we have demonstrated that antibodyorientation improves the binding a?nity and the binding capacity of immobilized antibodies.

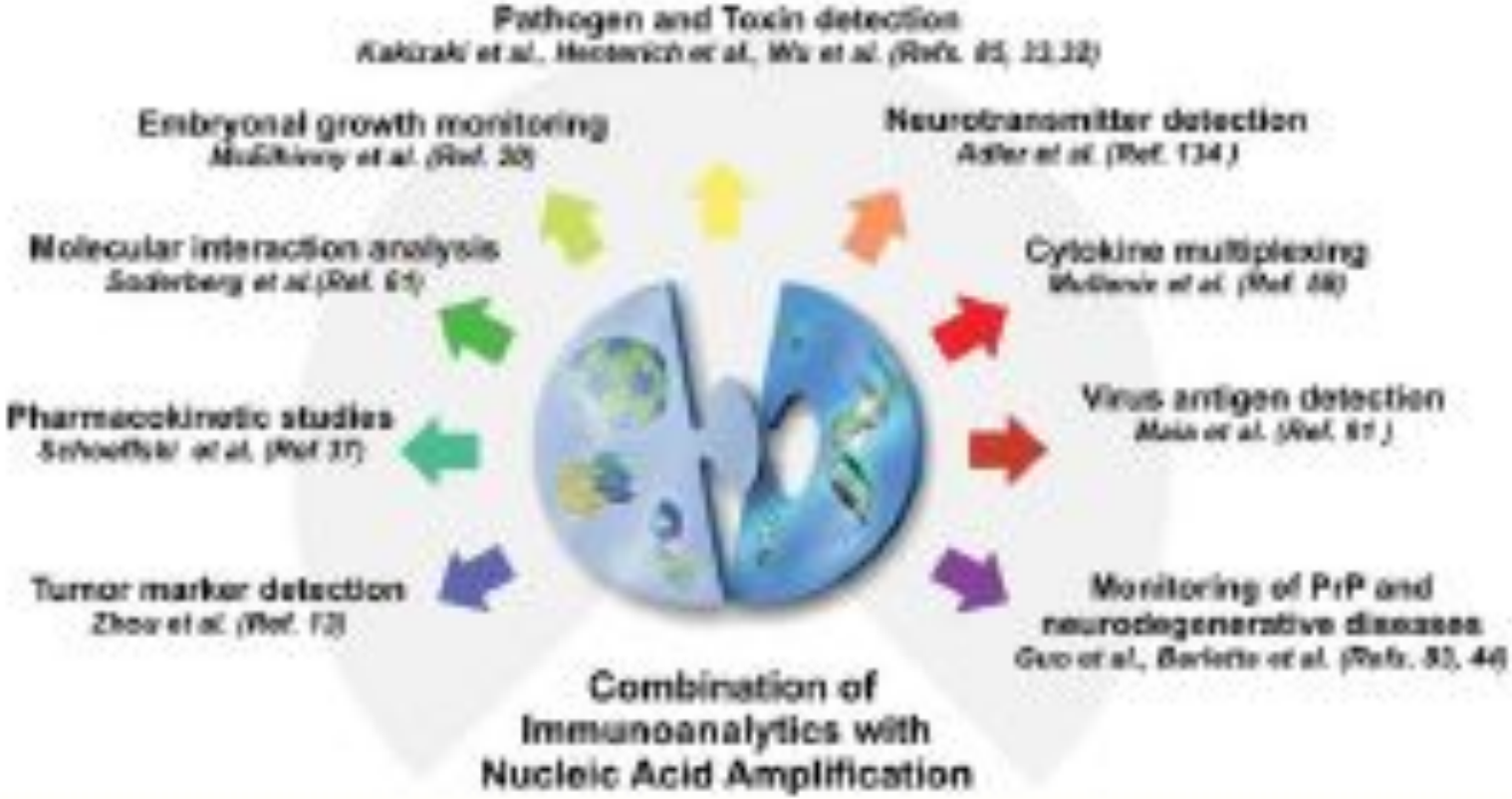

Fig. 2 The intrinsic properties of DNA molecules can be used to improve almost all fields of immunoassays. The scheme summarizes the range of different targets studied by exemplary applications including IPCR with protein chimeras,[20,21] Universal-IPCR,[18] immuno-RCA,[58] PD-IPCR,[46] Imperacer™,[17,63] competitive assays for small molecules[134] or proximity ligation.[62]

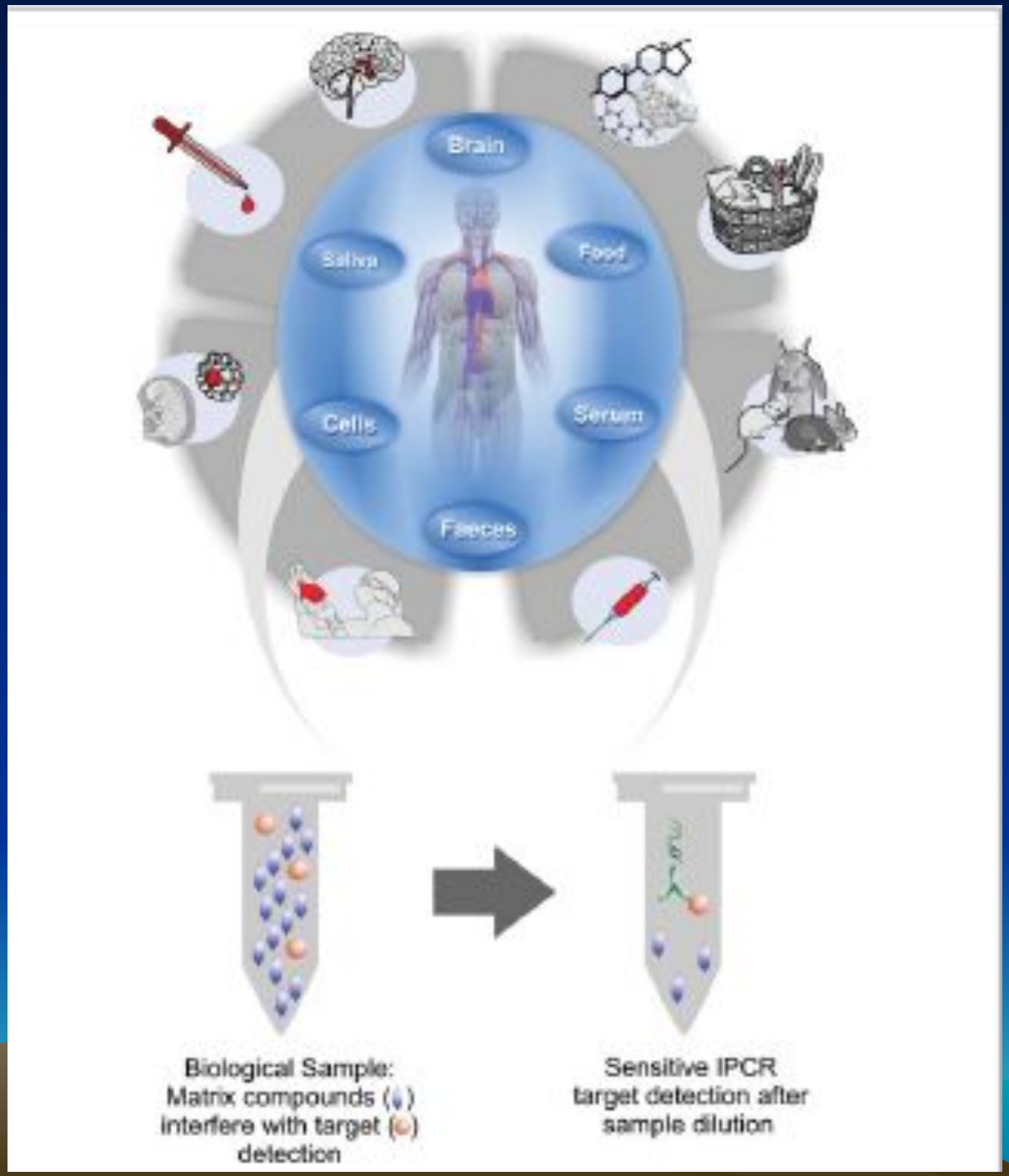
Brain
Saliva
Foot
Cells
Serum
Faeces
Biological Sample:
Matrix compounds (●)
interfere with target (●)
detection
Sensitive IPCR
target detection after
sample dilution

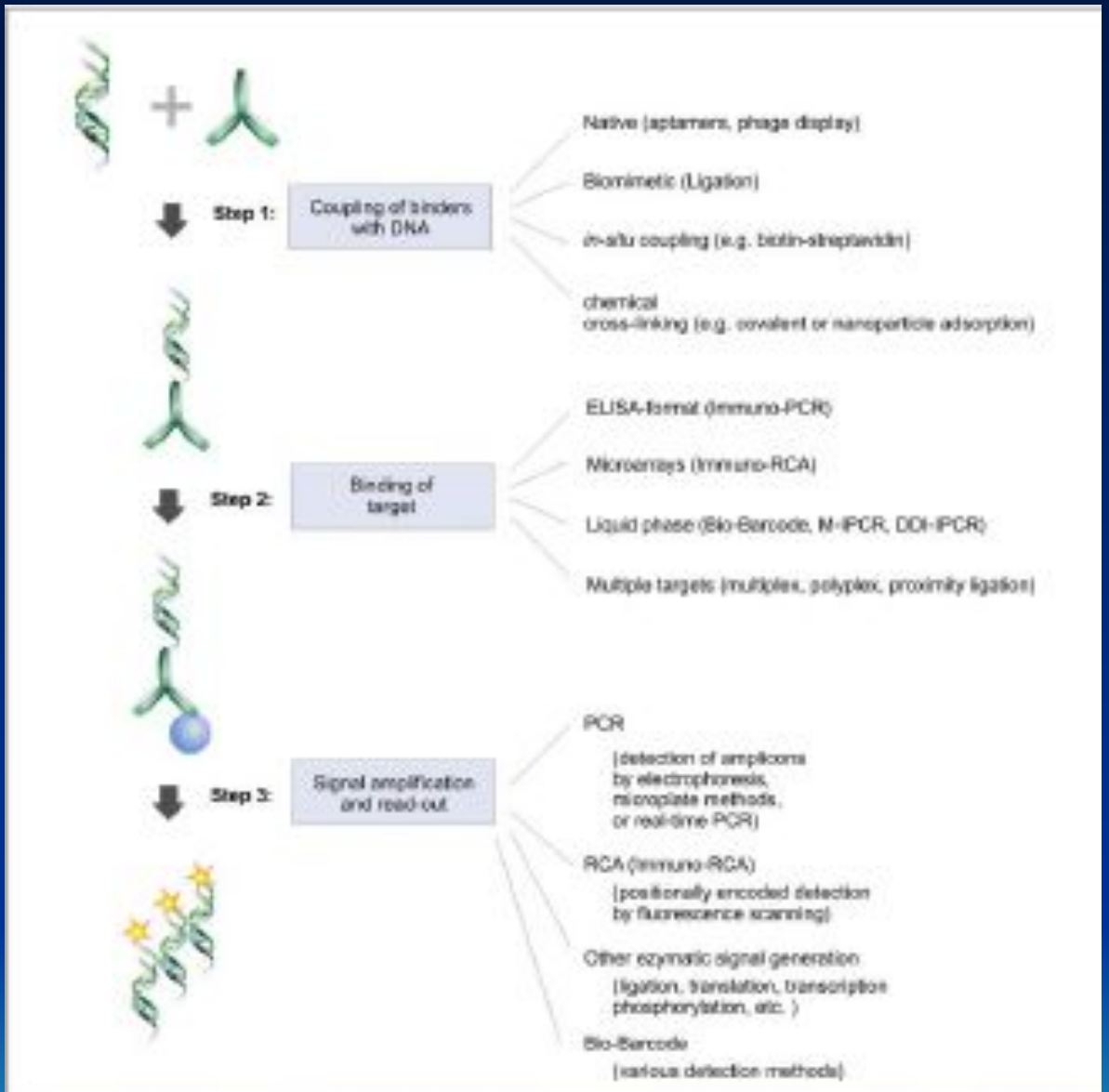

Fig. 1 Key steps of DNA-enhanced immunoassays. Note that additional details regarding antibody–DNA coupling are summarized in (Fig. 3) while aspects regarding signal-generation and DNA detection are further illustrated in (Fig. 6 and 7).

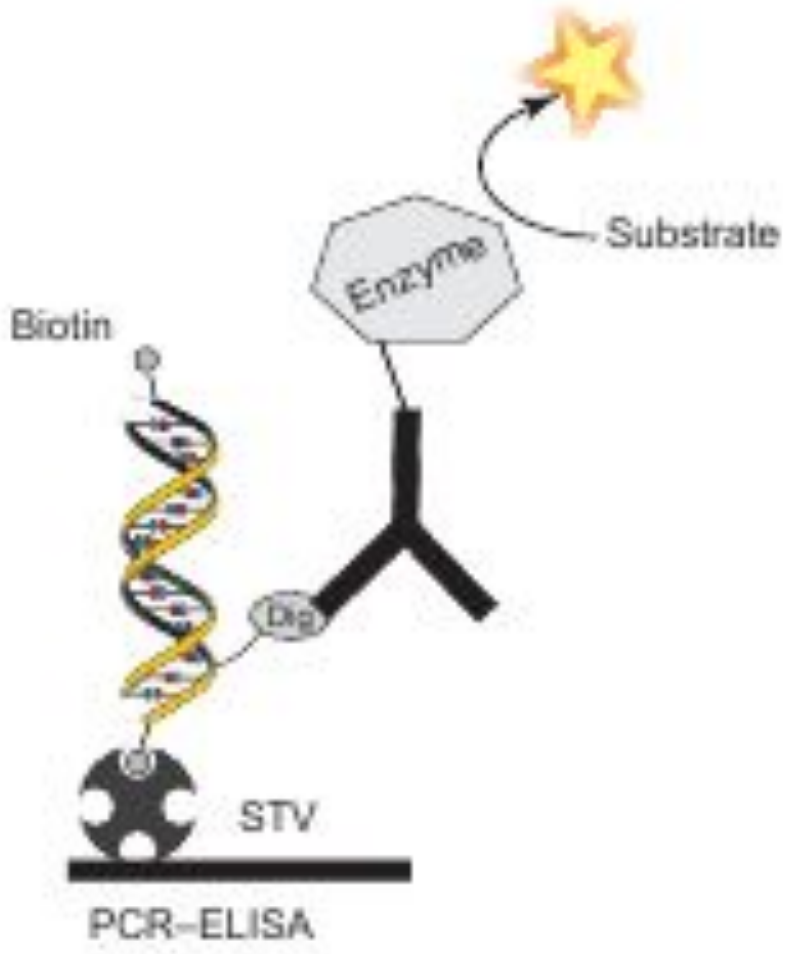
Substrate
Enzyme
Biotin
Dig
STV
PCR–ELISA

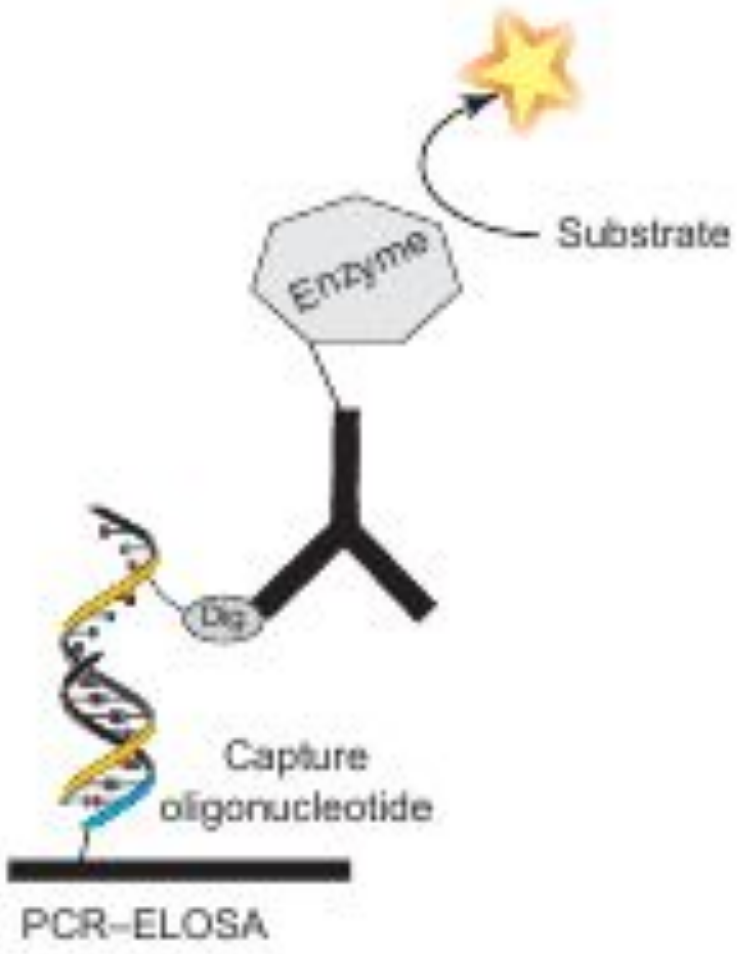
Substrate
Enzyme
Dig
Capture
oligonucleotide
PCR–ELOSA

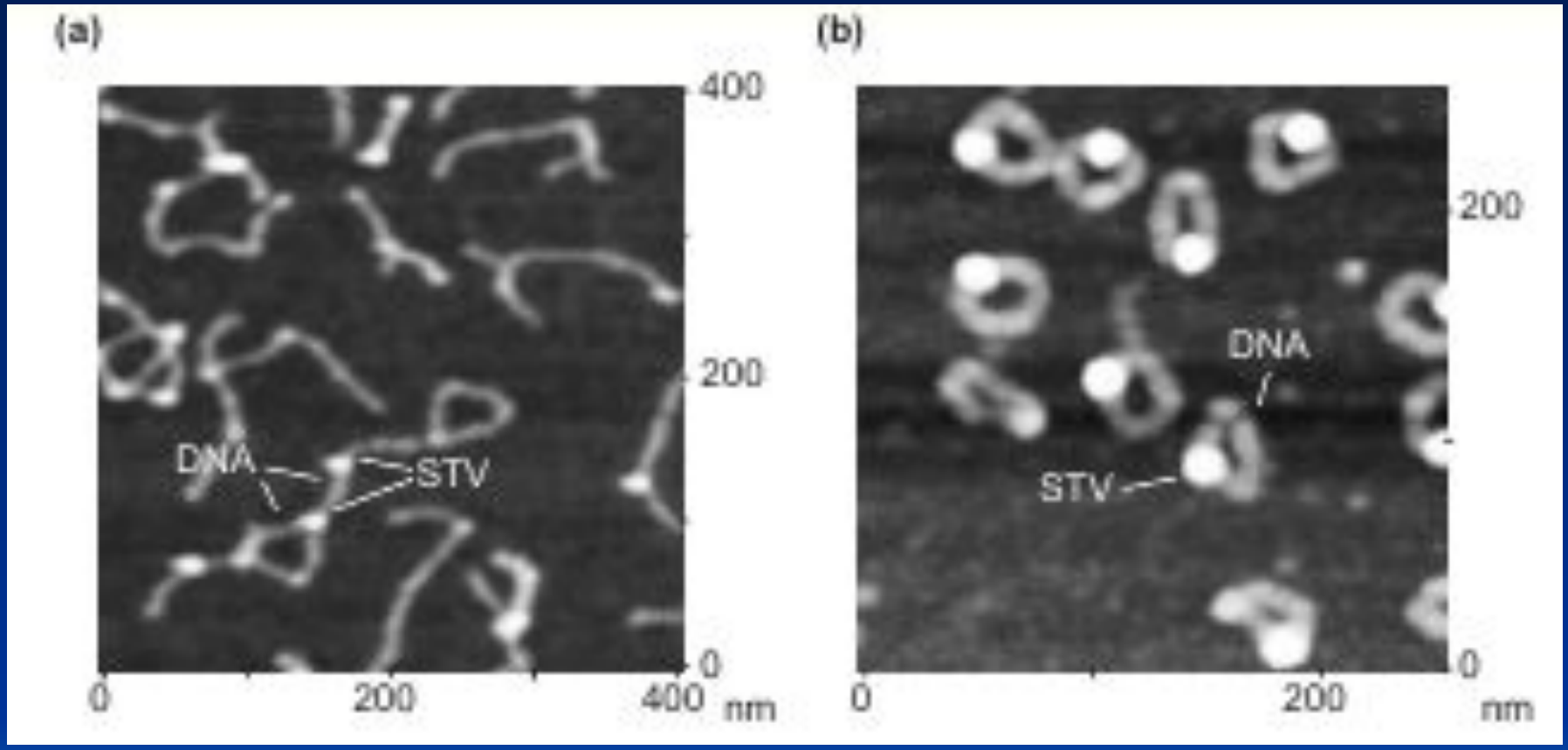

Representative atomic force microscope images of self-assembled oligomeric DNA–STV conjugates (a) and DNA–STV nanocircles (b).
The nanostructured conjugates form the basis of powerful reagents for IPCR assays.

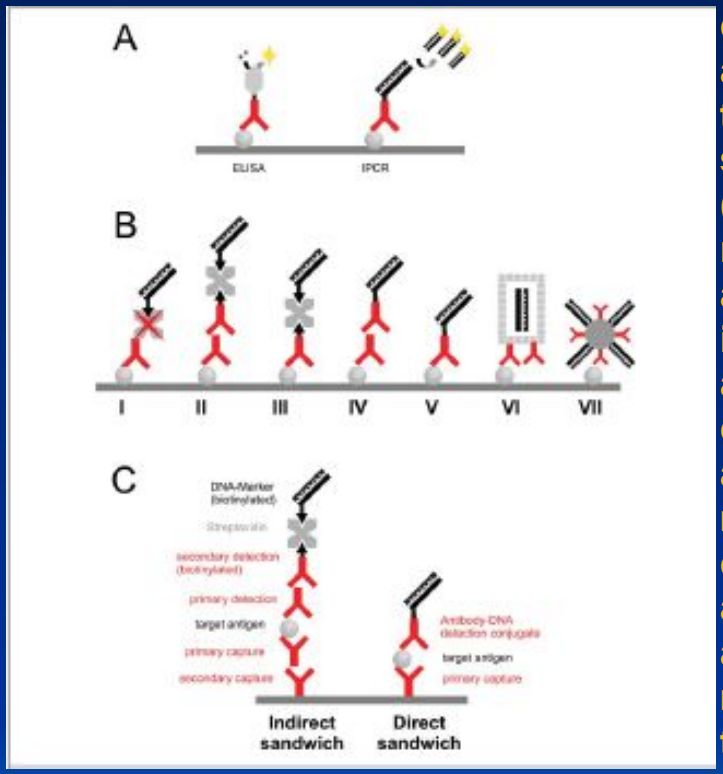

The evolution of immuno-PCR (IPCR): (A) the set-up of ELISA and IPCR is similar.
Instead of an enzyme marker, such as alkaline phosphatase (left), IPCR uses amplification of attached DNA for signal generation (right). (B) Different strategies for coupling antibodies and DNA: in the initial version of IPCR2 a Streptavidin (STV)–protein A chimeric fusion protein was used for tagging the detection antibody with biotinylated DNA (I). In the universal IPCR protocol, the signal generating complex is assembled in situ by subsequent incubation steps of biotinylated detection antibody, (strept-)avidin and biotinylated DNA; either using a non-biotinylated primary and a species specific secondary antibody (II) or a directly biotinylated primary antibody (III). The introduction of pre-assembled antibody–DNA conjugates takes advantage of either species- or marker-specific secondary conjugates92 (IV) or direct conjugation of target-specific antibodies and DNA14 (V). Approaches such as phage display mediated IPCR,44 tadpoles of antibodies and DNA,38 or native chemical ligation introduce elegant ways of coupling antibodies and DNA by circumventing artificial modifications such as biotin and complex crosslinking chemistries (VI). The linkage of multiple antibodies and DNA molecules with particles, as used in the bio-barcode technology92 has led to polyvalent reagents, which allow one to connect single antibody–antigen binding events to a larger number of DNA markers (VII). (C) Comparison of the multiple steps required for the in situ stepwise reagent assembly of the classical universal IPCR approach with the simplicity of specific antibody–DNA conjugates. Note that each coupling step requires optimization of reaction parameters and leads to a loss in sensitivity.

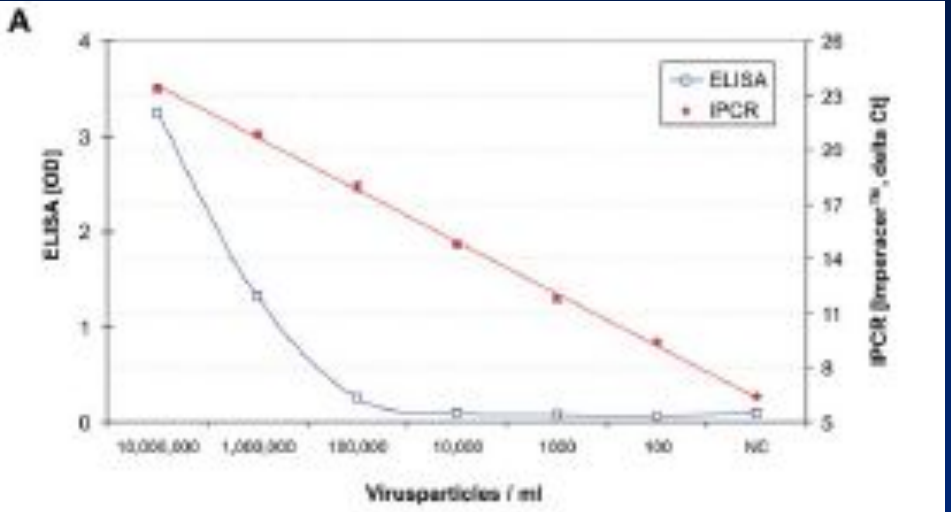

Typical results of immuno-PCR (IPCR) experiments. (A) Comparison of IPCR, the
analogous conventional ELISA for the detection of Rotavirus antigens.108 Note the high linearity and broad dynamic range of IPCR. (B) Comparison of different IPCR assay techniques for the detection of human TNFa: the use of target-specific antibody–DNA conjugates enables an increased sensitivity. The dark and light blue bars represent signals obtained by sequential IPCR (see Fig. 3B III) and direct IPCR with pre-assembled antibody–
DNA conjugates (see Fig. 3B V), respectively. The red curve represents signals obtained in the analogous ELISA.

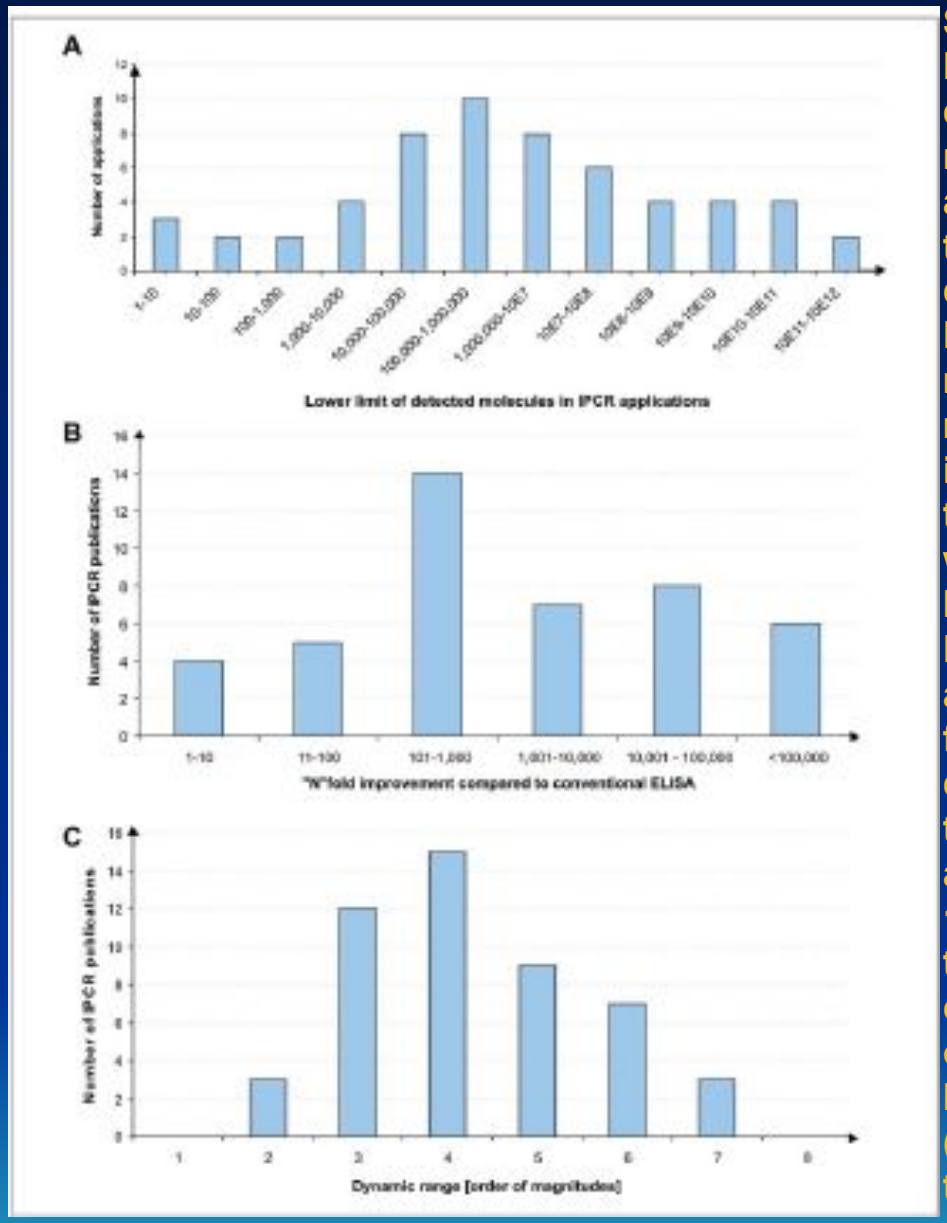

Statistical analysis of references reporting DNA-enhanced immunoassays: (A) summary of detection limits reported. The majority of examples revealed a maximum sensitivity in the 0.016 amol–16 amol range (1000–100 000 molecules, respectively), thus
defining the standard performance of the method. Note that the broad detection range of about ≤10 molecules2,74,102 or single cells18 up to 1010 molecules in all cases involves a significant improvement of the analogous ELISA.137,138 A typical LOD is found at approx. 1000 olecules/sample, which is in accordance with the expected theoretical kinetics of immunoassays.13 (B) Overview of the N-fold improvement of conventional ELISA by the analogous IPCR. The sensitivity enhancement varies from 5-fold31 to up to 1 000 000 000- fold82,86 depending on the design and optimization state of the assay as well as the performance of the antibodies. The majority of studies reported a 100–1000-fold improvement in LOD. (C) Overview of the linear dynamic range of IPCR applications. While conventional ELISA typically reveals a dynamic range of two orders of magnitude in antigen oncentration, IPCR shows a significantly broader dynamic range (see also Fig. 5). In the majority of IPCR applications, the dynamic range comprised about four orders of magnitude.

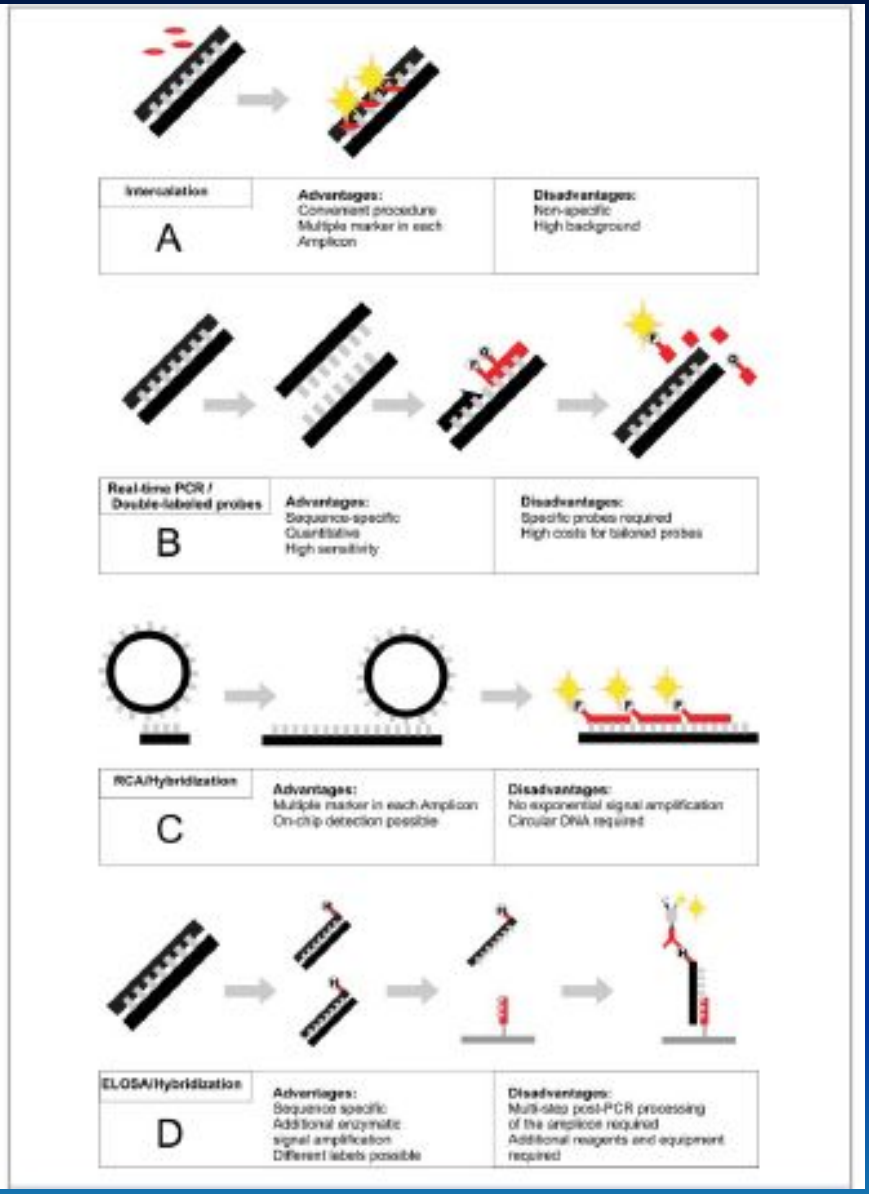

Comparison of the most prominent methods for the detection and quantification of DNA amplicons generated in DNA-enhanced immunoassays. (A) Intercalation fluorescence markers with increased specificity for double-stranded DNA, such as ethidiumbromide or SYBR greenTM, are used in gel-electrophoresis or real-time PCR analyses. Note that for multiplex IPCR, it is necessary to separate amplicons of different length by gel-ectrophoresis while multiplex real-time detection can not be performed using intercalation marks. (B) Different types of sequence-specific fluorophore-labeled nucleic acid probes, e.g. TaqManTM or ScorpionTM are typically used for real-time quantitative PCR. During elongation of primers, the probes are modified and thereby, a fluorescent signal is generated. (C & D) Hybridization assays for sequence-specific DNA-detection. Sensitivity can be increased by binding of multiple fluorophores to the amplified DNA by means of hybridization of fluorophore-labeled probes to
products of RCA (C) or PCR (D) processes. In the case of immuno-RCA, the antibody–DNA–conjugate remains intact during DNA amplification and thus, a multitude of hybridization probes can bind to spots of microarrays, containing the immobilized antigen. In PCR-ELOSA
(D), hapten-labeled amplicons, generated during PCR, are immobilized by means of surface-bound capture oligonucleotides and subsequent detection is carried out by using hapten- specific antibody–enzyme conjugates.

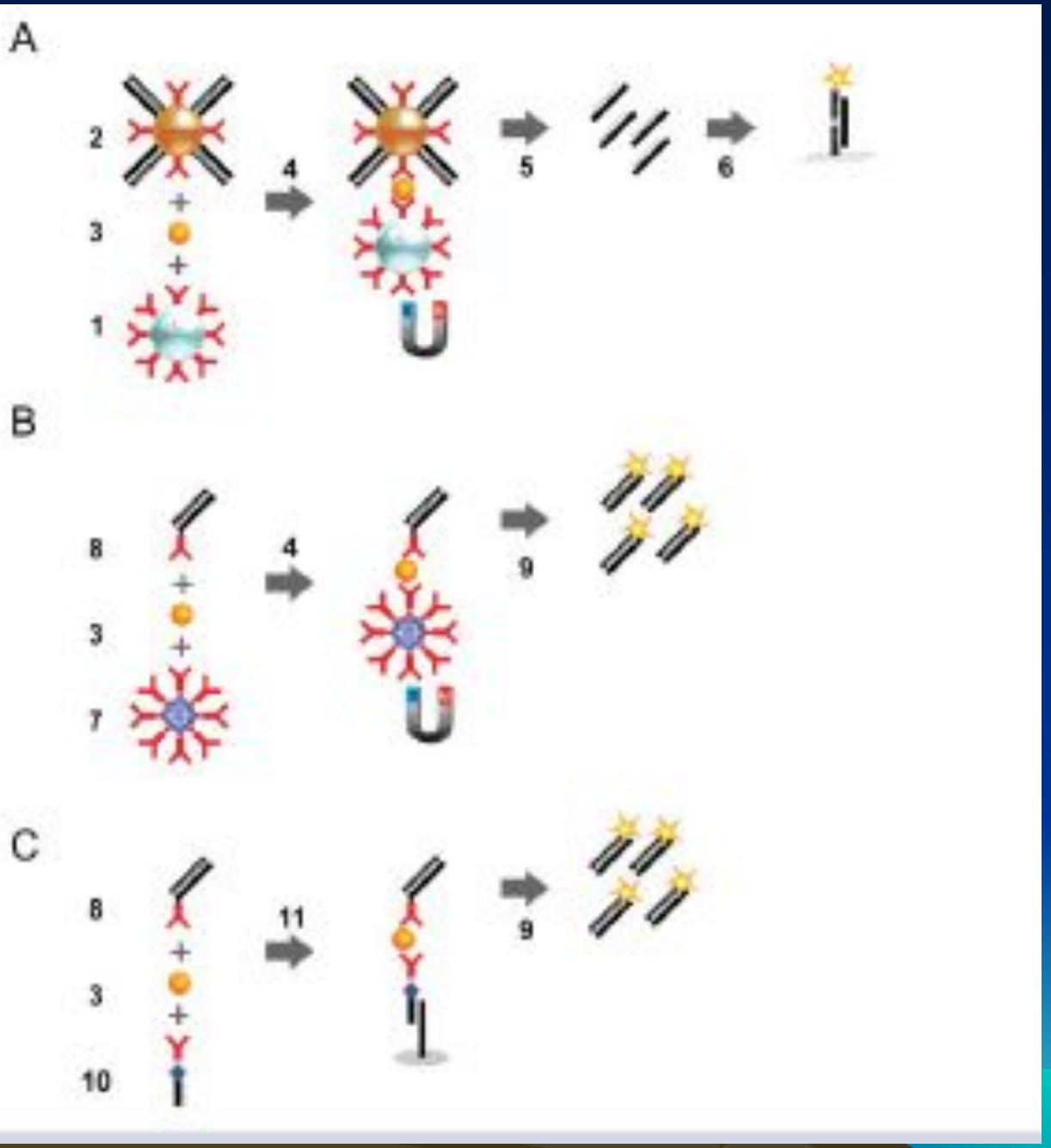
A
2
3
1
4
5
6
B
8
3
7
4
9
C
8
3
10
11
9

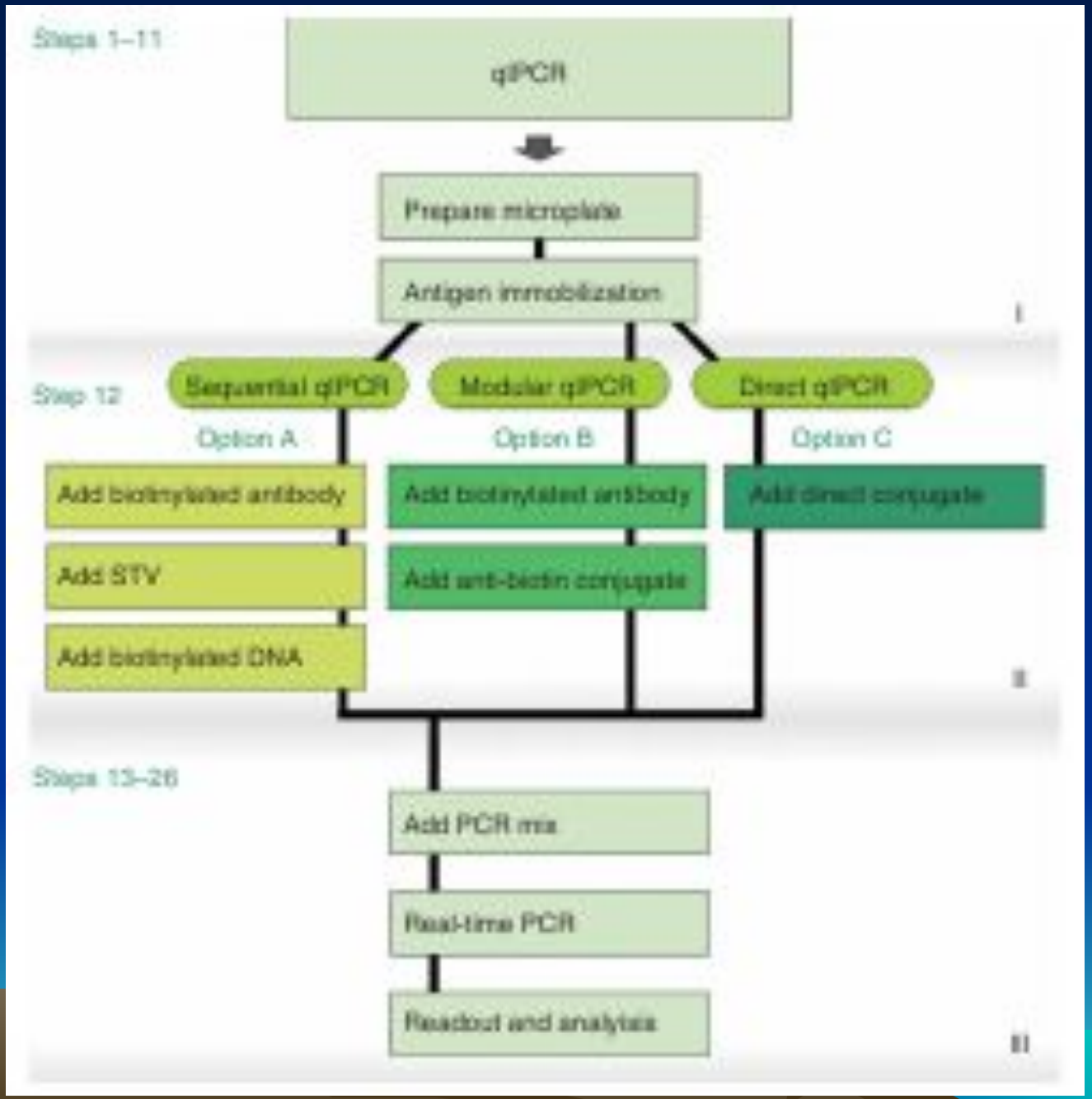
Steps 1–11
qPCR
Prepare microplate
Antigen immobilization
I
Step 12
Sequential qPCR
Modular qPCR
Direct qPCR
Option A
Option B
Option C
Add biotinylated antibody
Add biotinylated antibody
Add direct conjugate
Add STV
Add anti-biotin conjugate
Add biotinylated DNA
II
Steps 13–26
Add PCR mix
Real-time PCR
Readout and analysis
III

Table 1. Overview of IPCR applications

Protein class	Antigen	Year	Limit of detection (LOD); IPCR enhancement compared with ELISA	Remarks
Tumor marker	Human proto-oncogene ETS1	1993	100 000-fold; LOD: 9.6×10^{-21} mol	Universal IPCR
	PIVKA-II, tumor marker of hepatocellular carcinoma	1995	1 000 000 000-fold; LOD: 10^{-19} dilution sample of PIVKA antigen	
	Ganglioside GM3	1998	Detection level of <10 cells, melanoma cells diluted in 2 million healthy blood lymphocytes	
	MG7-Ag	2000	10 000-fold; LOD: 3.8×10^{-14} mol	
	Prostate-specific-antigen (PSA)	2000	1000-fold; LOD: 0.1 pg/ml	Immuno-RCA
	VEGF	2000	5-fold; LOD: 0.2 pg/ml	Real-time IPCR
	Carcinoembryonic antigen (CEA)	2001	92.3% of patients with high CEA levels and 50% of patients with 'normal' CEA levels were found positive	
	TNF-α	2001	50 000-fold; LOD: 1 fg/ml	
	PSA	2002	100-fold; LOD: 2.4×10^{6} molecules PSA	Real-time IPCR
	CEA	2003	1000-fold; LOD: 10 pg/ml	IPCR; real-time IPCR
	PSA	2003	1 000 000-fold; LOD: 30 amol/L	Biobarcode
Viral proteins	Hepatitis B surface-antigen (HbsAg)	1995	100-fold (compared with radioimmunoassay); LOD: 0.5 pg/sample	Sandwich IPCR, PCR-ELOSA
	Bovine herpesvirus I	1996	1 000 000-fold (antigen); 10 000-fold (antibody)	
	Recombinant HBsAg	1997	700-fold; LOD: 2 pg/ml	PCR-ELISA
	Hepatitis B surface-antigen (HBsAg)	2000	Specificity: 14 of 17 liver samples positive	*In situ* IPCR
	HIV core protein p24	2004	25-fold (compared with RT-PCR); LOD: 2 viral copies/ml	
Pathogens, micro-organisms and toxins	Fish pathogen from *Pasteurella piscicida*	1996	10 000-fold; LOD: 3.4 colony-forming units/ml	
	Beta-glucuronidase from *Escherichia coli*	1997	100 000 000-fold; LOD: 0.01 fg/ml	
	Clostridium botulinum neurotoxin type A	2001	1000-fold; LOD: 3.33×10^{-17} mol	
	Gliadin (food allergen)	2003	30-fold; LOD: 160 pg/ml	Real-time IPCR
	Group A Streptococcus	2003	LOD: $\sim1\times10^{-3}$ of a single cell	
	Antigen to *Angiostrongylus cantonensis* circulating fifth-stage worms	2004	100–1000-fold; LOD: 0.1 pg/ml	
	Clostridium botulinum neurotoxin type A	2004	100 000-fold; LOD: 50 fg/sample	
Metabolism, immune system	hTSH, hCG and β-Gal	1995	100–1000-fold; LOD: hTSH 1×10^{-19} mol, hCG 1×10^{-17} mol 5×10^{-18}, β-Gal: 1×10^{-17} mol	Multiplex IPCR
	Soluble murine T cell receptor	1995	125-fold; LOD: 0.8 pg/ml	
	Murine major histocompatibility complex	1997	10-fold; LOD: one embryo	
	Qa-2 antigen	1998	No comparison carried out, used in addition to RT-PCR for the study of blastocysts	
	Human angiotensinogen	2000	250 000-fold; LOD: 0.1 pg/ml	
	Human interleukin 18	2000	16 000-fold; LOD: 2.5 fg/ml	
	Qa-2 protein expression	2000	No comparison carried out, used in addition to RT-PCR for the study of expression in mouse embryos	
	Homodimeric osteoprotegerin	2001	25 000-fold; LOD: 5 fg/ml homodimer	
	Serotonin	2005	1000-fold, LOD: 0.4 pg/ml	Competitive IPCR
Diagnostics, analysis	Recombinant mistletoe lectin (rVis)	1999	1000-fold; LOD: 200 fg/ml	
	Mumps-specific IgG in serum	2002	Compared with ELISA, IPCR was 98.6% (71/72) sensitive and 92.9% (13/14) specific	Real-time IPCR
	rVis	2003	1000–10 000-fold; LOD: 100 fg/ml	
	IgG from several species (mouse, rabbit, goat and human), rViscumin, research antibody in cell culture media	2003	100–1000-fold; LOD: 0.1–0.01 amol IgG, 40 pg/ml rViscumin in serum, 100 pg/ml research antibody	Routine application real-time IPCR
Other	Bovine serum albumin	1992	100 000-fold; LOD: 9.6×10^{-23} mol	First IPCR publication
	Mouse antibody against apolipoprotein E	1993	No comparable ELISA data are given; LOD: 0.5 fg/sample	
	Fluorescein	2000	1000-fold; LOD: 300 amol/ml	Competitive IPCR
	p185(her2/neu) receptor from crude lysate of T6–17 cells	2001	1 000 000 000-fold; LOD: 10^{-13} dilution of cell solution	

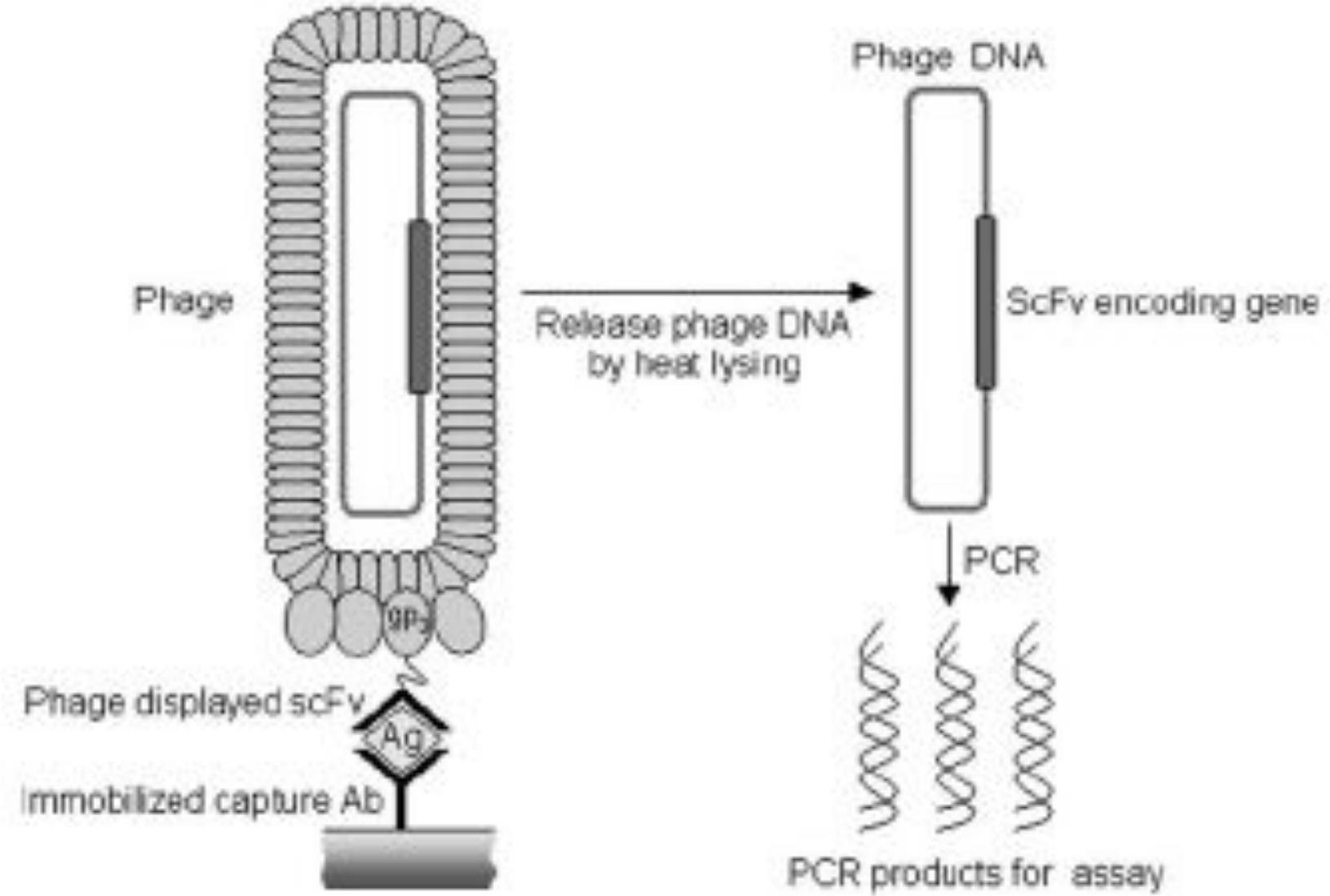
Phage DNA
Phage
Release phage DNA
by heat lysing
ScFv encoding gene
PCR
gP3
Phage displayed scFv
Ag
Immobilized capture Ab
PCR products for assay

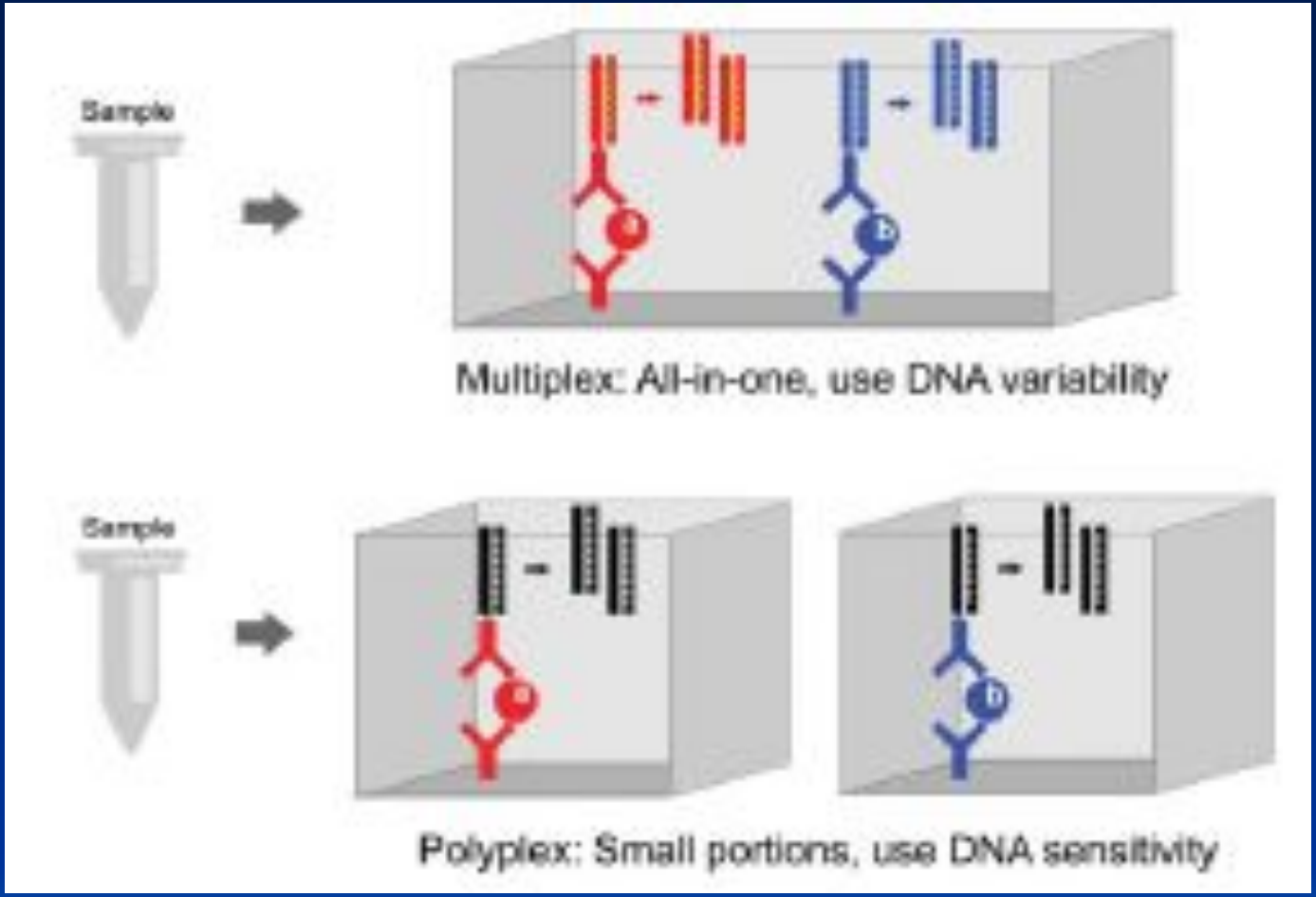

Multiplex and polyplex assays for the detection of several antigens in a single sample: in multiplex assays, different antigens (a and b) are tagged with different DNA sequences. Inpolyplex assays the sample is divided into small aliquots, each of which is analyzed individually by a target specific assay.

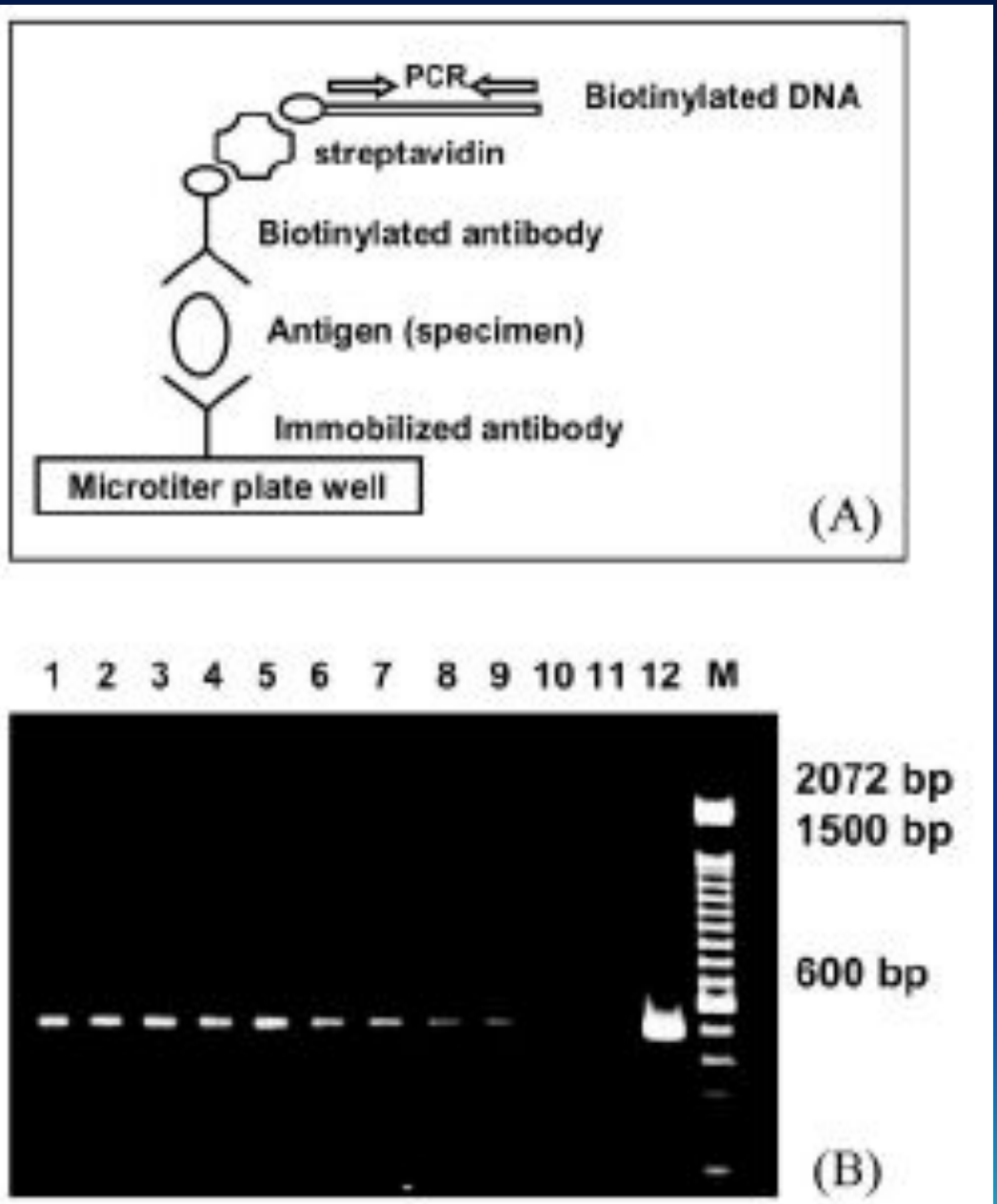

Fig. 1. Schematic representation of immuno-PCR assay (*A*), and detection of protein A from *S. aureus* by immuno-PCR (*B*).

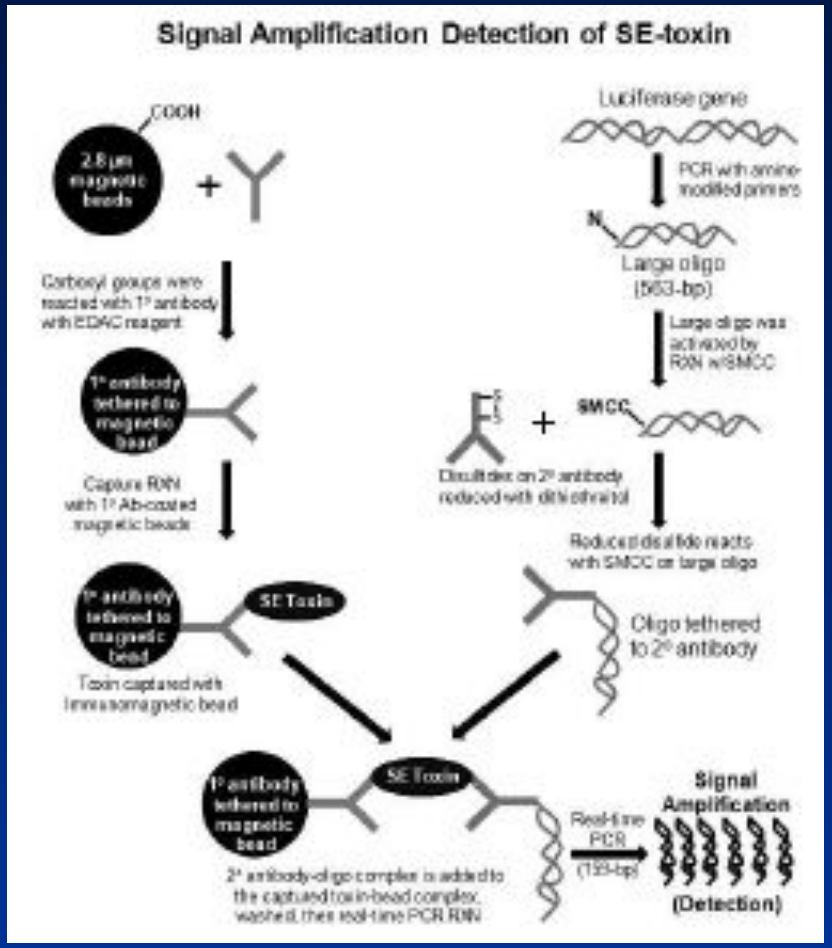

Schematic representing the flow of reactions involved in the immuno-PCR signal amplification assay for detection of SEA and SEB. The Bead Retriever facilitated recovery of magnetic beads during chemical reactions and SE recovery during the assays.

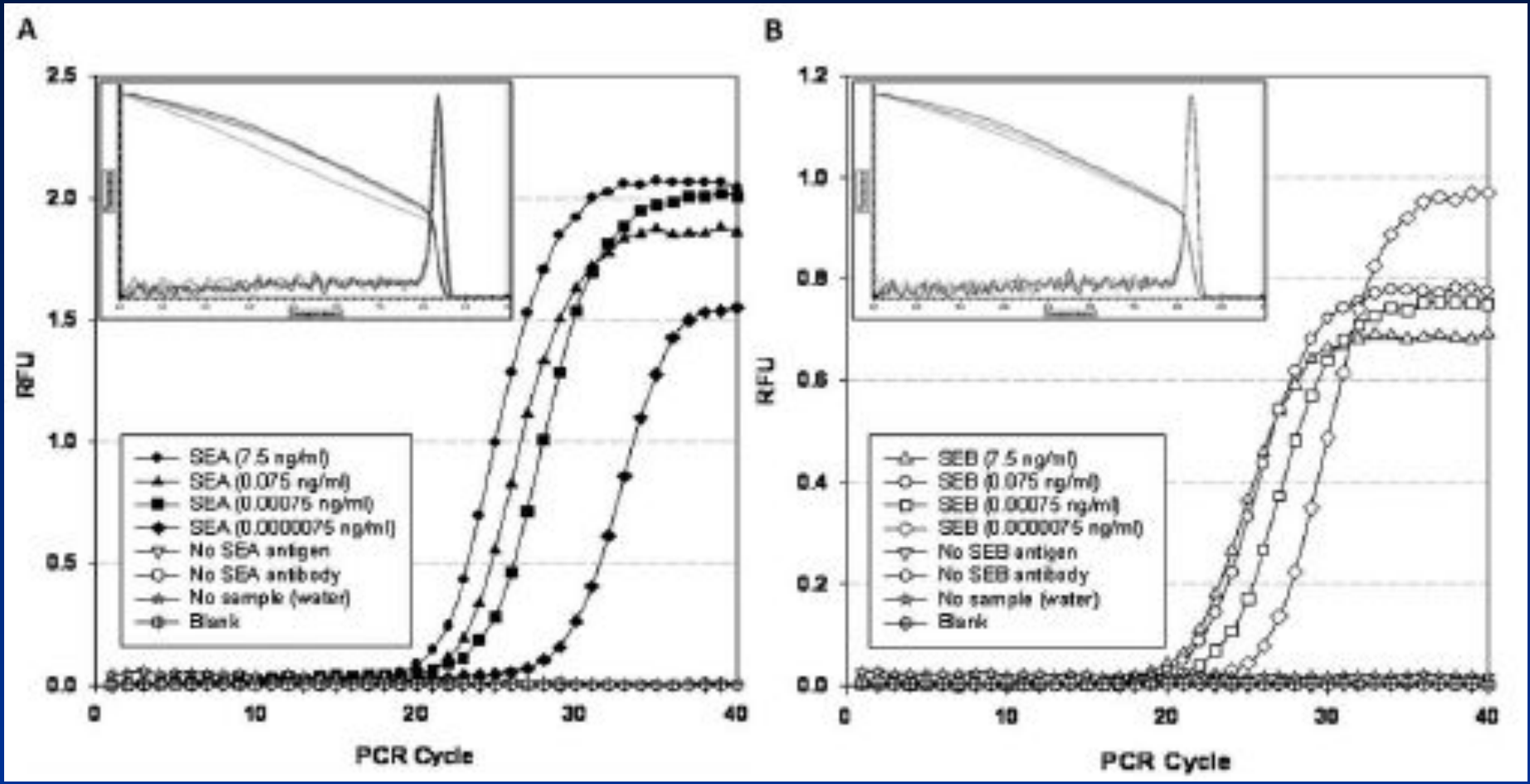

iPCR-SA assay detection of SEA (A) or SEB (B) spiked into tryptic soy broth at select levels. Controls consisted of lowest dilution without added SEA or SEB antigen (but processed accordingly), without SEA or SEB antibody, use of water as a sample, and a blank well with PCR reagents only. Inset shows overlapping melting curves of amplified products of all PCR-positive samples.

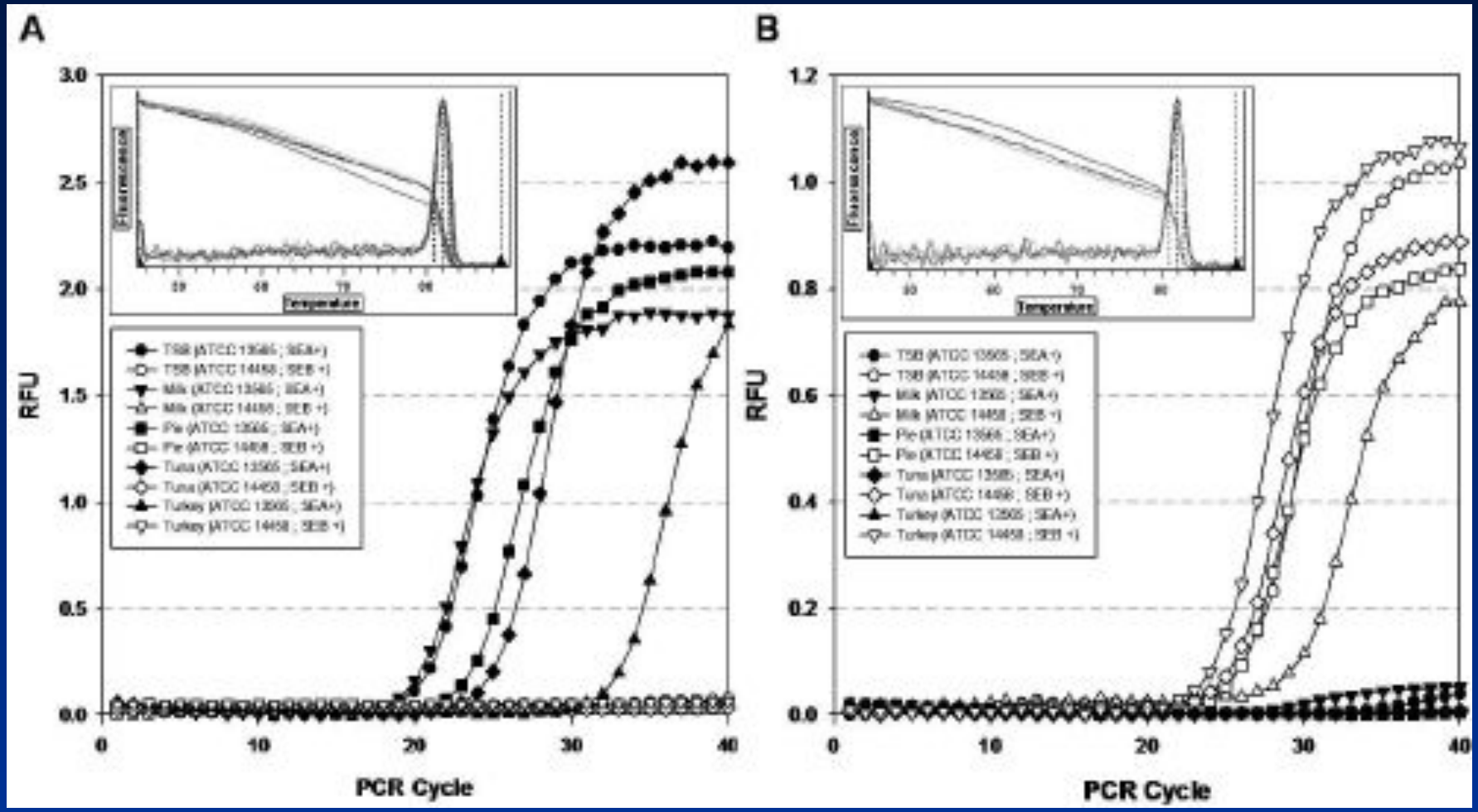

iPCR-SA assay detection of staphylococcal enterotoxins A and B produced bySEz S. aureus strains incubated in TSB, milk, lemon cream pie, tuna salad, and deli turkey. (A) Detection of SEA after incubation of S. aureus ATCC 13565 (SEA) in the various matrices using anti-SEA–coated magnetic beads. Control assays were performed with ATCC 14458 (SEB). (B) Detection of SEB after incubation with S. aureus ATCC 14458 (SEB) using anti-SEB–coated magnetic beads. Control assays were performed with ATCC 13565 (SEA). Insets show melting curves of amplified by-products obtained with a real-time PCR.

TABLE 2. *iPCR-SA detection of SEA and SEB spiked in foods*[a]

	Milk		Cream pie		Tuna salad		Ground turkey	
Spiked concn (ng/ml or g)	Detected	C_T (cycles)	Detected	C_T (cycles)	Detected	C_T (cycles)	Detected	C_T (cycles)
SEA								
7.5	+	26	+	28	NA		+	27
0.75	+	27	NA[b]		NA		+	27
0.075	+	28	+	29	NA		+	28
0.0075[c]	+	29	NA		NA		+	29
0.00075	+	30	+	30	NA		+	30
0.000075	+	30	NA		NA		+	31
0.0000075[d]	+	31	+	31	NA		+	32
SEB								
7.5	+	23	NA		+	26	+	22
0.75	+	24	NA		NA		+	21
0.075	+	25	NA		+	27	+	23
0.0075[c]	+	26	NA		NA		+	24
0.00075	+	26	NA		+	30	+	25
0.000075	+	27	NA		NA		+	26
0.0000075[d]	+	28	NA		+	32	+	27

[a] C_T, threshold cycle. The control samples for no antigen, no primary antibody, no secondary antibody, no sample, and blank were negative for all samples tested (i.e., $C_T > 40$).

[b] NA, not assayed.

[c] Equivalent to 7.5 pg/ml or g.

[d] Equivalent to 7.5 fg/ml or g.

TABLE 3. *Detection of toxin by the iPCR-SA assay in heated food samples*

Spiked concn or control type	iPCR-SA for SEA			iPCR-SA for SEB		
	Ground turkey (77°C, 30 min)	Milk[a]		Ground turkey (77°C, 30 min)	Milk	
		100°C, 10 min	121°C, 2.75 h		100°C, 10 min	121°C, 2.75 h
SEA or SEB (ng/ml or g)						
7.5	+	+	+	+	+	+
0.75	+	+	+	+	+	+
0.075	+	+	+	+	+	−
0.0075	+	+	+	+	+	−
0.00075	+	+	−	+	+	−
0.000075	+	+	−	+	+	−
0.0000075[b]	+	+	−	+	+	−
Control type						
No toxin	−	−	−	−	−	−
No 1° antibody	−	−	−	−	−	−
No 2° antibody	−	−	−	−	−	−
No sample (water)	−	−	−	−	−	−
Blank	−	−	−	−	−	−

[a] Milk was heated in an autoclave at 15 psi.

[b] Equivalent to 7.5 fg/ml or g.

TABLE 4. *Comparison of sensitivity of iPCR-SA assay with that of several commercial kits for detection of SEA and SEB diluted in TSB*

Spiked concn (ng/ml or g)	iPCR-SA		SET VIA[a]		ELISA for SEB[b]
	SEA	SEB	SEA	SEB	
7.5	+	+	+	+	+
0.75	+	+	−	−	−
0.075	+	+	−	−	−
0.0075[c]	+	+	−	−	−
0.00075	+	+	−	−	−
0.000075	+	+	−	−	−
0.0000075[d]	+	+	−	−	−

[a] From TECRA.
[b] From Toxin Technologies.
[c] Equivalent to 7.5 pg/ml or g.
[d] Equivalent to 7.5 fg/ml or g.

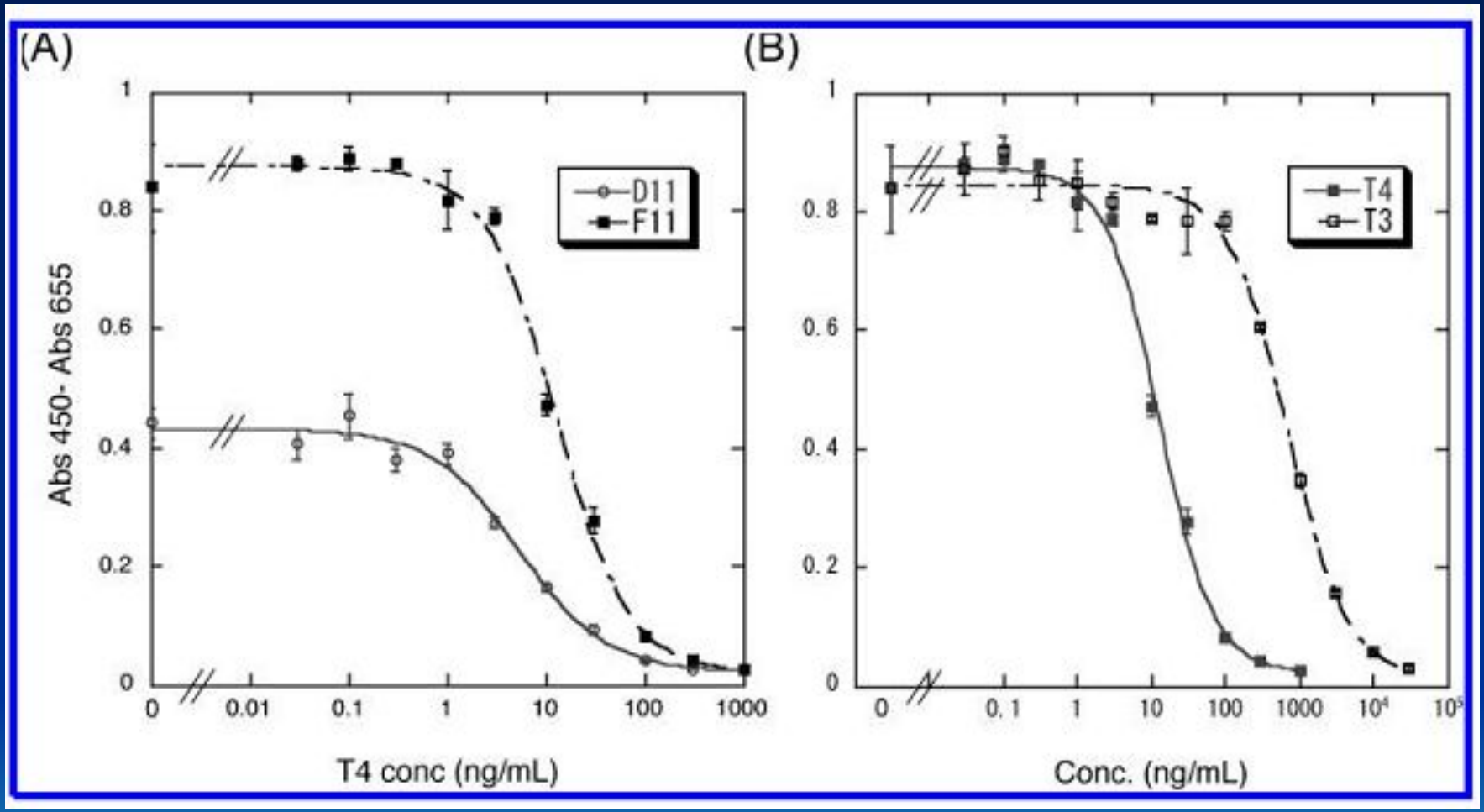
(A)
(B)
Abs 450- Abs 655
T4 conc (ng/mL)
Conc. (ng/mL)
D11
F11
T4
T3
0
0.2
0.4
0.6
0.8
1
0.01
0.1
10
100
1000

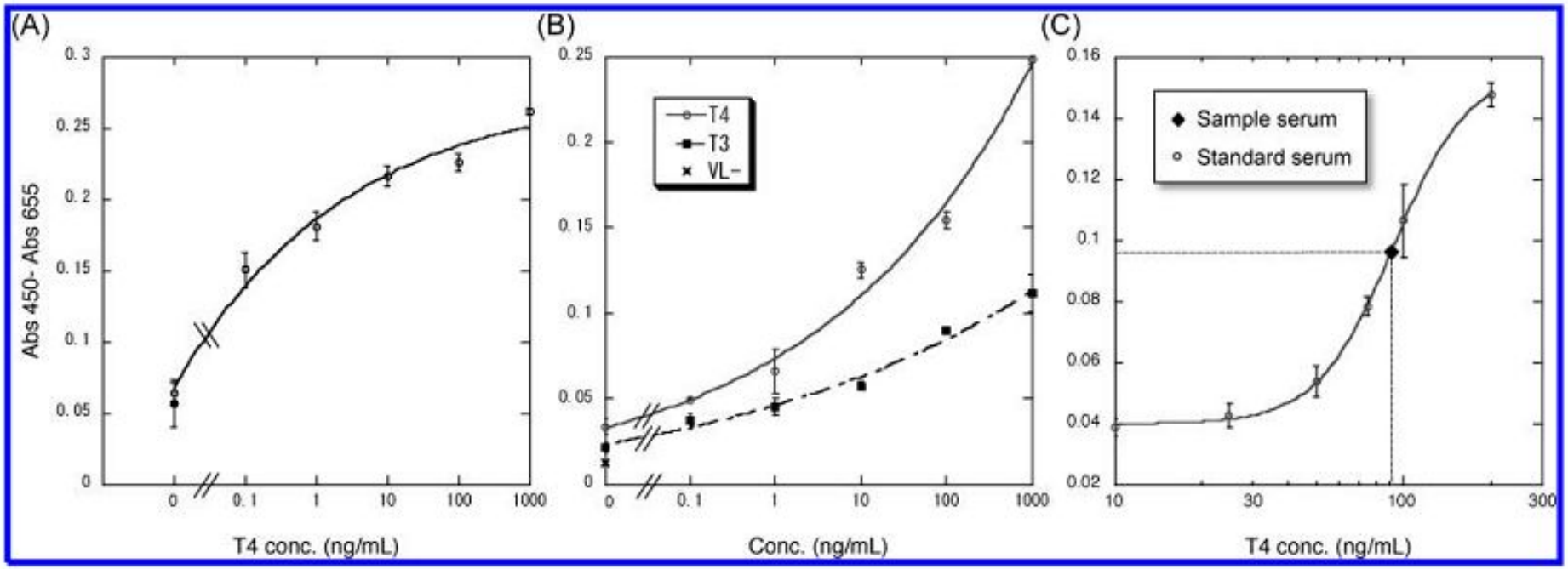

Figure 4. OS-ELISA using purified MBP−V_L and HRP−MBP−V_H of D11. Average of three measurements with 1 SD is shown. (A) A representative dose−response curve. Open and closed circles represent values with and without immobilized antihuman kappa chain antibody, respectively. (B) Cross reactivity with T3. Free T4 and T3 were incubated with HRP−MBP−V_H in the plate immobilized with MBP−V_L. V_L− shows the value without immobilized antibody. (C) Estimation of total T4 in serum using MBP−V_L and HRP−MBP−V_H.

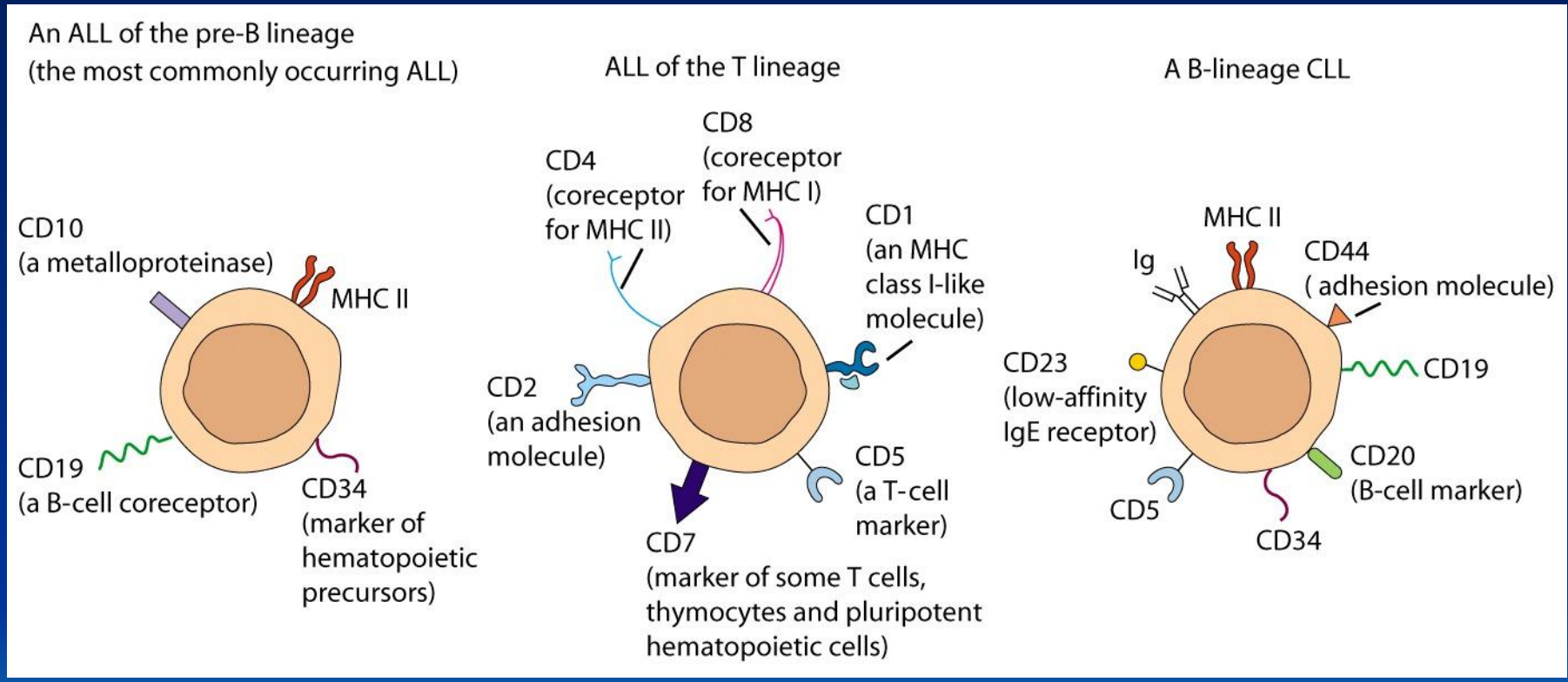
An ALL of the pre-B lineage
(the most commonly occurring ALL)
CD10
(a metalloproteinase)
MHC II
CD19
(a B-cell coreceptor)
CD34
(marker of
hematopoietic
precursors)
ALL of the T lineage
CD8
(coreceptor
for MHC I)
CD4
(coreceptor
for MHC II)
CD1
(an MHC
class I-like
molecule)
CD2
(an adhesion
molecule)
CD5
(a T-cell
marker)
CD7
(marker of some T cells,
thymocytes and pluripotent
hematopoietic cells)
A B-lineage CLL
MHC II
Ig
CD44
(adhesion molecule)
CD23
(low-affinity
IgE receptor)
CD19
CD20
(B-cell marker)
CD5
CD34

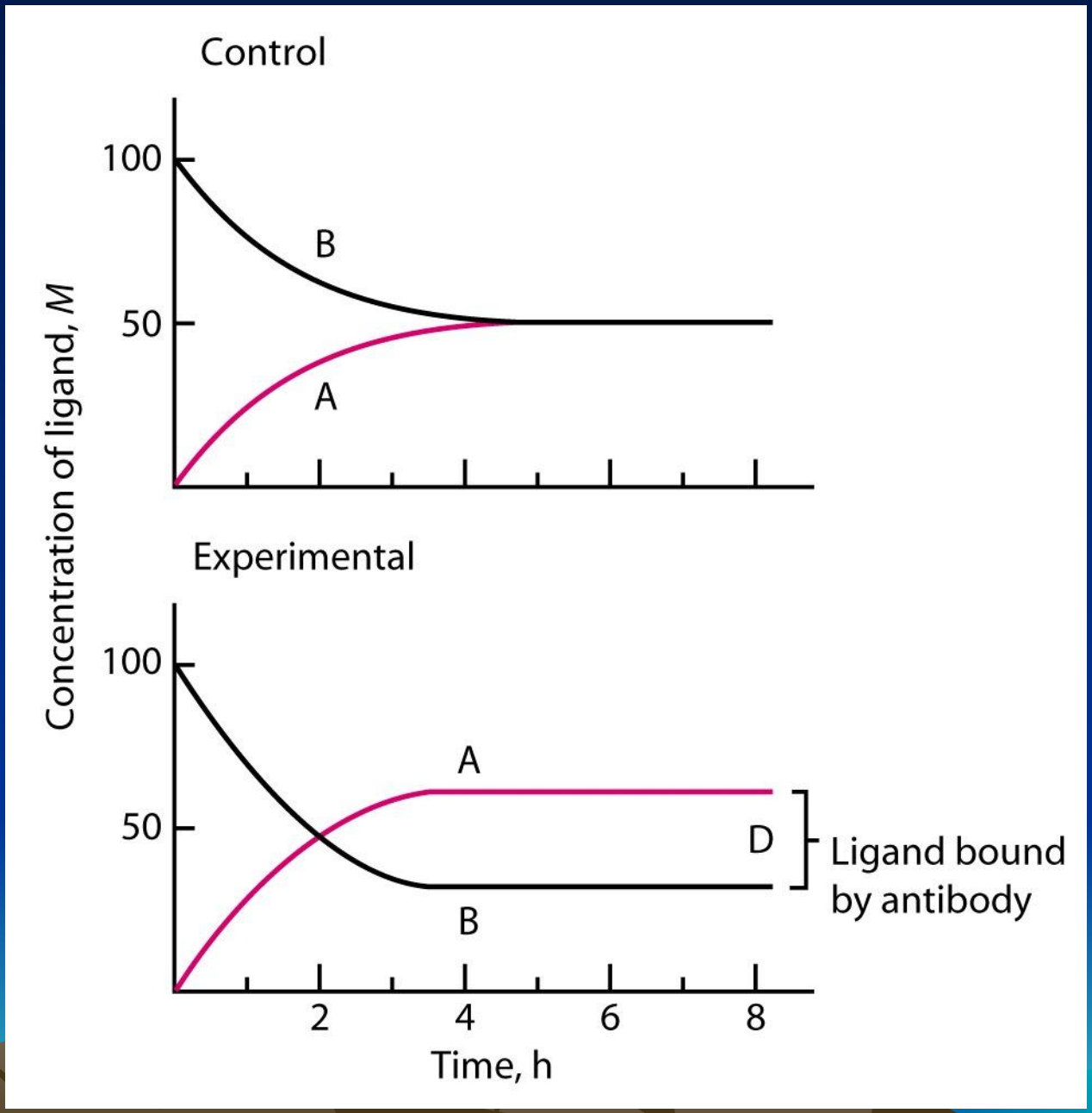
Control
100
50
B
A
Concentration of ligand, M
Experimental
100
50
A
D
Ligand bound by antibody
B
2
4
6
8
Time, h

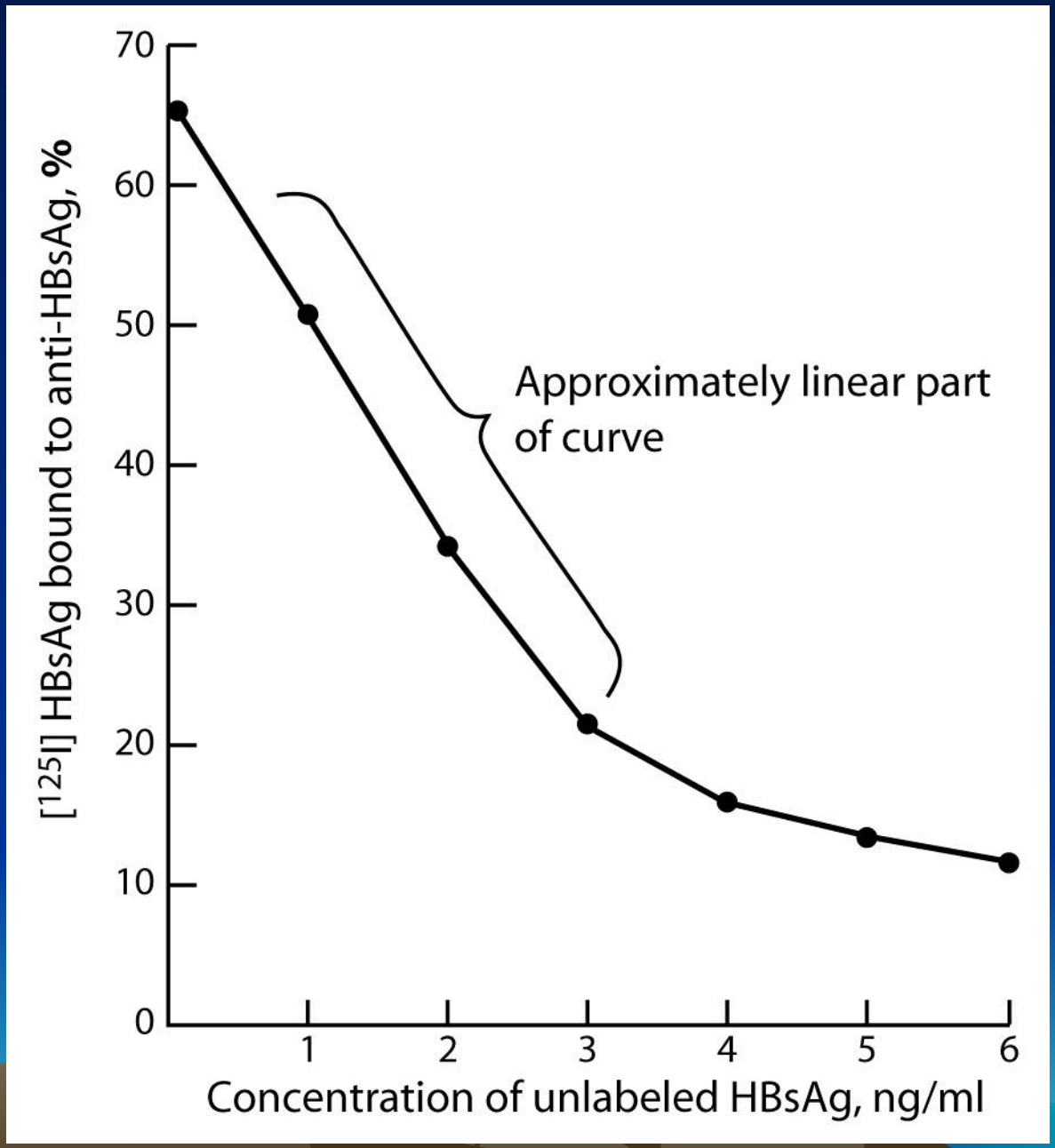
70
60
50
40
30
20
10
0
[125I] HBsAg bound to anti-HBsAg, %
Approximately linear part of curve
1
2
3
4
5
6
Concentration of unlabeled HBsAg, ng/ml

An ALL of the pre-B lineage
(the most commonly occurring ALL)

CD10
(a metalloproteinase)

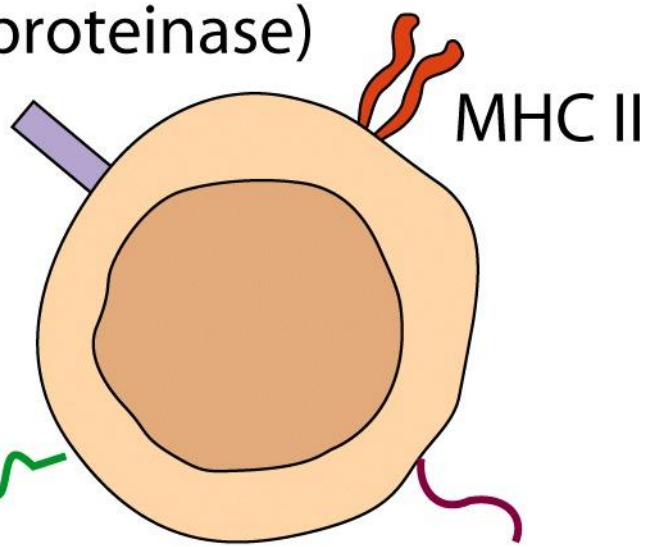

ALL of the T lineage

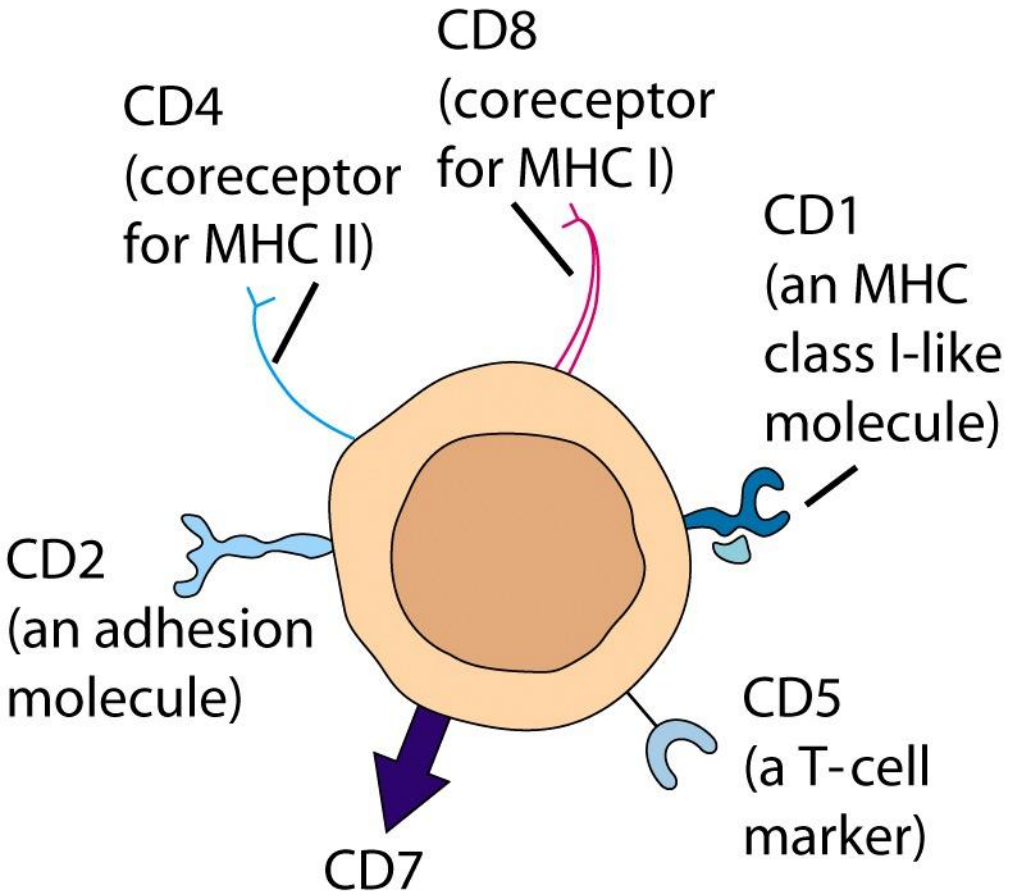

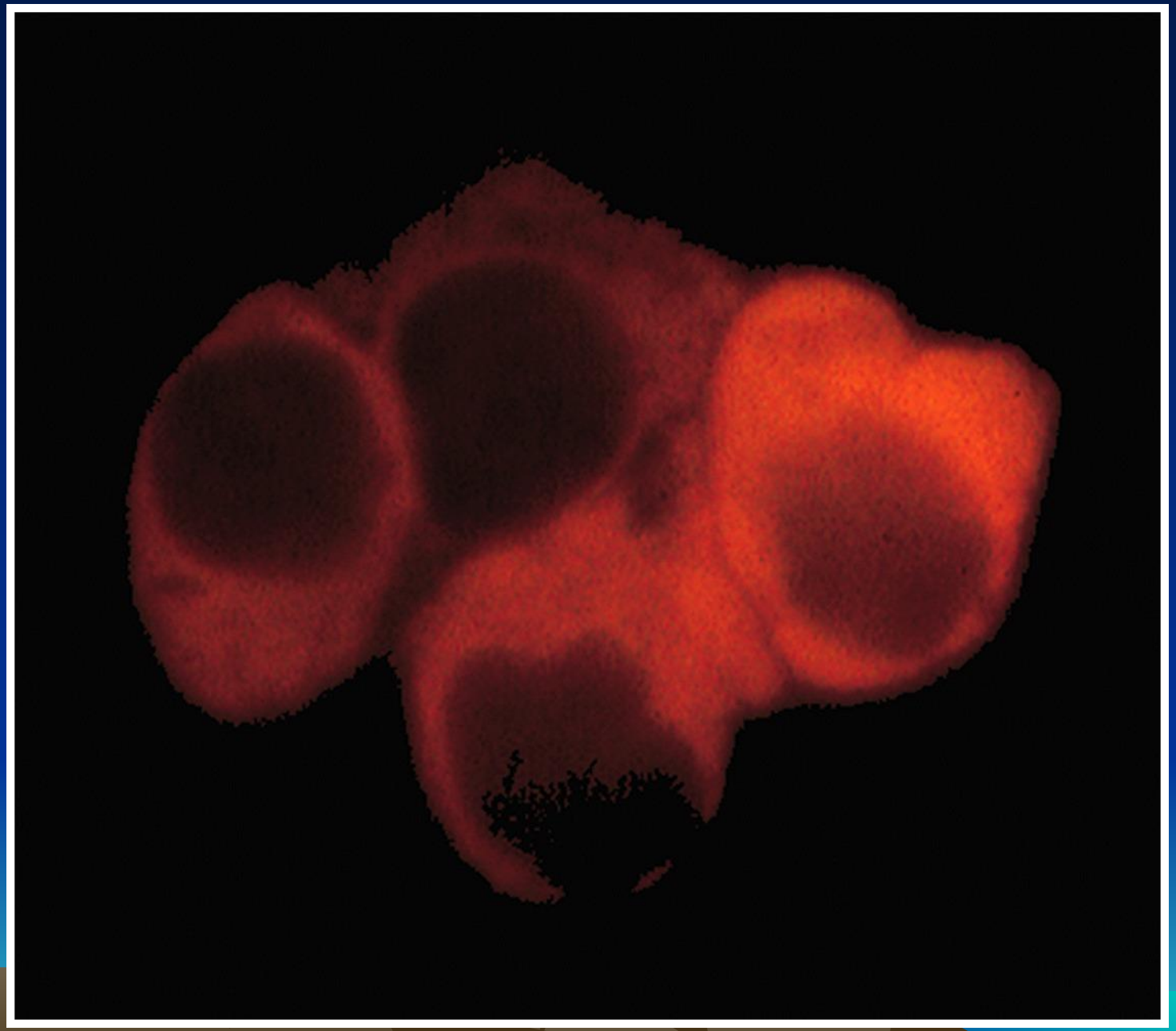

A B-lineage CLL